



Evidence of off-shell Higgs boson production from ZZ leptonic decay channels and constraints on its total width with the ATLAS detector



The ATLAS Collaboration*

ARTICLE INFO

Article history:

Received 5 April 2023

Received in revised form 27 September 2023

Accepted 28 September 2023

Available online 5 October 2023

Editor: M. Doser

Dataset link: <https://hepdata.cedar.ac.uk>

ABSTRACT

This Letter reports on a search for off-shell production of the Higgs boson using 139 fb^{-1} of pp collision data at $\sqrt{s} = 13 \text{ TeV}$ collected by the ATLAS detector at the Large Hadron Collider. The signature is a pair of Z bosons, with contributions from both the production and subsequent decay of a virtual Higgs boson and the interference of that process with other processes. The two observable final states are $ZZ \rightarrow 4\ell$ and $ZZ \rightarrow 2\ell 2\nu$ with $\ell = e$ or μ . In the $ZZ \rightarrow 4\ell$ final state, a dense Neural Network is used to enhance analysis sensitivity with respect to matrix element-based discrimination. The background-only hypothesis is rejected with an observed (expected) significance of 3.3 (2.2) standard deviations, representing experimental evidence for off-shell Higgs boson production. Assuming that no new particles enter the production of the virtual Higgs boson, its total width can be deduced from the measurement of its off-shell production cross-section. The measured total width of the Higgs boson is $4.5^{+3.3}_{-2.5} \text{ MeV}$, and the observed (expected) upper limit on the total width is found to be 10.5 (10.9) MeV at 95% confidence level.

© 2023 The Author(s). Published by Elsevier B.V. This is an open access article under the CC BY license (<http://creativecommons.org/licenses/by/4.0/>). Funded by SCOAP³.

1. Introduction

The discovery of the Higgs boson in 2012 by the ATLAS and CMS collaborations at the Large Hadron Collider (LHC) [1,2] was a major milestone in particle physics, and since then this particle has been put under the spotlight for further scrutiny to uncover its fundamental nature. Great progress has been made in measuring the properties and couplings of the Higgs boson [3,4], and to date no deviations from the Standard Model (SM) predictions have been found. The total width of the Higgs boson (Γ_H) is a key prediction of the SM. The expected value in the SM (Γ_H^{SM}) for a 125 GeV Higgs boson is only 4.1 MeV [5], which is inaccessible via any direct measurement of the width in the resonance region due to limited detector resolution. To probe this parameter, a method relying on both off-shell and on-shell production of the Higgs boson has been developed, as documented in [6–9]. In this method, the relationship between the Higgs boson coupling constants in the on-shell and off-shell regimes is assumed to be given by the SM prediction, assuming that no new particles enter into the Higgs boson production process. On-shell Higgs boson production (only gluon-gluon fusion (ggF) is considered in the equations below, but the principle is the same in other production modes) is inversely proportional to the width:

$$\sigma_{gg \rightarrow H \rightarrow ZZ}^{\text{on-shell}} \sim \frac{g_{ggF}^2 g_{HZZ}^2}{m_H \Gamma_H}.$$

However, off-shell Higgs boson production has no width dependence:

$$\sigma_{gg \rightarrow H \rightarrow ZZ}^{\text{off-shell}} \sim \frac{g_{ggF}^2 g_{HZZ}^2}{m_{ZZ}^2}.$$

Therefore, if the HZZ and effective ggH couplings in the two regimes (where the effective coupling is obtained by treating the quark loop as a single vertex) have a known relationship, Γ_H can be extracted from the ratio of yields of observed Higgs boson events. Off-shell production is accessible in the ZZ decay channel because the available phase space for the decay increases rapidly as the off-shell mass approaches the $2m_Z$ threshold, counteracting the expected drop in the production at higher masses [10–22], where m_Z is the mass of the Z boson.

Multiple searches for off-shell Higgs boson production have been carried out by the ATLAS and CMS collaborations using LHC Run 1 and Run 2 data [23–29]. In practice the signal of off-shell Higgs boson production is a deficit in $gg \rightarrow ZZ$ or electroweak $q\bar{q} \rightarrow ZZ$ production, due to the negative interference between the off-shell Higgs boson process and the continuum background. Throughout this Letter, the notation $gg \rightarrow (H^* \rightarrow) ZZ$ is used to refer to the inclusive process that combines the Higgs boson signal $gg \rightarrow H^* \rightarrow ZZ$, the continuum background process $gg \rightarrow ZZ$, and their interference. Similarly, the notation $q\bar{q} \rightarrow (H^* \rightarrow) ZZ + 2j$

* E-mail address: atlas.publications@cern.ch.

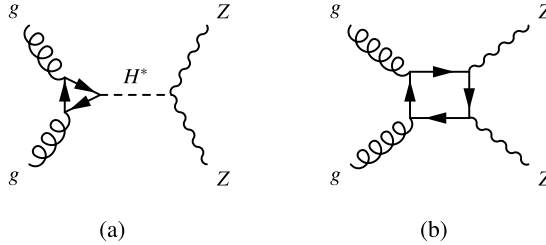


Fig. 1. The leading-order Feynman diagrams for the (a) $gg \rightarrow H^* \rightarrow ZZ$ signal and (b) background processes. In the signal process the quark loop is dominated by top and bottom, while for the continuum background it is mainly light quarks.

refers to the inclusive electroweak process that combines the processes $q\bar{q} \rightarrow H^* \rightarrow ZZ + 2j$, $q\bar{q} \rightarrow ZZ + 2j$, and their interference.

The corresponding leading-order Feynman diagrams for the signal and background processes are shown in Figs. 1 and 2. Owing to the clean signature and accessible branching fractions, the four-lepton final states (4ℓ and $2\ell 2\nu$ with $\ell = e$ or μ), originating from the decays of a pair of on-shell Z bosons induced by a virtual Higgs boson, offer the main signal sensitivity. The latest CMS search [29], using 138 fb^{-1} in the $2\ell 2\nu$ channel and 78 fb^{-1} in the 4ℓ channel, led to an observed (expected) detection significance of about 3.6σ (2.4) standard deviations (σ) for off-shell Higgs boson production and a measured Γ_H of $3.2^{+2.4}_{-1.7} \text{ MeV}$. The analysis described in this Letter updates the previous ATLAS result [27] with more data – the full Run-2 dataset is used in both decay channels – a more powerful discriminant in the 4ℓ channel, and a data-driven approach to estimating the leading $q\bar{q} \rightarrow ZZ$ background. Additionally, in this analysis for the first time ggF and EW off-shell production are probed separately as well as together.

This Letter presents a search for off-shell Higgs boson production in four-lepton final states using the full Run 2 data at a centre-of-mass energy $\sqrt{s} = 13 \text{ TeV}$ collected by the ATLAS detector. Two decay channels, 4ℓ and $2\ell 2\nu$, are separately analysed and then combined to obtain the final results. Events with a pair of Z bosons are categorised into several signal regions (SRs) to probe off-shell contributions from the two leading production modes, ggF and electroweak production (EW), and their respective interference with the continuum background $gg \rightarrow ZZ$ and electroweak $q\bar{q} \rightarrow ZZ + 2j$ processes. Electroweak production includes the contributions from vector-boson fusion (VBF) and vector-boson associated production (VH), since these two processes both interfere with the electroweak $q\bar{q} \rightarrow ZZ + 2j$ background and hence cannot be separated. The main irreducible background is Z boson pair production via quark-antiquark annihilation ($q\bar{q} \rightarrow ZZ$); the interfering backgrounds described above also contribute. In the 4ℓ channel, these are the only significant backgrounds, with sub-percent-level contributions from the production of Z bosons with associated jets and $t\bar{t}$ production. In the $2\ell 2\nu$ channel, background processes from diboson production (both WZ and WW), $t\bar{t}$ and single top production, and the production of Z bosons with associated jets constitute roughly half of the total background. Control regions (CRs) are defined to ensure control of the background modelling. In both channels, the background from the combination of vector-boson associated production to a top-quark pair ($t\bar{t} + V$, $V = W$ or Z) and triboson production (ZZZ , WZZ , or WWZ) is at the percent level. Distributions of discriminating variables are fitted simultaneously in all SRs to extract the off-shell contribution by measuring the signal strength $\mu_{\text{off-shell}}$, the off-shell production cross-section normalised to the SM prediction, with the CRs also included in the fit to constrain the normalisation of the main background processes. In the 4ℓ channel, an observable is constructed from the output of neural networks (NN) that are trained with

kinematic variables and matrix-element discriminants sensitive to the signal process (see Ref. [27]). The $2\ell 2\nu$ channel uses the transverse mass of the ZZ system,

$$m_T^{ZZ} = \sqrt{\left[\sqrt{m_Z^2 + (p_T^{\ell\ell})^2} + \sqrt{m_Z^2 + (E_T^{\text{miss}})^2} \right]^2 - |\vec{p}_T^{\ell\ell} + \vec{E}_T^{\text{miss}}|^2}, \quad (1)$$

where m_Z is the Z boson mass [30], $\vec{p}_T^{\ell\ell}$ and \vec{E}_T^{miss} are the transverse momentum vector of the lepton pair and the missing transverse momentum vector with magnitudes of $p_T^{\ell\ell}$ and E_T^{miss} , respectively. Finally, the constraint on Γ_H is derived by using both the measured $\mu_{\text{off-shell}}$ and the signal strength for on-shell Higgs boson contributions ($\mu_{\text{on-shell}}$) in the 4ℓ channel obtained from Ref. [31], relying on the equation (valid under the assumptions discussed above) $\mu_{\text{off-shell}}/\mu_{\text{on-shell}} = \Gamma_H/\Gamma_H^{\text{SM}}$. Similarly to the previous ATLAS paper [27], this search also reports the ratio of effective Higgs boson–gluon couplings (R_{gg}) and the ratio of Higgs boson and vector-boson couplings (R_{VV}) between the off-shell and on-shell regions, assuming that the Higgs boson total width takes its SM value.

2. ATLAS detector

ATLAS is a multipurpose detector with a forward–backward symmetric cylindrical geometry and a solid-angle¹ coverage of nearly 4π , described in detail in Ref. [32]. The inner tracking detector (ID), covering the region $|\eta| < 2.5$, consists of a silicon pixel detector, a silicon microstrip detector, and a transition-radiation tracker. The innermost layer of the pixel detector, the insertable B-layer [33], was installed between Run 1 and Run 2 of the LHC. The inner detector is surrounded by a thin superconducting solenoid providing a 2 T magnetic field, and by a finely segmented lead/liquid-argon (LAr) electromagnetic calorimeter covering the region $|\eta| < 3.2$. A steel/scintillator-tile hadron calorimeter provides coverage in the central region $|\eta| < 1.7$. The endcap and forward regions, covering the pseudorapidity range $1.5 < |\eta| < 4.9$, are instrumented with LAr electromagnetic and hadron calorimeters, with steel, copper, or tungsten as the absorber material. A muon spectrometer (MS) system incorporating large superconducting toroidal air-core magnets surrounds the calorimeters. Three layers of precision wire chambers provide muon tracking in the range of $|\eta| < 2.7$, while dedicated fast chambers are used for triggering in the region $|\eta| < 2.4$. The trigger system, composed of two stages, was upgraded [34] before Run 2. The first stage, implemented with custom hardware, uses information from the calorimeters and muon chambers to select events from the 40 MHz bunch crossings at a maximum rate of 100 kHz. The second stage, called the high-level trigger (HLT), reduces the data acquisition rate to about 1 kHz on average. The HLT is software-based and runs reconstruction algorithms similar to those used in offline reconstruction. An extensive software suite [35] is used in data simulation, in reconstruction and analysis of real and simulated data, in detector operations, and in the trigger and data acquisition systems of the experiment.

¹ The ATLAS experiment uses a right-handed coordinate system with its origin at the nominal interaction point (IP) in the centre of the detector and the z -axis along the beam pipe. The x -axis points from the IP to the centre of the LHC ring, and the y -axis points upward. Cylindrical coordinates (r, ϕ) are used in the transverse plane, ϕ being the azimuthal angle around the z -axis. The pseudorapidity is defined in terms of the polar angle θ as $\eta = -\ln \tan(\theta/2)$.

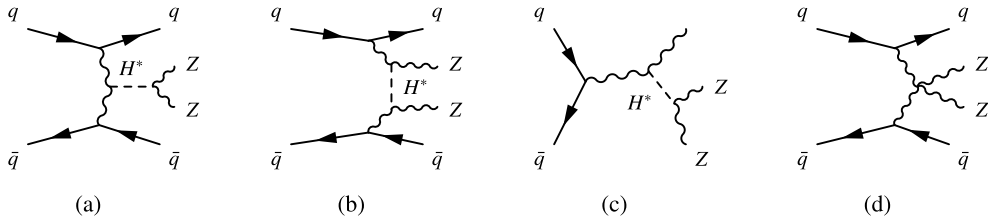


Fig. 2. The leading-order Feynman diagrams for (a) the s -channel vector-boson fusion signal, (b) the t -channel vector-boson fusion signal, (c) the vector-boson associated production signal, and (d) the vector-boson scattering background.

3. Data and Monte Carlo simulation

The proton–proton (pp) collision data used in this search were collected from 2015 to 2018, corresponding to an integrated luminosity of 139 fb^{-1} . Events in the 4ℓ final state were recorded with a combination of single-lepton, dilepton and trilepton triggers, while the $2\ell 2\nu$ events were collected via multiple single-lepton triggers. The overall trigger efficiency for the off-shell signal process is more than 98% in each final state after the application of the SR selections defined below.

Monte Carlo (MC) simulation is used to predict the normalisation and event kinematics of the signal process and some of the backgrounds. Event samples for each process were first produced by a corresponding event generator and then passed through detector simulation [36] within the GEANT4 framework [37]. Additional inelastic pp interactions (pile-up) modelled with PYTHIA8.186 [38] were overlaid on the simulated events to mimic the real collision events, and further corrections were applied to the simulated samples to match the pile-up conditions in the data. The lepton and jet momentum scale and resolution, and the lepton reconstruction, identification, isolation and trigger efficiencies in the simulation were corrected to match those measured in data.

Separate simulated samples were generated for each of the off-shell signal from ggF production, the $gg \rightarrow ZZ$ background, and the inclusive production $gg \rightarrow (H^* \rightarrow) ZZ$, which also includes the interference between the two. These loop-induced processes were modelled by SHERPA v2.2.2 [39] with OPENLOOPS [40–42] at leading-order (LO) accuracy in quantum chromodynamics (QCD), with up to one additional parton in the final state, using the NNPDF3.0 parton distribution function (PDF) set [43]. Signal and background were simulated separately from the inclusive process for NN training and template fitting. The merging with the parton shower was performed using the MEPS@NLO prescription [44] and the SHERPA built-in algorithm was used for parton showering and hadronisation. The samples are corrected to next-to-leading order (NLO) in QCD using corrections calculated separately as a function of the invariant mass of the ZZ system (m_{ZZ}) [45,46] for the signal, background, and inclusive processes. These corrections are similar for each process and range from 1.5 to 2. The total normalisation of all three processes was then corrected to next-to-next-to-next-to-leading order (N3LO) in QCD using a constant correction of 1.32, derived for the off-shell signal [47,48]. The use of the same correction for all processes is justified as the N3LO corrections are expected to be very similar for signal, background, and interference [49,50].

EW production of ZZ and two jets, also denoted by $q\bar{q} \rightarrow (H^* \rightarrow) ZZ + 2j$, contains inclusively the off-shell signal from VBF production, VH production, the non-Higgs boson EW $ZZjj$ process, and their interferences. Those processes were modelled by MADGRAPH5_AMC@NLO [51] at LO QCD accuracy using the NNPDF3.0 NLO PDF set [52]. PYTHIA8.244 [38] was used for parton showering and hadronisation with the A14 set of tuned parameters (tune) for the underlying event [53]. The t -channel exchange of the Higgs boson is treated as a contribution to the VBF signal process.

The ggF- and VBF-induced contributions can be straightforwardly parameterised as a function of $\mu_{\text{off-shell}}$, where the off-shell signal and the interference depend on $\mu_{\text{off-shell}}$ and $\sqrt{\mu_{\text{off-shell}}}$, respectively. More details of this parameterisation are given in Section 8.

The $q\bar{q} \rightarrow ZZ$ background was simulated by SHERPA v2.2.2 with OPENLOOPS using the NNPDF3.0 NNLO PDF set. The matrix elements were calculated to NLO accuracy in QCD for 0- and 1-jet final states, and to LO accuracy for 2- and 3-jet final states. The merging with the SHERPA parton shower was performed using the MEPS@NLO prescription [54]. NLO EW corrections calculated on top of the LO QCD prediction were applied as a function of m_{ZZ} for the 4ℓ final state [55,56], while the m_{ZZ} -based corrections for the $2\ell 2\nu$ channel were averaged from the additive (NLO EW + NLO QCD) and multiplicative (NLO EW \times NLO QCD) approaches following Ref. [57]. A cross-check was performed in the 4ℓ channel, and the results of the two approaches were found to agree within their uncertainties, while the uncertainties of both approaches (described in detail below) were also found to be similar.

The WZ diboson events from both QCD and EW production, with the subsequent leptonic decays of both the W and Z bosons, were simulated using SHERPA with a similar set-up to that of the $q\bar{q} \rightarrow ZZ$ background. The WZ events with the Z boson decaying leptonically and the W boson decaying hadronically were modelled with SHERPA v2.2.1. For the $2\ell 2\nu$ final state, the contribution from WW production was removed in the SHERPA simulation of the $q\bar{q} \rightarrow ZZ$ and $gg \rightarrow ZZ$ processes by requiring the charged leptons and the neutrinos to have different lepton flavours (the prediction was then scaled up by 1.5 to compensate). The $q\bar{q} \rightarrow WW$ and $gg \rightarrow WW$ processes were then modelled with POWHEG Box v2 [58] and SHERPA v2.2.2, respectively. The interference between WW and ZZ production in the $2\ell 2\nu$ final state is expected to be negligible in the phase space of the analysis [57] and was therefore not considered.

The $Z+jets$ background was simulated using the SHERPA v2.2.1 event generator, where the matrix elements were calculated for up to two partons at NLO and four partons at LO. The $Z+jets$ events were normalised using the NNLO cross-sections [59]. The $t\bar{t}$ background, as well as single-top (including s -channel, t -channel, and the dominant Wt component) production, were modelled using Powheg Box v2 interfaced to PYTHIA8.230 with the A14 tune. The total cross-sections for $t\bar{t}$ production and single-top production were normalised to the predictions at NNLO and NLO accuracy in QCD [60–62], respectively.

The triboson backgrounds ZZZ , WZZ , and WWZ with fully leptonic decays were modelled with SHERPA v2.2.2 at NLO QCD accuracy. The $ZZZ \rightarrow 4\ell + 2j$ process is included in the $q\bar{q} \rightarrow (H^* \rightarrow) ZZ + 2j$ sample described above. The simulation of $t\bar{t} + V$ production ($V = W$ or Z) with at least one of the top quark decaying leptonically and the vector boson decaying inclusively was performed with MADGRAPH5_AMC@NLO interfaced to PYTHIA8.210 for parton showering and hadronisation with the A14 tune. The total cross-sections for the $t\bar{t} + V$ backgrounds were normalised to the NLO QCD and EW predictions from Ref. [63].

4. Reconstruction of physics objects

To describe the event signature and obtain a good signal-to-background ratio, this search relies on the successful reconstruction of collision vertices, electrons, muons, jets, \vec{E}_T^{miss} , as well as identification of jets containing b -hadrons (b -jets). The reconstruction is identical to that in Ref. [64], and briefly summarised as follows.

Events are first required to have a collision vertex associated with at least two tracks each with transverse momentum $p_T > 0.5$ GeV. The vertex with the highest sum of p_T^2 of the associated tracks is referred to as the primary vertex.

Muons are primarily identified by tracks or segments (tracks using the hits of a single MS station) reconstructed in the MS and matched to tracks reconstructed in the ID, with exceptions in areas where the MS lacks coverage. In the region $2.5 < |\eta| < 2.7$, muons can also be identified by tracks from the muon spectrometer alone (standalone muons). In the gap region ($|\eta| < 0.1$) of the MS, muons can be identified by a track from the ID associated with a compatible calorimeter energy deposit (calorimeter-tagged muons). Candidate muons are required to have $p_T > 5$ GeV and $|\eta| < 2.7$, with the exception of calorimeter-tagged muons for which the p_T threshold is raised to 15 GeV. Muons must satisfy the ‘loose’ identification criterion [65] in the 4ℓ channel with at most one standalone or calorimeter-tagged muon allowed per Higgs boson candidate. In the $2\ell 2\nu$ channel muons are selected with $|\eta| < 2.5$ and must satisfy the ‘medium’ identification criterion. Electrons are reconstructed from energy deposits in the electromagnetic calorimeter matched to a track in the ID. Candidate electrons must have $p_T > 7$ GeV and $|\eta| < 2.47$, and satisfy the ‘loose’ and ‘medium’ identification criteria [66] in the 4ℓ and $2\ell 2\nu$ channels, respectively. All electrons and muons used in both channels must be isolated and satisfy the ‘FixedCutPFlowLoose’ isolation criteria [65,66]. Furthermore, electrons (muons) are required to have associated tracks satisfying $|d_0/\sigma_{d_0}| < 5$ (3) and $|z_0 \times \sin\theta| < 0.5$ mm, where d_0 is the transverse impact parameter relative to the beam line, σ_{d_0} is its uncertainty, and z_0 is the z coordinate of the r- ϕ impact point, defined relative to the primary vertex. The event is rejected if the minimum angular separation between two leptons is $\Delta R_{\ell\ell} < 0.1$, where $\Delta R_{\ell\ell} = \sqrt{(\Delta\phi_{\ell\ell})^2 + (\Delta\eta_{\ell\ell})^2}$.

Jets are reconstructed from particle-flow objects [67] using the anti- k_t algorithm [68,69] with radius parameter $R = 0.4$. The jet-energy scale is calibrated using simulation and further corrected with in situ methods [70]. Candidate jets are required to have $p_T > 30$ GeV and $|\eta| < 4.5$. A jet-vertex tagger [71] is applied to jets with $p_T < 60$ GeV and $|\eta| < 2.4$ to suppress jets that originate from pile-up. To mitigate the impact of pile-up jets in the forward region, another tagger, based on jet shapes and topological jet correlations [72], is used to suppress jets originating from the pile-up with $p_T < 50$ GeV and $2.5 < |\eta| < 4.5$. In addition, b -jets are identified using a multivariate b -tagging algorithm [73] and events containing them are rejected. The chosen b -tagging algorithm has an efficiency of 85% for b -jets and a rejection factor of 33 against light-flavour jets, measured in $t\bar{t}$ events [74].

The presence of neutrinos is identified using the missing transverse momentum vector \vec{E}_T^{miss} , which is computed as the opposite of the vector sum of transverse momenta of all the leptons and jets, as well as the tracks originating from the primary vertex but not associated with any of the leptons or jets [75]. Missing transverse momentum may also arise from the mismeasurement of the momentum of particles or jets. To avoid accepting events due to the presence of this kind of fake \vec{E}_T^{miss} , the statistical significance of the E_T^{miss} , $S(E_T^{\text{miss}})$, is used. $S(E_T^{\text{miss}})$ is calculated from the resolution information of the physics objects used in the E_T^{miss} reconstruction [76].

5. $ZZ \rightarrow 4\ell$ analysis

The selection of candidate events used in the signal and control regions of the 4ℓ channel closely follows that described in Ref [64]. The four-lepton invariant mass is required to be above the on-shell ZZ production threshold, $m_{4\ell} > 180$ GeV. Candidate 4ℓ quadruplets are formed by selecting two opposite-sign, same-flavour dilepton pairs in each event. In the $4e$ and 4μ channels, in which there are two possible pairings, the one that includes the lepton pair with mass closest to the Z boson mass is chosen. The p_T thresholds for the three leading leptons are 20, 15 and 10 GeV, respectively. In each quadruplet, the lepton pair with mass closest to the Z boson mass, m_{12} , is referred to as the leading pair and required to have $50 < m_{12} < 106$ GeV. The sub-leading pair, m_{34} , must satisfy $50 < m_{34} < 115$ GeV when $m_{4\ell} > 190$ GeV. Due to the increased probability of one off-shell Z boson at lower values of $m_{4\ell}$, the lower threshold for m_{34} decreases linearly to 45 GeV for $180 < m_{4\ell} < 190$ GeV.

Three SRs are designed to provide sensitivity to both the EW and ggF production modes. The SRs are defined such that $m_{4\ell}$ is well above the Higgs boson mass, including only events with $m_{4\ell} > 220$ GeV. Events in the range $180 < m_{4\ell} < 220$ GeV are expected to have the lowest signal-to-background ratio in the $m_{4\ell}$ range of the analysis and so are reserved for the control regions defined below. Events containing two or more jets with p_T greater than 30 GeV, where the two leading jets are well separated in η , $|\Delta\eta_{jj}| > 4$, are classified into the EW SR. Events falling outside the EW SR but featuring exactly one jet in the forward direction ($|\eta_j| > 2.2$) are assigned to a mixed SR. All the remaining events are then assigned to the ggF SR.

The main background in the 4ℓ channel is the $q\bar{q} \rightarrow ZZ$ process. The overall normalisation of this background is constrained by data in three different CRs defined with $180 < m_{4\ell} < 220$ GeV and with zero, one, or ≥ 2 jets. The signal contamination in these CRs is below 2%. The kinematic distributions are modelled with simulation, described in Section 3. Events in the zero- and one-jet CRs are binned in four and two intervals of equal width in $m_{4\ell}$, respectively, to provide further information about event kinematics. The interfering background processes $gg \rightarrow ZZ$ and EW $q\bar{q} \rightarrow ZZ$, as well as the small backgrounds from triboson production and $t\bar{t}Z$, are estimated from simulation. The contribution of the reducible backgrounds where hadrons or their decay products are mis-reconstructed as prompt leptons, such as $Z+jets$, WZ and $t\bar{t}$ processes, are estimated by using data-driven methods described in Ref. [64] and found to be negligible.

To maximise the signal sensitivity, a multi-class dense NN is employed in the SRs to enhance events with a Higgs boson candidate. The NN, implemented using Keras [77] with TensorFlow [78] as the backend, is designed to differentiate among the three event classes: the off-shell Higgs boson signal (S), the interfering background (B), and the non-interfering (NI) background. The interfering backgrounds to the ggF and EW signals are the $gg \rightarrow ZZ$ and EW $q\bar{q} \rightarrow ZZ + 2j$ processes, respectively. The non-interfering background is the $q\bar{q} \rightarrow ZZ$ process in both production modes.

The outputs of the NN use a normalised exponential function so that they can be interpreted as probabilities of an event belonging to a particular class (P_S , P_B and P_{NI}) and their ratio is used to define the final observable:

$$O_{\text{NN}} = \log_{10} \left(\frac{P_S}{P_B + P_{NI}} \right).$$

As the analysis attempts to constrain both the ggF- and EW-induced off-shell signals independently, two separate NNs are trained, one in the ggF SR and the other in the EW SR. The observable from the first NN ($O_{\text{NN}}^{\text{ggF}}$) is then used as the discriminating

variable in both the ggF and mixed SRs, while that of the second NN ($O_{\text{NN}}^{\text{EW}}$) is used in the EW SR.

The first NN is trained to discriminate among the ggF-induced signal, the $gg \rightarrow ZZ$ background, and the $q\bar{q} \rightarrow ZZ$ process. The features used by this NN include the kinematic information of the four leptons from MC simulation and also the square of the modulus of the values of the LO matrix element (ME) for the four leptons. The LO MEs are calculated for the gluon-induced signal and background processes and the $q\bar{q} \rightarrow ZZ$ process from the final-state variables in the Higgs boson rest frame using the MCFM program [8,27]. The kinematic variables are the leading Z boson production angle and four decay angles defined in Ref [79], and the three invariant masses $m_{4\ell}$, m_{12} and m_{34} . These are used as inputs to the ME calculation, and, along with the transverse momentum of the four-lepton system, as inputs to the NN as well.

The second NN is used to separate the EW-induced off-shell signal process from the non-Higgs boson EW $q\bar{q} \rightarrow ZZjj$ background and the QCD-induced $q\bar{q} \rightarrow ZZjj$ process. In addition to the variables used in the first NN, with matrix elements calculated specifically for the final state with two jets, several supplementary variables are included to exploit the kinematics of the dijet system: the invariant mass and azimuthal separation of the two leading jets, and the two Zeppenfeld angular variables, calculated for each Z boson as $\eta_{\text{Zep}} = \eta_{Z_1} - (\eta_{j_1} + \eta_{j_2})/2$ [80].

The two networks have 7 and 9 hidden layers respectively, with [90, 80, 80, 75, 75, 40, 40] and [60, 65, 70, 85, 90, 80, 75, 50, 30] neurons. The sparse categorical cross-entropy loss was used to optimise the network structure as well as the learning rate of the Adam optimiser. Input features were chosen to fully describe the event kinematics. The networks were trained on samples of the signal and the interfering and non-interfering backgrounds.

Fig. 3 shows the distributions of the observed and expected NN-based observables in all three signal regions. The data is shown after the simultaneous fit described in Section 8, except that the fit is carried out only in the 4ℓ channel and the value of $\mu_{\text{off-shell}}$ is set equal to one. All systematic uncertainties, which are described in Section 7, are included.

6. $ZZ \rightarrow 2\ell 2\nu$ analysis

The $2\ell 2\nu$ final state consists of a pair of isolated leptons (e or μ) and large $E_{\text{T}}^{\text{miss}}$. It has a larger branching fraction than the 4ℓ channel, but is subject to larger background contamination. Candidate events are preselected by requiring exactly two electrons or muons with opposite charges and $p_{\text{T}} > 20$ GeV. The leading lepton must have $p_{\text{T}} > 30$ GeV to surpass the trigger thresholds. To suppress the WZ background, events containing any additional lepton satisfying the loose identification criteria with $p_{\text{T}} > 7$ GeV are rejected. Requiring the dilepton invariant mass ($m_{\ell\ell}$) to be between 76 and 106 GeV largely reduces the contamination from the non-resonant- $\ell\ell$ background, originating from $t\bar{t}$, single-top (dominated by the Wt process), and $q\bar{q} \rightarrow WW$ production. Events that satisfy this preselection are then further separated into the SRs and CRs. To suppress the remaining background dominated by the $Z + \text{jets}$ and non-resonant- $\ell\ell$ processes, further selections based on $E_{\text{T}}^{\text{miss}}$ and the topology of the candidate events are applied. Candidate events are required to have $E_{\text{T}}^{\text{miss}} > 120$ GeV and $S(E_{\text{T}}^{\text{miss}}) > 10$. The azimuthal-angle difference between the dilepton system and $\vec{E}_{\text{T}}^{\text{miss}}$, $\Delta\phi(\vec{p}_{\text{T}}^{\ell\ell}, \vec{E}_{\text{T}}^{\text{miss}})$, must be larger than 2.5 radians, and the selected leptons must be close to each other, with the distance $\Delta R_{\ell\ell}$ below 1.8. Furthermore, the azimuthal-angle difference between any of the selected jets with $p_{\text{T}} > 100$ GeV and $\vec{E}_{\text{T}}^{\text{miss}}$ must be larger than 0.4 radians to suppress events with poorly measured jet energies. Finally, events containing one or more b -jets are rejected to further suppress the

$t\bar{t}$ and Wt backgrounds. The selected events are then categorised into three SRs in the same way as for the 4ℓ channel.

The shape and normalisation of the main background contribution from $q\bar{q} \rightarrow ZZ$ production are estimated from simulation, while in the combined result the overall normalisation factors are constrained by the ZZ CRs defined in the 4ℓ channel as described in the previous section. As is shown later in Table 4, the measured normalisations generally agree fairly well with the simulated ones, so this is a safe approach for developing the analysis in this final state.

To estimate the background from WZ production, control regions enriched in WZ events, with a purity of over 90%, are defined using the full event selection given above, except that the presence of a third lepton with $p_{\text{T}} > 20$ GeV is required. Several further selections such as $S(E_{\text{T}}^{\text{miss}}) > 3$, a b -jet veto, and $m_{\text{T}}^W > 60$ GeV, where m_{T}^W is constructed from the third lepton's transverse momentum and the $\vec{E}_{\text{T}}^{\text{miss}}$ vector², are applied to suppress non- WZ contributions. Three separate WZ CRs are defined according to the number of jets (zero, one, and ≥ 2 jets), and the CRs are included in the statistical fit to separately constrain the normalisation of the WZ background in each N_{jets} bin. The shapes of the kinematic distributions are estimated from simulation.

To estimate the non-resonant- $\ell\ell$ background, arising from $qq \rightarrow WW$, $t\bar{t}$, and single-top production, a control region dominated by the non-resonant- $\ell\ell$ processes (with a purity of about 95%) is defined with all the event selection criteria except that the final state is required to contain an opposite-sign $e\mu$ pair. The non-resonant- $\ell\ell$ contribution with the ee ($\mu\mu$) pair is quite similar to that with the $e\mu$ pair, and the difference in lepton reconstruction is taken into account in the simulation. This CR is then used to constrain the total normalisation of the non-resonant- $\ell\ell$ background in all three SRs, and the kinematic shapes are modelled with simulation. The $Z + \text{jets}$ background contribution is estimated from simulation and constrained by a normalisation factor derived in a control region enriched in $Z + \text{jets}$ events. The control region is defined with all event selection criteria except that $S(E_{\text{T}}^{\text{miss}})$ is required to be less than 9, and no requirements on the azimuthal angle difference between jets with $p_{\text{T}} > 100$ GeV and $\vec{E}_{\text{T}}^{\text{miss}}$ are made. The resulting control region is about 73% pure. The kinematic distributions for the $Z + \text{jets}$ background are modelled with simulation. The CRs for the non-resonant- $\ell\ell$ and the $Z + \text{jets}$ backgrounds are not further divided to match the categorisation of SRs depending on jet multiplicity, due to insufficient events in the data. Finally, minor backgrounds from the VVV and $t\bar{t}V$ processes are estimated from simulation.

The distributions of the final observable m_T^{ZZ} in the $2\ell 2\nu$ channel, as defined in Eq. (1), are presented in Fig. 4. The data is shown after the simultaneous fit described in Section 8, except that the fit is carried out only in the $2\ell 2\nu$ channel and the value of $\mu_{\text{off-shell}}$ is set equal to one. All three SRs are shown together with the total systematic uncertainty from the sources described in Section 7.

7. Systematic uncertainties

The sources of systematic uncertainty impacting the analysis of both channels can be divided into two categories: uncertainties in the theoretical description of the signal and background processes and experimental uncertainties related to the detector response.

The largest source of systematic uncertainties arises from the theoretical modelling of the signal and background processes, including those related to the production of jets associated with the Higgs boson. Experimental uncertainties related to the reconstruc-

² $m_{\text{T}}^W \equiv \sqrt{2p_{\text{T}}^{\ell} E_{\text{T}}^{\text{miss}} [1 - \cos \Delta\phi(\vec{p}_{\text{T}}^{\ell}, \vec{E}_{\text{T}}^{\text{miss}})]}$.

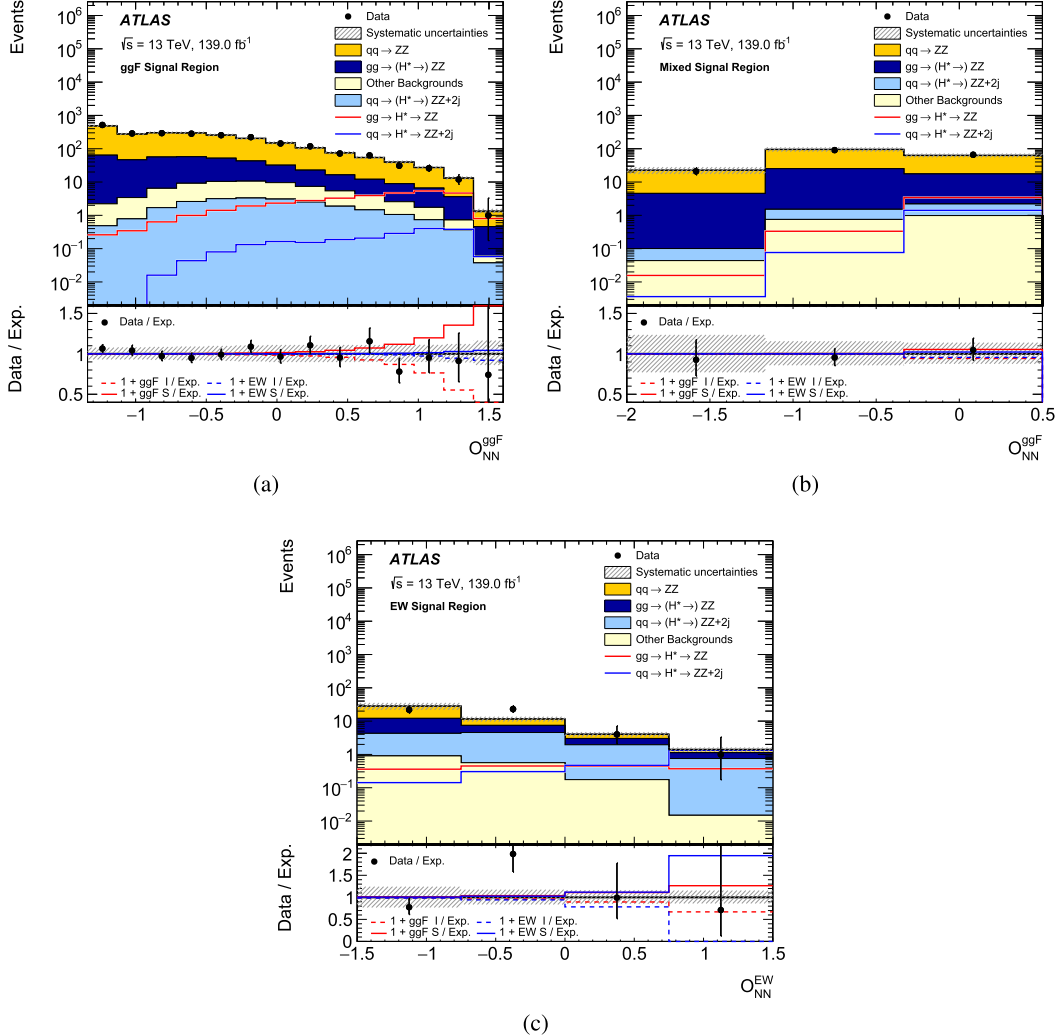


Fig. 3. The observed and expected Standard Model distributions in the 4ℓ channel for (a) O_{NN}^{ggF} in the ggF signal region, (b) O_{NN}^{ggF} in the mixed signal region, and (c) O_{NN}^{EW} in the EW signal region. The observed data are shown following the fit described in Section 8, except that the fit is carried out only in the 4ℓ channel and the off-shell Higgs boson signal is fixed to the SM expectation. The total systematic uncertainty, including all uncertainties described in Section 7, is shown as the hatched area including correlations between uncertainties. The expectation includes the inclusive (signal plus background plus interference) $gg \rightarrow (H^* \rightarrow ZZ)$ (dark blue) and $q\bar{q} \rightarrow (H^* \rightarrow ZZ + 2j)$ (light blue) processes, as well as the backgrounds from QCD $q\bar{q} \rightarrow ZZ$ production (orange) and other processes (Z-jets, $t\bar{t}$, triboson and $t\bar{t}V$) (yellow). The expected $gg \rightarrow H^* \rightarrow ZZ$ and EW $q\bar{q} \rightarrow H^* \rightarrow ZZ + 2j$ signals are also shown as red and blue lines. The first and last bins include the underflow and overflow, respectively. The lower panel of each plot shows the ratio of data to expectation (black points) and the total systematic uncertainty (hatched area), as well as the ratio of the signal (solid lines) and the interference (dashed lines) to the expectation for ggF (red) and EW (blue) production. (For ease of display, for the last four curves one plus the ratio is plotted.)

tion of jets are also prominent while other experimental uncertainties are generally small. To help understand the impact of the leading uncertainties, their relative size before the statistical fit for a specific process is provided in this section, with the largest uncertainties for the main processes in the signal and control regions summarised in Table 1. The impact of these uncertainties on the observed upper limits of $\mu_{\text{off-shell}}$ is given in Section 8.

The theoretical uncertainties arise from the choice of PDF, from the missing higher-order corrections in both QCD and EW perturbative calculations, and from the modelling of the parton shower.

The PDF uncertainties are evaluated using the NNPDF prescription with MC replicas. The PDF covariance matrix between each channel of the analysis is estimated from the 100 replicas from the NNPDF3.0 NNLO set. Only the principal component of the covariance matrix has a non-negligible impact on the yields and it is used as a representation of the PDF uncertainty including its bin-by-bin correlations. The uncertainties due to missing higher-order QCD corrections are estimated by varying the renormalisation and factorisation scales independently, ranging from a factor of one-half to two (excluding the cases in which one scale

is varied down by one-half and the other up by two). For the $q\bar{q} \rightarrow ZZ$ background, the uncertainty is evaluated independently in bins of N_{jets} . For the gluon-induced processes, including the signal, the $gg \rightarrow ZZ$ background, and their interference, the missing higher-order uncertainties are evaluated by their impact on the respective NLO K -factors [81]. The uncertainties are increased in the kinematic regions of the SRs where the K -factor calculations are less precise due to missing effects from on-shell top quarks and high- p_T jets [27]: the uncertainty is doubled in the phase space containing a jet with $p_T > 150$ GeV and increased by 50% for m_{ZZ} around twice the top-quark mass. In both the 4ℓ and $2\ell 2\nu$ channels, the uncertainty from missing higher order corrections in the $q\bar{q} \rightarrow ZZ$ background is one of the largest uncertainties, ranging from a few percent up to 40% depending on jet multiplicity and observable bin. In both channels, the same uncertainty in the gluon-gluon processes ranges from 10% to 20%.

The uncertainties due to missing higher-order EW corrections (HOEW) are considered for the main $q\bar{q} \rightarrow ZZ$ background and handled differently in the two channels. For the $2\ell 2\nu$ channel, the difference in the NLO EW correction between the multiplicative

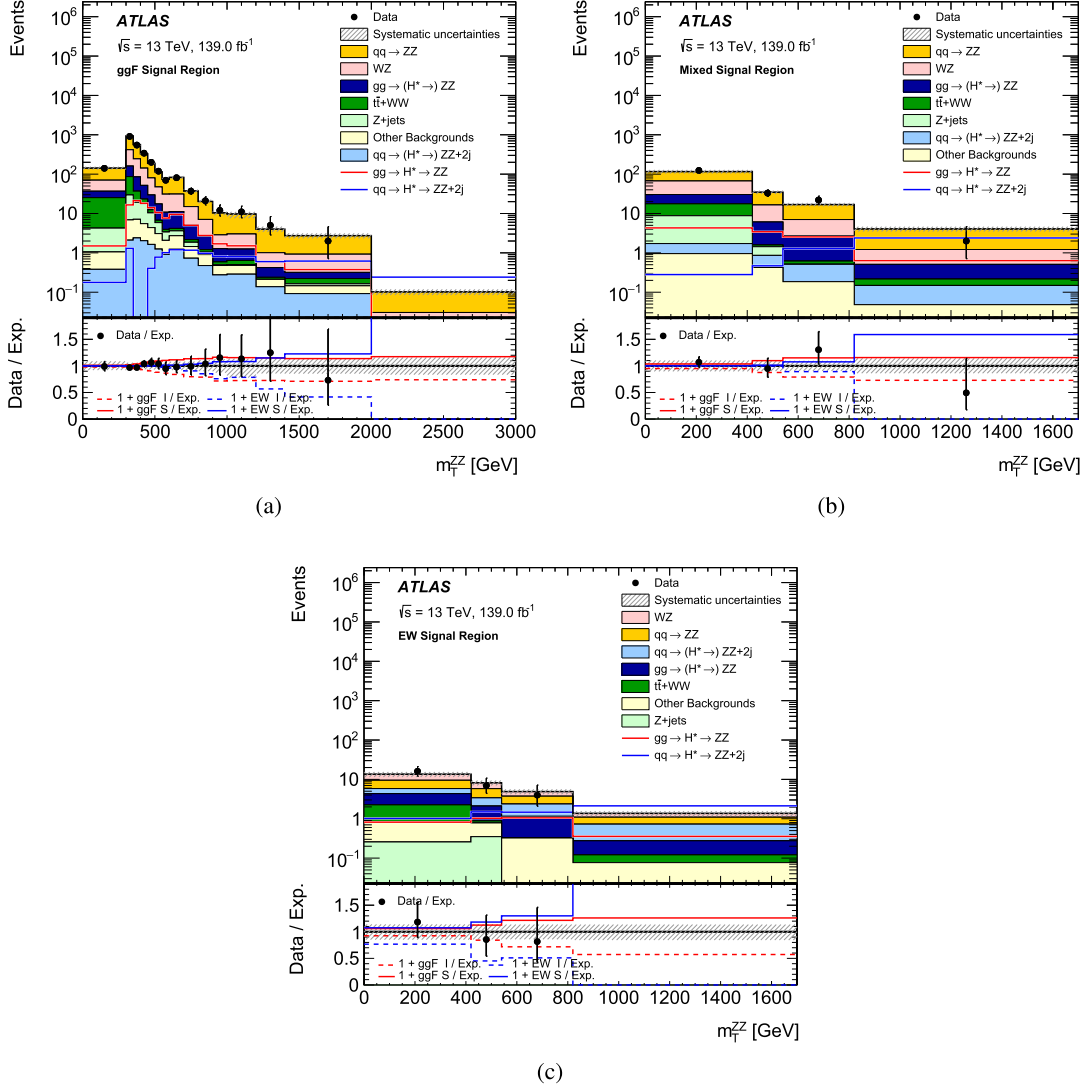


Fig. 4. The observed and expected Standard Model m_T^{ZZ} distributions in the $2\ell 2\nu$ channel for (a) the ggF SR, (b) the mixed SR, and (c) the EW SR. The data are shown after the simultaneous fit described in Section 8, except that the fit is carried out only in the $2\ell 2\nu$ channel and the off-shell Higgs boson signal is fixed to the SM expectation. The hatched area shows the total systematic uncertainty after the fit, comprising all uncertainties described in Section 7 and including correlations between uncertainties. The expectation includes the inclusive (signal plus background plus interference) $gg \rightarrow (H^* \rightarrow) ZZ$ (dark blue) and EW $q\bar{q} \rightarrow (H^* \rightarrow) ZZ + 2j$ (light blue) production, as well as the backgrounds from QCD $q\bar{q} \rightarrow ZZ$ production (orange), WZ (pink), non-resonant $\ell\ell$ (dark green), $Z+jets$ (light green), and other (triboson and $t\bar{t}V$) (yellow) processes. The expected $gg \rightarrow H^* \rightarrow ZZ$ and $q\bar{q} \rightarrow H^* \rightarrow ZZ + 2j$ signals are also shown as red and blue lines. The last bins include the overflow. The lower panels show the ratio of data to expectation (black points) and the total systematic uncertainty (hatched area), as well as the ratio of the signal (solid lines) and the interference (dashed lines) to the expectation for ggF (red) and EW (blue) production. (For ease of display, for the last four curves one plus the ratio is plotted.)

and additive methods as a function of m_{ZZ} is assigned as the uncertainty [57]. This uncertainty ranges from 1% to at most 20% of the cross-section depending on the bins of observables. For the 4ℓ channel, the NLO EW corrections are calculated on top of the LO QCD cross-section. Therefore, a specific prescription [82], also applied in Ref. [27], is used to derive the uncertainty to account for missing NLO QCD+EW diagrams. A study of the compatibility between the two methods in the 4ℓ channel shows that the central values agree to within a few percent while the uncertainties have a similar size.

The uncertainties due to the modelling of the parton shower and hadronisation play an important role in this search, as jet multiplicity, a key variable used to define both the SRs and the CRs, is particularly sensitive to the modelling of matrix elements, parton showering, and the merging and matching between the two. The parton shower (PS) uncertainties are evaluated by varying resummation and matching scales for the processes simulated with the SHERPA generator. These variations for SHERPA samples are ex-

pected to further account for the shape uncertainties relating to missing high-order QCD effects beyond those from the usual QCD scale variations, i.e. migrations between jet bins. For those processes simulated with the PYTHIA shower program, the uncertainty is assessed by varying the PYTHIA configurations, such as the parameter values of the A14 tune, the multi-parton models and the final-state radiation models. For ggF production, the PS uncertainties are correlated between the signal and background processes. The uncertainties are split into shape and normalisation components, with the latter being more significant.

In the $2\ell 2\nu$ channel, the systematic uncertainties arising from the PS are parameterised using only the ZZ transverse momentum. In this channel, the PS uncertainty in the ggF processes is quite important: it is about 25% in the yields and ranges from a few percent to a maximum of 15% in the observable shapes. For the EW processes, this uncertainty reaches 15% in the yields and a few percent in the shapes. The PS uncertainties for the $q\bar{q} \rightarrow ZZ$ background are at percentage level for the bulk of ob-

Table 1

The dominant uncertainties in the leading processes in the signal and background regions. Uncertainties may depend on the value of the observable: if so, a range is given in the table. Detailed descriptions of the uncertainties are given in the text.

Process	Uncertainty	Final State	Value (%)
ggF Signal Region			
$q\bar{q} \rightarrow ZZ$	QCD Scale	$2\ell 2\nu$	4–40
$q\bar{q} \rightarrow ZZ$	QCD Scale	4ℓ	21–28
$q\bar{q} \rightarrow ZZ$	HOEW	4ℓ	1–7
$q\bar{q} \rightarrow ZZ$	HOEW	$2\ell 2\nu$	2–20
$q\bar{q} \rightarrow ZZ$	Parton Shower	$2\ell 2\nu$	1–67
$q\bar{q} \rightarrow ZZ + 2j$	Parton Shower	$2\ell 2\nu$	1–33
$q\bar{q} \rightarrow ZZ + 2j$	Parton Shower	4ℓ	2–10
$gg \rightarrow H^* \rightarrow ZZ$	Parton Shower	4ℓ	27
$gg \rightarrow H^* \rightarrow ZZ$	Parton Shower	$2\ell 2\nu$	8–45
$gg \rightarrow ZZ$	Parton Shower	4ℓ	38
$gg \rightarrow ZZ$	Parton Shower	$2\ell 2\nu$	6–43
$WZ + 0j$	QCD Scale	$2\ell 2\nu$	1–54
1-jet Signal Region			
$gg \rightarrow H^* \rightarrow ZZ$	Parton Shower	4ℓ	27
$gg \rightarrow H^* \rightarrow ZZ$	QCD Scale	$2\ell 2\nu$	13–18
$gg \rightarrow ZZ$	Parton Shower	4ℓ	38
$gg \rightarrow ZZ$	QCD Scale	$2\ell 2\nu$	18–20
$q\bar{q} \rightarrow ZZ + 2j$	QCD Scale	$2\ell 2\nu$	7–18
$q\bar{q} \rightarrow ZZ + 2j$	QCD Scale	4ℓ	3–10
2-jet Signal Region			
$q\bar{q} \rightarrow ZZ$	QCD Scale	4ℓ	18–26
$q\bar{q} \rightarrow ZZ$	QCD Scale	$2\ell 2\nu$	8–32
$gg \rightarrow H^* \rightarrow ZZ$	Parton Shower	4ℓ	27
$gg \rightarrow H^* \rightarrow ZZ$	QCD Scale	$2\ell 2\nu$	14–18
$gg \rightarrow ZZ$	Parton Shower	4ℓ	38
$gg \rightarrow ZZ$	QCD Scale	$2\ell 2\nu$	18–20
$WZ + 2j$	QCD Scale	$2\ell 2\nu$	20–22
$q\bar{q} \rightarrow ZZ + 2j$	QCD Scale	4ℓ	8–14
$q\bar{q} \rightarrow ZZ + 2j$	QCD Scale	$2\ell 2\nu$	8–16
$qq \rightarrow ZZ$ Control Regions			
$q\bar{q} \rightarrow ZZ$	QCD Scale	4ℓ	26
Three-lepton Control Regions			
$WZ + 2j$	QCD Scale	$2\ell 2\nu$	28

servable bins but can reach up to 30% in some parts of the phase space.

In the 4ℓ channel, these uncertainties are parameterised using the 4ℓ invariant mass, transverse momentum, and the kinematics of the leading jets. NNs are trained to estimate the density ratio between the nominal and the varied samples in this multi-dimensional space [83]. This novel method ensures a detailed description of the systematic uncertainty while reducing statistical fluctuations due to the interpolation provided by the differentiable NN. In the 4ℓ channel, PS uncertainties are the leading source of uncertainties for the gluon-gluon processes in the SRs, and are about 30% and 40% in the yields of the signal and the background. The impact of PS uncertainties in the shape of observables is found to be no more than 10% in the 4ℓ channel. The PS uncertainties for the EW processes are less significant, ranging from a few percent to 10%. The PS uncertainties for the QCD $q\bar{q} \rightarrow ZZ$ background are generally smaller, at percentage level for most observable bins.

Experimental systematic uncertainties are generally less important than the theoretical ones. However, uncertainties related to jet reconstruction are important in the $2\ell 2\nu$ channel as mismeasurement of the jet energy can mimic E_T^{miss} . The main jet uncertainties are those in the jet energy scale (JES) and resolution (JER), which can amount to about 10% for processes in the EW SRs. The effect of pile-up and the differences between the energy responses for jets with different hadron flavour compositions are particularly important. Uncertainties originating from the electron and muon reconstruction and selection, and from E_T^{miss} reconstruction are

less important. The uncertainty in the Run-2 luminosity measurement is 1.7% [84], obtained using the LUCID-2 detector [85] for the primary luminosity measurements.

8. Results and interpretations

The statistical model used to translate the results into constraints on the off-shell signal strength $\mu_{\text{off-shell}}$ is based on the profile likelihood technique [86]. A binned likelihood function is constructed as a product of Poisson probability terms over all bins in all the SRs and CRs considered in the analysis, as introduced in Sections 5 and 6. The likelihood depends on the parameters of interest and a set of nuisance parameters θ that include the effects of systematic uncertainties and statistical uncertainties from the limited number of simulated events. They are constrained using Gaussian and Poisson terms, respectively. Different parameters of interest are used depending on the interpretation. The first interpretation explores two signal strength parameters ($\mu_{\text{off-shell}}^{\text{ggF}} = \kappa_g^2 \cdot \kappa_V^2$, off-shell and $\mu_{\text{off-shell}}^{\text{EW}} = \kappa_V^4$, off-shell) corresponding to the ggF- and EW-induced off-shell contributions, respectively. Here, κ_g (κ_V) refers to the Higgs boson coupling to gluons (vector bosons) normalised to the SM prediction. In the second interpretation, a single off-shell signal-strength parameter ($\mu_{\text{off-shell}}$) is applied for all production modes, assuming that $\mu_{\text{off-shell}}^{\text{ggF}} = \mu_{\text{off-shell}}^{\text{EW}} = \mu_{\text{off-shell}}$.

Given the sizeable interference effects, the off-shell signal cannot be treated independently of the interfering backgrounds. The interference term, which is proportional to $\sqrt{\mu_{\text{off-shell}}}$, must be taken into account when building the probability model. The expected number of events from the $gg \rightarrow (H^* \rightarrow) ZZ$ process for a given $\mu_{\text{off-shell}}^{\text{ggF}}$, referred as v^{ggF} , can be obtained for a bin of the input distributions from the following parameterisation:

$$\begin{aligned} v^{\text{ggF}}(\mu_{\text{off-shell}}^{\text{ggF}}, \theta) \\ = \mu_{\text{off-shell}}^{\text{ggF}} \cdot n_S^{\text{ggF}}(\theta) \\ + \sqrt{\mu_{\text{off-shell}}^{\text{ggF}} \cdot (n_{S\text{BI}}^{\text{ggF}}(\theta) - n_S^{\text{ggF}}(\theta) - n_B^{\text{ggF}}(\theta)) + n_B^{\text{ggF}}(\theta)} \\ = (\mu_{\text{off-shell}}^{\text{ggF}} - \sqrt{\mu_{\text{off-shell}}^{\text{ggF}}}) \cdot n_S^{\text{ggF}}(\theta) \\ + \sqrt{\mu_{\text{off-shell}}^{\text{ggF}} \cdot n_{S\text{BI}}^{\text{ggF}}(\theta) + (1 - \sqrt{\mu_{\text{off-shell}}^{\text{ggF}}}) \cdot n_B^{\text{ggF}}(\theta)} \end{aligned}$$

where n_S^{ggF} , n_B^{ggF} and $n_{S\text{BI}}^{\text{ggF}}$ represent the corresponding expected yields of the signal, the $gg \rightarrow ZZ$ background and the full $gg \rightarrow (H^* \rightarrow) ZZ$ process, respectively. The expected number of events from the EW $q\bar{q} \rightarrow (H^* \rightarrow) ZZ + 2j$ process for a given $\mu_{\text{off-shell}}^{\text{EW}}$ can be modelled similarly, and the parameterisation is determined by using three simulation samples: that for the full process $q\bar{q} \rightarrow (H^* \rightarrow) ZZ + 2j$ with $\mu_{\text{off-shell}}^{\text{EW}}$ set to 1, that for the same process with $\mu_{\text{off-shell}}^{\text{EW}}$ set to 10, and the non-Higgs boson EW $q\bar{q} \rightarrow ZZ + 2j$ background³. The description in terms of a single signal component as performed for ggF production is not possible in the EW case because the requirement on high m_{ZZ} , used to ensure that the Higgs boson is off-shell, does not apply to the t -channel Higgs boson exchange in EW production, even though it is also off-shell (with $t < 0$). The parameterisation described here ensures that this component scales with $\mu_{\text{off-shell}}^{\text{EW}}$.

The total normalisation of the $q\bar{q} \rightarrow ZZ$ background is left as a free parameter in the profile likelihood fit, separately for each jet multiplicity. Three parameters are introduced in the likelihood

³ The values of $\mu_{\text{off-shell}}^{\text{EW}} = 0, 1$, and 10 are chosen for technical reasons involving the production of simulated samples but in principle any three numbers could be used.

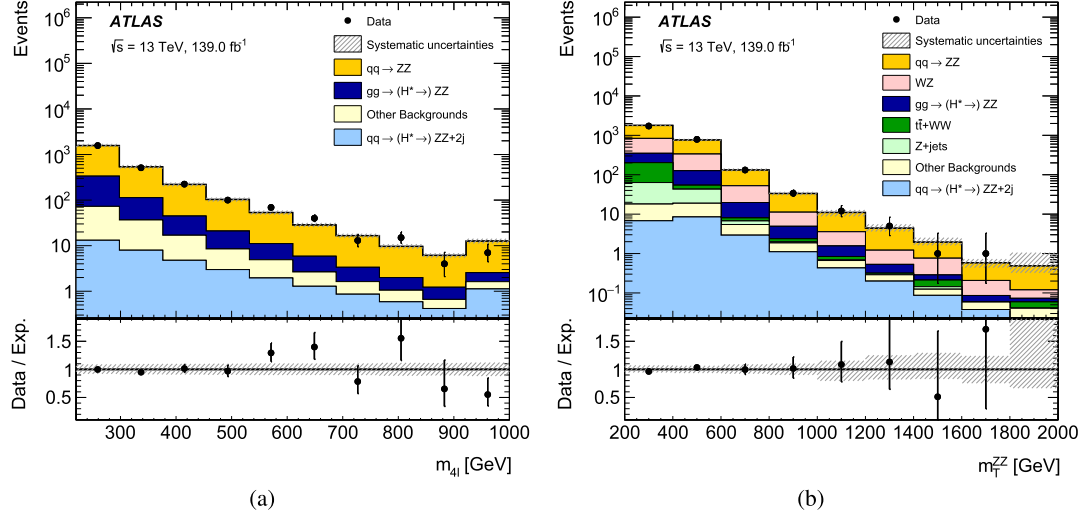


Fig. 5. Comparisons between data and the SM prediction for the (a) $m_{4\ell}$ and (b) m_T^{ZZ} distributions in the inclusive off-shell signal regions in the $ZZ \rightarrow 4\ell$ and $ZZ \rightarrow 2\ell 2\nu$ channels, respectively. The scenario with the off-shell signal strength equal to one is considered in the fit. The hatched area represents the total systematic uncertainty. The last bin in both figures contains the overflow.

model to constrain the normalisation of this dominant background in both final states, a normalisation factor for 0-jet events, μ_{qqZZ} , and two additional parameters to represent the relative contributions of higher jet multiplicities, μ_{qqZZ}^{1j} and μ_{qqZZ}^{2j} . The expected yield of 0-jet $q\bar{q} \rightarrow ZZ$ events is scaled by μ_{qqZZ} , that of 1-jet events by $\mu_{qqZZ} \cdot \mu_{qqZZ}^{1j}$, and that of events with at least two jets by $\mu_{qqZZ} \cdot \mu_{qqZZ}^{1j} \cdot \mu_{qqZZ}^{2j}$. These parameters are largely constrained by the three CRs defined in Section 5, especially at high jet multiplicity.

The normalisations of the WZ , $Z + \text{jets}$ and non-resonant- $\ell\ell$ backgrounds are also obtained from the simultaneous fit, using the dedicated control regions described in Section 6. Similarly to the $q\bar{q} \rightarrow ZZ$ background, events from the WZ process are treated separately for each jet multiplicity. Five additional free parameters, $\mu_{3\ell}$, $\mu_{3\ell}^{1j}$, $\mu_{3\ell}^{2j}$, μ_{Zj} , and $\mu_{e\mu}$, are therefore introduced in the likelihood model specifically for the $2\ell 2\nu$ channel and for its combination with the 4ℓ channel.

The likelihood function for the combination of both channels is built as a product of the likelihoods of the individual channels. Theoretical and experimental uncertainties with common sources are treated as correlated between the two channels. The NLO EW uncertainty is uncorrelated between the two channels, due to the different schemes used to derive the uncertainties. The hypothesis of systematic uncertainty correlation between the 4ℓ and $2\ell 2\nu$ channels is tested for the dominant sources of uncertainties, including the PS uncertainties that use models with different complexity in the two channels, and the NLO EW uncertainty. The difference in the result when using different correlation hypotheses is found to be negligible.

The $m_{4\ell}$ distribution for the 4ℓ channel and the m_T^{ZZ} distribution for the $2\ell 2\nu$ channel are shown in Fig. 5 after the full fit to data with $\mu_{\text{off-shell}} = 1$. The total systematic uncertainty from the sources described in Section 7 are shown in the figure. The distributions of the NN observables used in the 4ℓ channel are shown in Fig. 3.

The expected numbers of events in the SRs after the maximum-likelihood fit to the data performed in all SRs and CRs, together with the corresponding observed yields, are shown in Tables 2 and 3 for the $ZZ \rightarrow 4\ell$ and $ZZ \rightarrow 2\ell 2\nu$ channels, respectively. The fitted background normalisation factors together with their total uncertainties are summarised in Table 4.

Table 2

The observed and expected yields together with their uncertainties, for the ggF -and EW-enriched categories in the 4ℓ channel. The results are obtained after the simultaneous fit to both the 4ℓ and $2\ell 2\nu$ channels with $\mu_{\text{off-shell}} = 1$. The first row represents the inclusive ZZ process from gg production, including the signal, background, and interference components. The signal and background components are shown separately in rows 2–3: they do not add up to match the inclusive yield due to the presence of negative interference. The other backgrounds include contributions from $t\bar{t}V$ and VVV processes. The uncertainties in the expected number of events include the statistical and systematic uncertainties. The uncertainties in the $q\bar{q} \rightarrow ZZ$ background are quoted as the sum in quadrature of all three jet multiplicity contributions for purposes of illustration.

Process	ggF SR	Mixed SR	EW SR
$gg \rightarrow (H^* \rightarrow) ZZ$	341 ± 117	42.5 ± 14.9	11.8 ± 4.3
$gg \rightarrow H^* \rightarrow ZZ$	32.6 ± 9.07	3.68 ± 1.03	1.58 ± 0.47
$gg \rightarrow ZZ$	345 ± 119	43.0 ± 15.2	11.9 ± 4.4
$q\bar{q} \rightarrow (H^* \rightarrow) ZZ + 2j$	23.2 ± 1.0	2.03 ± 0.16	9.89 ± 0.96
$q\bar{q} \rightarrow ZZ$	1878 ± 151	135 ± 23	22.0 ± 8.3
Other backgrounds	50.6 ± 2.5	1.79 ± 0.16	1.65 ± 0.16
Total expected (SM)	2293 ± 209	181 ± 29	45.3 ± 10.0
Observed	2327	178	50

To obtain the results for a given parameter of interest, profile likelihood ratios (denoted by λ) are computed for different values of each parameter. The $-2\ln\lambda$ curve as a function of $\mu_{\text{off-shell}}$ is presented in Fig. 6(a). The expected curve is constructed from a fit to an Asimov dataset which is built from the SM expectation. The expected curve is flatter than the observed due to the effect of a downward fluctuation in the data and the parabolic shape of the yield versus μ curve, which arises due to the $\sqrt{\mu}$ dependence of the interference. In particular, for electroweak production, the expected yield is minimised at the value of $\mu = 0.8$, close to the value $\mu = 1$ at which the expected $-2\ln\lambda$ curve is minimised. In this case, a downward fluctuation in the data, observed for this production mode, does not appreciably move the minimum, because a lower yield cannot reduce the best-fit value of μ below 0.8. Instead, the lower yield makes values further from the minimum less likely, thus narrowing the profile likelihood.

Due to the quadratic parameterisation of the yield as a function of the parameter of interest, the distribution of the test statistic $-2\ln\lambda$ is slightly different from the asymptotic χ^2 distribution predicted by Wilks' theorem [87]. Therefore confidence intervals on $\mu_{\text{off-shell}}$ are built based on the Neyman construction [88] using the distribution of $-2\ln\lambda$ for different values of the parameter of

Table 3

The observed and expected yields together with their uncertainties, for the ggF- and EW-enriched categories in the $2\ell 2\nu$ channel. The results are obtained after the simultaneous fit to both the 4ℓ and $2\ell 2\nu$ channels with $\mu_{\text{off-shell}} = 1$. The first row represents the inclusive ZZ process from gg production, including the signal, background, and interference components. The signal and background components are shown separately in rows 2–3: they do not add up to match the inclusive yield due to the presence of negative interference. The other backgrounds include contributions from VVV , $W+jets$ and top quark processes other than pair production. The uncertainties in the expected number of events include the statistical and systematic uncertainties. The uncertainties in the $qq \rightarrow ZZ$ and WZ backgrounds are quoted as the sum in quadrature of all three jet multiplicity contributions for purposes of illustration.

Process	ggF SR	Mixed SR	EW SR
$gg \rightarrow (H^* \rightarrow) ZZ$	$210 + 53$	$19.7 + 4.9$	$4.29 + 1.10$
$gg \rightarrow H^* \rightarrow ZZ$	$111 + 26$	$10.9 + 2.5$	$3.26 + 0.82$
$gg \rightarrow ZZ$	$251 + 66$	$23.4 + 6.2$	$5.31 + 1.46$
$q\bar{q} \rightarrow (H^* \rightarrow) ZZ + 2j$	$14.0 + 3.0$	$1.63 + 0.17$	$4.46 + 0.50$
$q\bar{q} \rightarrow ZZ$	$1422 + 112$	$80.4 + 11.9$	$7.74 + 2.99$
WZ	$678 + 54$	$51.9 + 6.9$	$7.89 + 2.50$
$Z+jets$	$62.3 + 24.3$	$7.51 + 6.94$	$0.62 + 0.54$
Non-resonant- $\ell\ell$	$106 + 39$	$9.17 + 2.73$	$1.55 + 0.42$
Other backgrounds	$22.6 + 5.2$	$1.62 + 0.25$	$1.40 + 0.10$
Total expected (SM)	$2515 + 165$	$172 + 17$	$28.0 + 4.1$
Observed	2496	181	27

Table 4

The fitted normalisation factors for the dominant $q\bar{q} \rightarrow ZZ$ background as well as the WZ , $Z+jets$ and non-resonant- $\ell\ell$ type backgrounds.

Normalisation factor	Fitted value
$\mu_{q\bar{q}ZZ}^{1j}$	1.11 ± 0.07
$\mu_{q\bar{q}ZZ}^{2j}$	0.90 ± 0.10
$\mu_{q\bar{q}ZZ}^{3j}$	0.88 ± 0.26
$\mu_{3\ell}^{1j}$	1.06 ± 0.03
$\mu_{3\ell}^{2j}$	0.92 ± 0.10
$\mu_{3\ell}^{3j}$	0.75 ± 0.19
μ_{Zj}	0.90 ± 0.19
$\mu_{e\mu}$	1.08 ± 0.09

Table 5

The impact of most important systematic uncertainties on the observed upper value of $\mu_{\text{off-shell}}$ for which $-2\ln\lambda = 4$, obtained by the combined fit. This value corresponds to the two standard deviation upper limit of $\mu_{\text{off-shell}}$ with the asymptotic method. The first column denotes the systematic uncertainty that was excluded from the fit. The last row gives the nominal upper limit, where all uncertainties are included. The further the upper limit is deviating from the last row value, the more important that uncertainty is.

Systematic Uncertainty Fixed	$\mu_{\text{off-shell}}$ value at which $-2\ln\lambda(\mu_{\text{off-shell}}) = 4$
Parton shower uncertainty for $gg \rightarrow ZZ$ (normalisation)	2.26
Parton shower uncertainty for $gg \rightarrow ZZ$ (shape)	2.29
NLO EW uncertainty for $q\bar{q} \rightarrow ZZ$	2.27
NLO QCD uncertainty for $gg \rightarrow ZZ$	2.29
Parton shower uncertainty for $q\bar{q} \rightarrow ZZ$ (shape)	2.29
Jet energy scale and resolution uncertainty	2.26
None	2.30

interest. The distributions of $-2\ln\lambda$ are estimated using simulated events sampled from the likelihood model of the analysis, profiled to the best fit results from data. The resulting confidence intervals are 5–10% more conservative than those obtained by assuming that the asymptotic assumption is correct. The intersections of the 1-sigma and 2-sigma curves in Fig. 6(a) with the likelihood curves allow the true 68 and 95% confidence intervals to be estimated. The expected uncertainty in $\mu_{\text{off-shell}}$, also obtained us-

ing the 1σ confidence intervals from the Neyman construction, is ± 0.9 . The observed value of $\mu_{\text{off-shell}}$ with the 1σ confidence intervals from the Neyman construction is $\mu_{\text{off-shell}} = 1.1^{+0.7}_{-0.6}$. The observed (expected) 95% confidence level (CL) upper limit on $\mu_{\text{off-shell}}$ is 2.4 (2.6). The background-only hypothesis ($\mu_{\text{off-shell}} = 0$) is rejected at an observed (expected) significance of 3.3σ (2.2σ). The $-2\ln\lambda = 2.30$ and $-2\ln\lambda = 5.99$ 2D contours for $\mu_{\text{off-shell}}^{\text{ggF}}$ and $\mu_{\text{off-shell}}^{\text{EW}}$, which correspond to the 68% and 95% CL limits in the asymptotic approximation, are shown in Fig. 6(b).

To estimate the importance of the most relevant sources of systematic uncertainty to the result, Table 5 shows the value of the largest $\mu_{\text{off-shell}}$ for which $-2\ln\lambda = 4$ when each source of uncertainty is removed one at a time. Due to the unusual shape of the yield curve, the impact of nuisance parameters on the best-fit value of $\mu_{\text{off-shell}}$ can be difficult to interpret. Additionally, the correlations between the nuisance parameters, and between the nuisance parameters and the normalisation parameters for the backgrounds, make it difficult to extract uncertainty components. Table 5 indicates the magnitude of the systematic uncertainties and shows their relative importance. The most important ones are the PS uncertainties, the NLO EW uncertainties, and the jet-related uncertainties.

The combination with the on-shell $H \rightarrow ZZ^* \rightarrow 4\ell$ analysis [89], where the on-shell signal strength is measured to be $\mu_{\text{on-shell}} = 1.01 \pm 0.11$, allows these results to be translated into limits on the width of the Higgs boson normalised to its SM expectation ($\mu_{\text{off-shell}}/\mu_{\text{on-shell}} = \Gamma_H/\Gamma_H^{\text{SM}}$) as well as the ratio of off-shell to on-shell couplings for ggF ($R_{gg} \equiv \kappa_{g,\text{off-shell}}^2/\kappa_{g,\text{on-shell}}^2$) and EW ($R_{VV} \equiv \kappa_{V,\text{off-shell}}^2/\kappa_{V,\text{on-shell}}^2$) production. The experimental uncertainties are correlated between the two measurements, while the theoretical uncertainties are assumed to be uncorrelated, considering that differences could exist in the structure of high-order corrections at different mass scales. The difference in the statistical results between the correlated and uncorrelated schemes is found to be negligible. The $\Gamma_H/\Gamma_H^{\text{SM}}$ interpretation assumes that the off- and on-shell coupling modifiers are the same for both ggF and EW production modes. The R_{gg} and R_{VV} interpretations assume that the total width of the Higgs boson is equal to its SM prediction, and that the scattering phase also follows the SM. Additionally, in the R_{gg} case it is assumed that the coupling scale factors associated with the on- and off-shell EW production are the same, while in the R_{VV} case the t -channel Higgs boson exchange process is assumed to scale in the same way as for the off-shell signal.

For the combination with the on-shell analysis, the combined likelihood is built as the product of the likelihood models for the two analyses. The values of $-2\ln\lambda$ as a function of $\Gamma_H/\Gamma_H^{\text{SM}}$, R_{gg} and R_{VV} are shown in Figs. 7(a), 7(b) and 7(c), respectively. The deviation of $-2\ln\lambda$ from a smooth parabolic curve in the region close to zero in Fig. 7(b) is due to the $\sqrt{\mu}$ dependence in the yield that arises from the interference, as discussed earlier in this section, combined with a slight excess observed in the data in the 4ℓ ggH SR, which leads to a maximum near $\mu = 0$. Confidence intervals are obtained using the Neyman construction, as described above. The corresponding measured values are the following: $\Gamma_H/\Gamma_H^{\text{SM}} = 1.1^{+0.7}_{-0.6}$, $R_{gg} = 1.4^{+1.1}_{-1.4}$ and $R_{VV} = 0.9^{+0.3}_{-0.3}$. Multiplying the measured $\Gamma_H/\Gamma_H^{\text{SM}}$ by the width of the SM Higgs boson, the measured Γ_H is $4.5^{+3.3}_{-2.5}$ MeV. The total uncertainty is dominated by its statistical component. The observed (expected) upper limit on $\Gamma_H/\Gamma_H^{\text{SM}}$ is 2.6 (2.7) at 95% confidence level using the Neyman construction, and the corresponding lower limit is 0.1 (0.01). Thus observed (expected) upper and lower limits can be placed on the total width of the Higgs boson of $0.5(0.1) < \Gamma_H < 10.5(10.9)$ MeV.

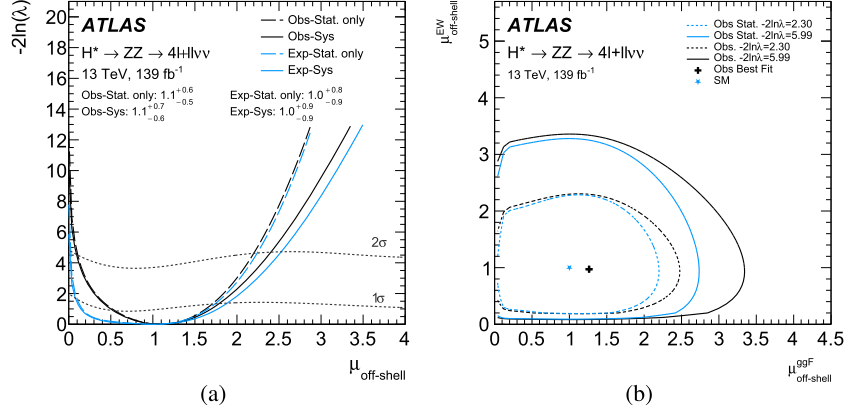


Fig. 6. The likelihood profile, $-2 \ln \lambda$, as a function of (a) the off-shell Higgs boson signal strength, $\mu_{\text{off-shell}}$, for the combination of the $ZZ \rightarrow 4\ell$ and $ZZ \rightarrow 2\ell 2\nu$ off-shell analyses, and (b) two off-shell signal strength parameters for the ggF and EW production modes, plotted in a plane ($\mu_{\text{ggF off-shell}}, \mu_{\text{EW off-shell}}$). In (a) the dotted curves correspond to the one and two standard deviation confidence intervals on the measurement obtained using the Newyman construction while (b) shows two-dimensional contours for $\mu_{\text{ggF off-shell}}$ and $\mu_{\text{EW off-shell}}$ corresponding to $-2 \ln \lambda = 2.30$ and $-2 \ln \lambda = 5.99$, which correspond to the 68% and 95% CL limits in the asymptotic approximation.

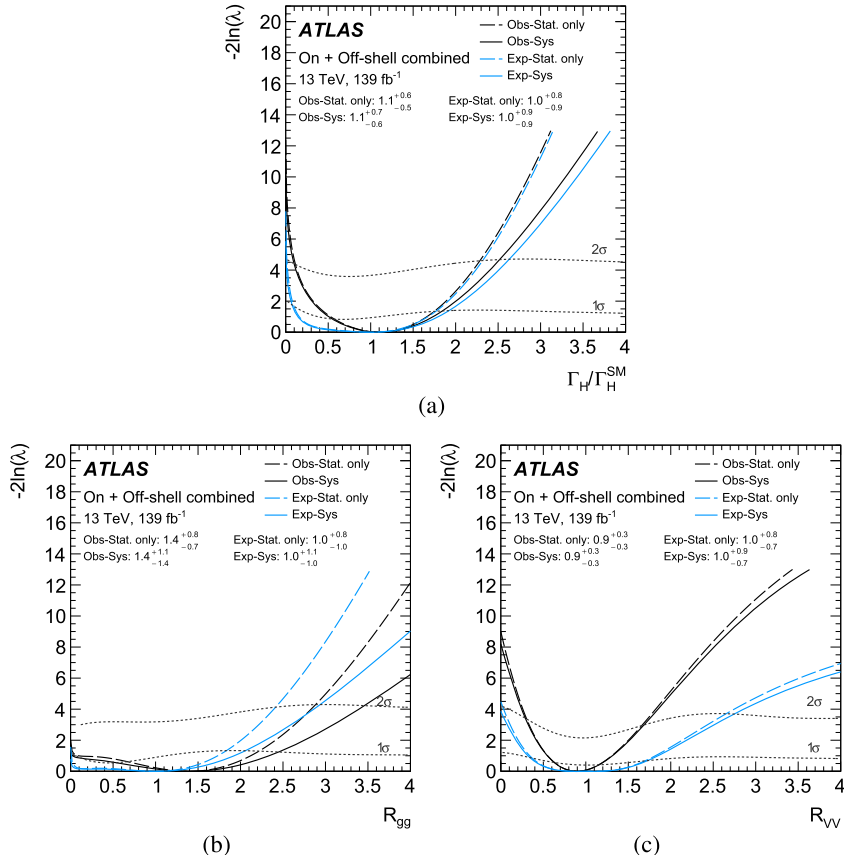


Fig. 7. The likelihood profile, $-2 \ln \lambda$, as a function of (a) $\Gamma_H/\Gamma_H^{\text{SM}}$, (b) R_{gg} and (c) R_{VV} for the combination with the on-shell signal strength measurement. The dotted curves correspond to the one and two standard deviation confidence intervals on the measurement obtained using the Neyman construction. For R_{gg} there are two additional negative crossings, near -1.2 and -0.84 from the best fit value: as these are very close to the $1-\sigma$ level, they are neglected.

9. Conclusion

This Letter presents a search for off-shell Higgs boson production in the $ZZ \rightarrow 4\ell$ and the $ZZ \rightarrow 2\ell 2\nu$ final states with the ATLAS detector using 139 fb^{-1} of pp collision data. The search is optimised for sensitivity to both the ggf- and EW-induced signal, and a simultaneous fit to all SRs and CRs is performed to extract the signal contribution. No deviations from the SM prediction are observed. The data reject the background-only hypothesis with an observed (expected) significance of 3.3σ (2.2σ). The observed (expected) upper limit at 95% confidence interval on the signal strength $\mu_{\text{off-shell}}$ is found to be 2.4 (2.6). A combination with the on-shell Higgs boson measurement gives a measured total width of the Higgs boson of $4.5^{+3.3}_{-2.5} \text{ MeV}$, and the observed (expected) upper limit on the total width is found to be 10.5 (10.9) MeV at 95% CL. These results are compatible with those previously obtained by the CMS experiment. Together with that result, this means that both experiments have observed evidence of off-shell Higgs boson production.

Declaration of competing interest

The authors declare that they have no known competing financial interests or personal relationships that could have appeared to influence the work reported in this paper.

Data availability

The data for this manuscript are not available. The values in the plots and tables associated to this article are stored in HEPDATA (<https://hepdata.cedar.ac.uk>).

Acknowledgements

We thank CERN for the very successful operation of the LHC, as well as the support staff from our institutions without whom ATLAS could not be operated efficiently.

We acknowledge the support of ANPCyT, Argentina; YerPhI, Armenia; ARC, Australia; BMWFW and FWF, Austria; ANAS, Azerbaijan; CNPq and FAPESP, Brazil; NSERC, NRC and CFI, Canada; CERN; ANID, Chile; CAS, MOST and NSFC, China; Minciencias, Colombia; MEYS CR, Czech Republic; DNRF and DNSRC, Denmark; IN2P3-CNRS and CEA-DRF/IRFU, France; SRNSFG, Georgia; BMBF, HGF and MPG, Germany; GSRI, Greece; RGC and Hong Kong SAR, China; ISF and Benoziyo Center, Israel; INFN, Italy; MEXT and JSPS, Japan; CNRST, Morocco; NWO, Netherlands; RCN, Norway; MEiN, Poland; FCT, Portugal; MNE/IFA, Romania; MESTD, Serbia; MSSR, Slovakia; ARRS and MIZŠ, Slovenia; DSI/NRF, South Africa; MICINN, Spain; SRC and Wallenberg Foundation, Sweden; SERI, SNSF and Canton of Bern and Geneva, Switzerland; MOST, Taiwan; TENMAK, Türkiye; STFC, United Kingdom; DOE and NSF, United States of America. In addition, individual groups and members have received support from BCKDF, CANARIE, Compute Canada and CRC, Canada; PRIMUS 21/SCI/017 and UNCE SCI/013, Czech Republic; COST, ERC, ERDF, Horizon 2020 and Marie Skłodowska-Curie Actions, European Union; Investissements d'Avenir Labex, Investissements d'Avenir Idex and ANR, France; DFG and AvH Foundation, Germany; Herakleitos, Thales and Aristeia programmes co-financed by EU-ESF and the Greek NSRF, Greece; BSF-NSF and MINERVA, Israel; Norwegian Financial Mechanism 2014–2021, Norway; NCN and NAWA, Poland; La Caixa Banking Foundation, CERCA Programme Generalitat de Catalunya and PROMETEO and GenT Programmes Generalitat Valenciana, Spain; Göran Gustafssons Stiftelse, Sweden; The Royal Society and Leverhulme Trust, United Kingdom.

The crucial computing support from all WLCG partners is acknowledged gratefully, in particular from CERN, the ATLAS Tier-1 facilities at TRIUMF (Canada), NDGF (Denmark, Norway, Sweden), CC-IN2P3 (France), KIT/GridKA (Germany), INFN-CNAF (Italy), NL-T1 (Netherlands), PIC (Spain), ASGC (Taiwan), RAL (UK) and BNL (USA), the Tier-2 facilities worldwide and large non-WLCG resource providers. Major contributors of computing resources are listed in Ref. [90].

References

- [1] ATLAS Collaboration, Observation of a new particle in the search for the Standard Model Higgs boson with the ATLAS detector at the LHC, Phys. Lett. B 716 (2012) 1, arXiv:1207.7214 [hep-ex].
- [2] CMS Collaboration, Observation of a new boson at a mass of 125 GeV with the CMS experiment at the LHC, Phys. Lett. B 716 (2012) 30, arXiv:1207.7235 [hep-ex].
- [3] ATLAS Collaboration, A detailed map of Higgs boson interactions by the ATLAS experiment ten years after the discovery, Nature 607 (2022) 52, arXiv:2207.00992 [hep-ex].
- [4] CMS Collaboration, A portrait of the Higgs boson by the CMS experiment ten years after the discovery, Nature 607 (2022) 60, arXiv:2207.00043 [hep-ex].
- [5] LHC Higgs Cross Section Working Group, Handbook of LHC Higgs cross sections: 4. Deciphering the nature of the Higgs sector, arXiv:1610.07922 [hep-ph], 2016, 2/2017.
- [6] N. Kauer, G. Passarino, Inadequacy of zero-width approximation for a light Higgs boson signal, J. High Energy Phys. 08 (2012) 116, arXiv:1206.4803 [hep-ph].
- [7] F. Caoila, K. Melnikov, Constraining the Higgs boson width with ZZ production at the LHC, Phys. Rev. D 88 (2013) 054024, arXiv:1307.4935 [hep-ph].
- [8] J.M. Campbell, R.K. Ellis, C. Williams, Bounding the Higgs width at the LHC using full analytic results for $gg \rightarrow e^+e^-\mu^+\mu^-$, J. High Energy Phys. 04 (2014) 060, arXiv:1311.3589 [hep-ph].
- [9] J.M. Campbell, R.K. Ellis, C. Williams, Bounding the Higgs width at the LHC: complementary results from $H \rightarrow WW$, Phys. Rev. D 89 (2014) 053011, arXiv:1312.1628 [hep-ph].
- [10] C. Englert, M. Spannowsky, Limitations and opportunities of off-shell coupling measurements, Phys. Rev. D 90 (2014) 053003, arXiv:1405.0285 [hep-ph].
- [11] G. Cacciapaglia, A. Deandrea, G.D. La Rochelle, J.-B. Flament, Higgs couplings: disentangling new physics with off-shell measurements, Phys. Rev. Lett. 113 (2014) 201802, arXiv:1406.1757 [hep-ph].
- [12] A. Azatov, C. Grojean, A. Paul, E. Salvioni, Taming the off-shell Higgs boson, J. Exp. Theor. Phys. 120 (2015) 354, arXiv:1406.6338 [hep-ph].
- [13] M. Ghezzi, G. Passarino, S. Uccirati, Bounding the Higgs width using effective field theory, PoS LL2014 072 (2014), arXiv:1405.1925 [hep-ph].
- [14] M. Buschmann, et al., Mass effects in the Higgs-gluon coupling: boosted vs off-shell production, J. High Energy Phys. 02 (2015) 038, arXiv:1410.5806 [hep-ph].
- [15] J.S. Gainer, J. Lykken, K.T. Matchev, S. Mrenna, M. Park, Beyond geolocating: constraining higher dimensional operators in $H \rightarrow 4\ell$ with off-shell production and more, Phys. Rev. D 91 (2015) 035011, arXiv:1403.4951 [hep-ph].
- [16] C. Englert, Y. Soreq, M. Spannowsky, Off-shell Higgs coupling measurements in BSM scenarios, J. High Energy Phys. 05 (2015) 145, arXiv:1410.5440 [hep-ph].
- [17] D. Gonçalves, T. Han, S. Mukhopadhyay, Off-shell Higgs probe of naturalness, Phys. Rev. Lett. 120 (2018) 111801, arXiv:1710.02149 [hep-ph].
- [18] D. Gonçalves, T. Han, S. Ching, Iris Leung, H. Qin, Off-shell Higgs couplings in $H^* \rightarrow ZZ \rightarrow \ell\ell\nu\nu$, Phys. Lett. B 817 (2021) 136329, arXiv:2012.05272 [hep-ph].
- [19] S.J. Lee, M. Park, Z. Qian, Probing unitarity violation in the tail of the off-shell Higgs boson in $V_L V_L$ mode, Phys. Rev. D 100 (2019) 011702, arXiv:1812.02679 [hep-ph].
- [20] H.-R. He, X. Wan, Y.-K. Wang, Anomalous $H \rightarrow ZZ \rightarrow 4\ell$ decay and its interference effects on gluon–gluon contribution at the LHC, Chin. Phys. C 44 (2020) 123101, arXiv:1902.04756 [hep-ph].
- [21] U. Haisch, G. Koole, Off-shell Higgs production at the LHC as a probe of the trilinear Higgs coupling, J. High Energy Phys. 02 (2022) 030, arXiv:2111.12589 [hep-ph].
- [22] M. Ruhdorfer, E. Salvioni, A. Weiler, A global view of the off-shell Higgs portal, SciPost Phys. 8 (2020) 027, arXiv:1910.04170 [hep-ph].
- [23] ATLAS Collaboration, Constraints on the off-shell Higgs boson signal strength in the high-mass ZZ and WW final states with the ATLAS detector, Eur. Phys. J. C 75 (2015) 335, arXiv:1503.01060 [hep-ex].
- [24] CMS Collaboration, Constraints on the Higgs boson width from off-shell production and decay to Z-boson pairs, Phys. Lett. B 736 (2014) 64, arXiv:1405.3455 [hep-ex].
- [25] CMS Collaboration, Limits on the Higgs boson lifetime and width from its decay to four charged leptons, Phys. Rev. D 92 (2015) 072010, arXiv:1507.06656.
- [26] CMS Collaboration, Search for Higgs boson off-shell production in proton-proton collisions at 7 and 8 TeV and derivation of constraints on its total decay width, J. High Energy Phys. 09 (2016) 051, arXiv:1605.02329 [hep-ex].

- [27] ATLAS Collaboration, Constraints on off-shell Higgs boson production and the Higgs boson total width in $ZZ \rightarrow 4\ell$ and $ZZ \rightarrow 2\ell 2\nu$ final states with the ATLAS detector, Phys. Lett. B 786 (2018) 223, arXiv:1808.01191 [hep-ex].
- [28] CMS Collaboration, Measurements of the Higgs boson width and anomalous HVV couplings from on-shell and off-shell production in the four-lepton final state, Phys. Rev. D 99 (2019) 112003, arXiv:1901.00174 [hep-ex].
- [29] CMS Collaboration, Measurement of the Higgs boson width and evidence of its off-shell contributions to ZZ production, Nat. Phys. 18 (2022) 1329, eprint: arXiv:2202.06923.
- [30] S. Schael, et al., Precision electroweak measurements on the Z resonance, Phys. Rep. 427 (2006) 257, arXiv:hep-ex/0509008.
- [31] ATLAS Collaboration, Measurements of the Higgs boson inclusive and differential fiducial cross sections in the 4ℓ decay channel at $\sqrt{s} = 13$ TeV, Eur. Phys. J. C 80 (2020) 942, arXiv:2004.03969 [hep-ex].
- [32] ATLAS Collaboration, The ATLAS experiment at the CERN large hadron collider, J. Instrum. 3 (2008) S08003.
- [33] ATLAS Collaboration, ATLAS Insertable B-Layer Technical Design Report, CERN-LHCC-2010-013, ATLAS-TDR-19, <https://cds.cern.ch/record/1291633>, 2010, ATLAS Insertable B-Layer Technical Design Report Addendum, ATLAS-TDR-19-ADD-1 <https://cds.cern.ch/record/1451888>, 2012.
- [34] ATLAS Collaboration, Performance of the ATLAS trigger system in 2015, Eur. Phys. J. C 77 (2017) 317, arXiv:1611.09661 [hep-ex].
- [35] ATLAS Collaboration, The ATLAS Collaboration software and firmware, ATL-SOFT-PUB-2021-001, <https://cds.cern.ch/record/2767187>, 2021.
- [36] ATLAS Collaboration, The ATLAS simulation infrastructure, Eur. Phys. J. C 70 (2010) 823, arXiv:1005.4568 [physics.ins-det].
- [37] S. Agostinelli, et al., GEANT4: a simulation toolkit, Nucl. Instrum. Methods A 506 (2003) 250.
- [38] T. Sjöstrand, S. Mrenna, P.Z. Skands, A brief introduction to PYTHIA 8.1, Comput. Phys. Commun. 178 (2008) 852, arXiv:0710.3820 [hep-ph].
- [39] E. Bothmann, et al., Event generation with Sherpa 2.2, SciPost Phys. 7 (2019) 034, arXiv:1905.09127 [hep-ph].
- [40] F. Buccioni, et al., OpenLoops 2, Eur. Phys. J. C 79 (2019) 866, arXiv:1907.13071 [hep-ph].
- [41] F. Cascioli, P. Maieröfer, S. Pozzorini, Scattering amplitudes with open loops, Phys. Rev. Lett. 108 (2012) 111601, arXiv:1111.5206 [hep-ph].
- [42] A. Denner, S. Dittmaier, L. Hofer, Collier: a fortran-based complex one-loop library in extended regularizations, Comput. Phys. Commun. 212 (2017) 220, arXiv:1604.06792 [hep-ph].
- [43] R.D. Ball, et al., Parton distributions for the LHC Run II, J. High Energy Phys. 04 (2015) 040, arXiv:1410.8849 [hep-ph].
- [44] F. Cascioli, et al., Precise Higgs-background predictions: merging NLO QCD and squared quark-loop corrections to four-lepton + 0, 1 jet production, J. High Energy Phys. 01 (2014) 046, arXiv:1309.0500 [hep-ph].
- [45] F. Caola, K. Melnikov, R. Röntsch, L. Tancredi, QCD corrections to ZZ production in gluon fusion at the LHC, Phys. Rev. D 92 (2015) 18, arXiv:1509.06734 [hep-ph].
- [46] F. Caola, M. Dowling, K. Melnikov, R. Röntsch, L. Tancredi, QCD corrections to vector boson pair production in gluon fusion including interference effects with off-shell Higgs at the LHC, J. High Energy Phys. 07 (2016) 087, arXiv:1605.04610 [hep-ph].
- [47] G. Passarino, Higgs CAT, Eur. Phys. J. C 74 (2014) 2866, arXiv:1312.2397 [hep-ph].
- [48] LHC Higgs Cross Section Working Group, D. de Florian, et al., Handbook of LHC Higgs Cross Sections: 4. Deciphering the Nature of the Higgs Sector, CERN-2017-002-M, CERN, Geneva, 2016, arXiv:1610.07922 [hep-ph].
- [49] M. Bonvini, F. Caola, S. Forte, K. Melnikov, G. Ridolfi, Signal-background interference effects for $gg \rightarrow H \rightarrow W^+W^-$ beyond leading order, Phys. Rev. D 88 (3 2013) 034032, <https://link.aps.org/doi/10.1103/PhysRevD.88.034032>.
- [50] F. Caola, K. Melnikov, R. Röntsch, L. Tancredi, QCD corrections to W^+W^- production through gluon fusion, Phys. Lett. B (ISSN 0370-2693) 754 (2016) 275.
- [51] J. Alwall, et al., The automated computation of tree-level and next-to-leading order differential cross sections, and their matching to parton shower simulations, J. High Energy Phys. 07 (2014) 079, arXiv:1405.0301 [hep-ph].
- [52] R.D. Ball, et al., Parton distributions with LHC data, Nucl. Phys. B 867 (2013) 244, arXiv:1207.1303 [hep-ph].
- [53] ATLAS Collaboration, ATLAS Pythia 8 tunes to 7 TeV data, ATL-PHYS-PUB-2014-021, <https://cds.cern.ch/record/1966419>, 2014.
- [54] S. Höche, F. Krauss, M. Schönherr, F. Siegert, QCD matrix elements + parton showers. The NLO case, J. High Energy Phys. 04 (2013) 027, arXiv:1207.5030 [hep-ph].
- [55] B. Biedermann, A. Denner, S. Dittmaier, L. Hofer, B. Jäger, Electroweak corrections to $pp \rightarrow \mu^+\mu^-e^+e^- + X$ at the LHC: a Higgs boson background study, Phys. Rev. Lett. 116 (2016) 161803, arXiv:1601.07787 [hep-ph].
- [56] B. Biedermann, A. Denner, S. Dittmaier, L. Hofer, B. Jäger, Next-to-leading-order electroweak corrections to the production of four charged leptons at the LHC, J. High Energy Phys. 01 (2017) 033, arXiv:1611.05338 [hep-ph].
- [57] S. Kallweit, J. Lindert, S. Pozzorini, M. Schönherr, NLO QCD+EW predictions for $2\ell 2\nu$ diboson signatures at the LHC, J. High Energy Phys. 11 (2017) 120, arXiv:1705.00598 [hep-ph].
- [58] P. Nason, G. Zanderighi, W^+W^- , WZ and ZZ production in the POWHEG-BOX-V2, Eur. Phys. J. C 74 (2014) 2702, arXiv:1311.1365 [hep-ph].
- [59] R. Gavin, Y. Li, F. Petriello, S. Quackenbush, FEWZ 2.0: a code for hadronic Z production at next-to-next-to-leading order, Comput. Phys. Commun. 182 (2011) 2388, arXiv:1011.3540 [hep-ph].
- [60] M. Czakon, A. Mitov, Top++: a program for the calculation of the top-pair cross-section at hadron colliders, Comput. Phys. Commun. 185 (2014) 2930, arXiv:1112.5675 [hep-ph].
- [61] P. Kant, et al., HATHor for single top-quark production: updated predictions and uncertainty estimates for single top-quark production in hadronic collisions, Comput. Phys. Commun. 191 (2015) 74, arXiv:1406.4403 [hep-ph].
- [62] M. Aliev, et al., HATHOR: Hadronic top and heavy quarks cross section calculator, Comput. Phys. Commun. 182 (2011) 1034, arXiv:1007.1327 [hep-ph].
- [63] S. Frixione, V. Hirschi, D. Pagani, H.-S. Shao, M. Zaro, Electroweak and QCD corrections to top-pair hadroproduction in association with heavy bosons, J. High Energy Phys. 06 (2015) 184, arXiv:1504.03446 [hep-ph].
- [64] ATLAS Collaboration, Search for heavy resonances decaying into a pair of Z bosons in the $\ell^+\ell^-\ell^+\ell^-$ and $\ell^+\ell^-\nu\bar{\nu}$ final states using 139fb^{-1} of proton-proton collisions at $\sqrt{s} = 13$ TeV with the ATLAS detector, Eur. Phys. J. C 81 (2020) 332, arXiv:2009.14791 [hep-ex].
- [65] ATLAS Collaboration, Muon reconstruction performance of the ATLAS detector in proton-proton collision data at $\sqrt{s} = 13$ TeV, Eur. Phys. J. C 76 (2016) 292, arXiv:1603.05598 [hep-ex].
- [66] ATLAS Collaboration, Electron reconstruction and identification in the ATLAS experiment using the 2015 and 2016 LHC proton-proton collision data at $\sqrt{s} = 13$ TeV, Eur. Phys. J. C 79 (2019) 639, arXiv:1902.04655 [hep-ex].
- [67] ATLAS Collaboration, Jet reconstruction and performance using particle flow with the ATLAS detector, Eur. Phys. J. C 77 (2017) 466, arXiv:1703.10485 [hep-ex].
- [68] M. Cacciari, G.P. Salam, G. Soyez, The anti- k_t jet clustering algorithm, J. High Energy Phys. 04 (2008) 063, arXiv:0802.1189 [hep-ph].
- [69] M. Cacciari, G.P. Salam, G. Soyez, FastJet user manual, Eur. Phys. J. C 72 (2012) 1896, arXiv:1111.6097 [hep-ph].
- [70] ATLAS Collaboration, Jet energy scale measurements and their systematic uncertainties in proton-proton collisions at $\sqrt{s} = 13$ TeV with the ATLAS detector, Phys. Rev. D 96 (2017) 072002, arXiv:1703.09665 [hep-ex].
- [71] ATLAS Collaboration, Performance of pile-up mitigation techniques for jets in pp collisions at $\sqrt{s} = 8$ TeV using the ATLAS detector, Eur. Phys. J. C 76 (2016) 581, arXiv:1510.03823 [hep-ex].
- [72] ATLAS Collaboration, Identification and rejection of pile-up jets at high pseudorapidity with the ATLAS detector, Eur. Phys. J. C 77 (2017) 580, Erratum: Eur. Phys. J. C 77 (2017) 712, arXiv:1705.02211 [hep-ex].
- [73] ATLAS Collaboration, ATLAS b-jet identification performance and efficiency measurement with $t\bar{t}$ events in pp collisions at $\sqrt{s} = 13$ TeV, Eur. Phys. J. C 79 (2019) 970, arXiv:1907.05120 [hep-ex].
- [74] ATLAS flavour-tagging algorithms for the LHC Run 2 pp collision dataset, arXiv: 2211.16345 [physics.data-an], 2022.
- [75] ATLAS Collaboration, Performance of missing transverse momentum reconstruction with the ATLAS detector in the first proton-proton collisions at $\sqrt{s} = 13$ TeV, ATL-PHYS-PUB-2015-027, <https://cds.cern.ch/record/2037904>, 2015.
- [76] ATLAS Collaboration, Object-based missing transverse momentum significance in the ATLAS detector, ATLAS-CONF-2018-038, <https://cds.cern.ch/record/2630948>, 2018.
- [77] F. Chollet, et al., <https://github.com/fchollet/keras>, 2015.
- [78] Martín Abadi, et al., TensorFlow: large-scale machine learning on heterogeneous systems, Software available from tensorflow.org, <https://www.tensorflow.org/>, 2015.
- [79] ATLAS Collaboration, Evidence for the spin-0 nature of the Higgs boson using ATLAS data, Phys. Lett. B 726 (2013) 120, arXiv:1307.1432 [hep-ex].
- [80] D. Rainwater, R. Szalapski, D. Zeppenfeld, Probing color-singlet exchange in $Z + 2$ -jet events at the CERN LHC, Phys. Rev. D 54 (11 1996) 6680, <https://link.aps.org/doi/10.1103/PhysRevD.54.6680>.
- [81] D. de Florian, et al., Handbook of LHC Higgs cross sections: 4. Deciphering the nature of the Higgs sector, arXiv:1610.07922 [hep-ph], 2016.
- [82] S. Gieseke, T. Kasprzik, J.H. Kühn, Vector-boson pair production and electroweak corrections in HERWIG++, Eur. Phys. J. C 74 (2014) 2988, arXiv:1401.3964 [hep-ph].
- [83] B. Nachman, J. Thaler, Neural conditional reweighting, Phys. Rev. D 105 (2022) 076015, arXiv:2107.08979 [physics.data-an].
- [84] ATLAS Collaboration, Luminosity determination in pp collisions at $\sqrt{s} = 13$ TeV using the ATLAS detector at the LHC, ATLAS-CONF-2019-021, <https://cds.cern.ch/record/2677054>, 2019.
- [85] G. Avoni, et al., The new LUCID-2 detector for luminosity measurement and monitoring in ATLAS, J. Instrum. 13 (2018) P07017.
- [86] G. Cowan, K. Cranmer, E. Gross, O. Vitells, Asymptotic formulae for likelihood-based tests of new physics, Eur. Phys. J. C 71 (2011).
- [87] S.S. Wilks, The large-sample distribution of the likelihood ratio for testing composite hypotheses, Ann. Math. Stat. 9 (1938) 60.
- [88] J. Neyman, Outline of a theory of statistical estimation based on the classical theory of probability, Philos. Trans. R. Soc. Lond. Ser. A, Math. Phys. Sci. 236 (1937) 333, issn: 00804614.

- [89] ATLAS Collaboration, Higgs boson production cross-section measurements and their EFT interpretation in the 4ℓ decay channel at $\sqrt{s} = 13\text{ TeV}$ with the ATLAS detector, Eur. Phys. J. C 80 (2020) 957, arXiv:2004.03447 [hep-ex], Erratum: Eur. Phys. J. C 81 (2021) 29, Erratum: Eur. Phys. J. C 81 (2021) 398.
- [90] ATLAS Collaboration, ATLAS computing acknowledgements, ATL-SOFT-PUB-2023-001, <https://cds.cern.ch/record/2869272>, 2023.

The ATLAS Collaboration

- G. Aad ^{102, ID}, B. Abbott ^{120, ID}, K. Abeling ^{55, ID}, S.H. Abidi ^{29, ID}, A. Aboulhorma ^{35e, ID}, H. Abramowicz ^{151, ID}, H. Abreu ^{150, ID}, Y. Abulaiti ^{117, ID}, A.C. Abusleme Hoffman ^{137a, ID}, B.S. Acharya ^{69a, 69b, ID, p}, C. Adam Bourdarios ^{4, ID}, L. Adamczyk ^{85a, ID}, L. Adamek ^{155, ID}, S.V. Addepalli ^{26, ID}, J. Adelman ^{115, ID}, A. Adiguzel ^{21c, ID}, S. Adorni ^{56, ID}, T. Adye ^{134, ID}, A.A. Affolder ^{136, ID}, Y. Afik ^{36, ID}, M.N. Agaras ^{13, ID}, J. Agarwala ^{73a, 73b, ID}, A. Aggarwal ^{100, ID}, C. Agheorghiesei ^{27c, ID}, J.A. Aguilar-Saavedra ^{130f, ID}, A. Ahmad ^{36, ID}, F. Ahmadov ^{38, ID, ab}, W.S. Ahmed ^{104, ID}, S. Ahuja ^{95, ID}, X. Ai ^{48, ID}, G. Aielli ^{76a, 76b, ID}, M. Ait Tamlihat ^{35e, ID}, B. Aitbenchikh ^{35a, ID}, I. Aizenberg ^{169, ID}, M. Akbiyik ^{100, ID}, T.P.A. Åkesson ^{98, ID}, A.V. Akimov ^{37, ID}, N.N. Akolkar ^{24, ID}, K. Al Khoury ^{41, ID}, G.L. Alberghi ^{23b, ID}, J. Albert ^{165, ID}, P. Albicocco ^{53, ID}, S. Alderweireldt ^{52, ID}, M. Aleksa ^{36, ID}, I.N. Aleksandrov ^{38, ID}, C. Alexa ^{27b, ID}, T. Alexopoulos ^{10, ID}, A. Alfonsi ^{114, ID}, F. Alfonsi ^{23b, ID}, M. Alhroob ^{120, ID}, B. Ali ^{132, ID}, S. Ali ^{148, ID}, M. Aliev ^{37, ID}, G. Alimonti ^{71a, ID}, W. Alkakhi ^{55, ID}, C. Allaire ^{66, ID}, B.M.M. Allbrooke ^{146, ID}, C.A. Allendes Flores ^{137f, ID}, P.P. Allport ^{20, ID}, A. Aloisio ^{72a, 72b, ID}, F. Alonso ^{90, ID}, C. Alpigiani ^{138, ID}, M. Alvarez Estevez ^{99, ID}, A. Alvarez Fernandez ^{100, ID}, M.G. Alvaggi ^{72a, 72b, ID}, M. Aly ^{101, ID}, Y. Amaral Coutinho ^{82b, ID}, A. Ambler ^{104, ID}, C. Amelung ³⁶, M. Amerl ^{101, ID}, C.G. Ames ^{109, ID}, D. Amidei ^{106, ID}, S.P. Amor Dos Santos ^{130a, ID}, K.R. Amos ^{163, ID}, V. Ananiev ^{125, ID}, C. Anastopoulos ^{139, ID}, T. Andeen ^{11, ID}, J.K. Anders ^{36, ID}, S.Y. Andrean ^{47a, 47b, ID}, A. Andreazza ^{71a, 71b, ID}, S. Angelidakis ^{9, ID}, A. Angerami ^{41, ID, ae}, A.V. Anisenkov ^{37, ID}, A. Annovi ^{74a, ID}, C. Antel ^{56, ID}, M.T. Anthony ^{139, ID}, E. Antipov ^{145, ID}, M. Antonelli ^{53, ID}, D.J.A. Antrim ^{17a, ID}, F. Anulli ^{75a, ID}, M. Aoki ^{83, ID}, T. Aoki ^{153, ID}, J.A. Aparisi Pozo ^{163, ID}, M.A. Aparo ^{146, ID}, L. Aperio Bella ^{48, ID}, C. Appelt ^{18, ID}, N. Aranzabal ^{36, ID}, V. Araujo Ferraz ^{82a, ID}, C. Arcangeletti ^{53, ID}, A.T.H. Arce ^{51, ID}, E. Arena ^{92, ID}, J-F. Arguin ^{108, ID}, S. Argyropoulos ^{54, ID}, J.-H. Arling ^{48, ID}, A.J. Armbruster ^{36, ID}, O. Arnaez ^{4, ID}, H. Arnold ^{114, ID}, Z.P. Arrubarrena Tame ¹⁰⁹, G. Artoni ^{75a, 75b, ID}, H. Asada ^{111, ID}, K. Asai ^{118, ID}, S. Asai ^{153, ID}, N.A. Asbah ^{61, ID}, J. Assahsah ^{35d, ID}, K. Assamagan ^{29, ID}, R. Astalos ^{28a, ID}, R.J. Atkin ^{33a, ID}, M. Atkinson ¹⁶², N.B. Atlay ^{18, ID}, H. Atmani ^{62b}, P.A. Atmasiddha ^{106, ID}, K. Augsten ^{132, ID}, S. Auricchio ^{72a, 72b, ID}, A.D. Auriol ^{20, ID}, V.A. Aastrup ^{171, ID}, G. Avner ^{150, ID}, G. Avolio ^{36, ID}, K. Axiotis ^{56, ID}, G. Azuelos ^{108, ID, ai}, D. Babal ^{28b, ID}, H. Bachacou ^{135, ID}, K. Bachas ^{152, ID, s}, A. Bachiu ^{34, ID}, F. Backman ^{47a, 47b, ID}, A. Badea ^{61, ID}, P. Bagnaia ^{75a, 75b, ID}, M. Bahmani ^{18, ID}, A.J. Bailey ^{163, ID}, V.R. Bailey ^{162, ID}, J.T. Baines ^{134, ID}, C. Bakalis ^{10, ID}, O.K. Baker ^{172, ID}, E. Bakos ^{15, ID}, D. Bakshi Gupta ^{8, ID}, R. Balasubramanian ^{114, ID}, E.M. Baldin ^{37, ID}, P. Balek ^{133, ID}, E. Ballabene ^{71a, 71b, ID}, F. Balli ^{135, ID}, L.M. Baltes ^{63a, ID}, W.K. Balunas ^{32, ID}, J. Balz ^{100, ID}, E. Banas ^{86, ID}, M. Bandieramonte ^{129, ID}, A. Bandyopadhyay ^{24, ID}, S. Bansal ^{24, ID}, L. Barak ^{151, ID}, E.L. Barberio ^{105, ID}, D. Barberis ^{57b, 57a, ID}, M. Barbero ^{102, ID}, G. Barbour ⁹⁶, K.N. Barends ^{33a, ID}, T. Barillari ^{110, ID}, M-S. Barisits ^{36, ID}, T. Barklow ^{143, ID}, P. Baron ^{122, ID}, D.A. Baron Moreno ^{101, ID}, A. Baroncelli ^{62a, ID}, G. Barone ^{29, ID}, A.J. Barr ^{126, ID}, L. Barranco Navarro ^{47a, 47b, ID}, F. Barreiro ^{99, ID}, J. Barreiro Guimarães da Costa ^{14a, ID}, U. Barron ^{151, ID}, M.G. Barros Teixeira ^{130a, ID}, S. Barsov ^{37, ID}, F. Bartels ^{63a, ID}, R. Bartoldus ^{143, ID}, A.E. Barton ^{91, ID}, P. Bartos ^{28a, ID}, A. Basan ^{100, ID}, M. Baselga ^{49, ID}, I. Bashta ^{77a, 77b, ID}, A. Bassalat ^{66, ID, b}, M.J. Basso ^{155, ID}, C.R. Basson ^{101, ID}, R.L. Bates ^{59, ID}, S. Batlamous ^{35e, ID}, J.R. Batley ^{32, ID}, B. Batool ^{141, ID}, M. Battaglia ^{136, ID}, D. Battulga ^{18, ID}, M. Bauce ^{75a, 75b, ID}, M. Bauer ^{36, ID}, P. Bauer ^{24, ID}, J.B. Beacham ^{51, ID}, T. Beau ^{127, ID}, P.H. Beauchemin ^{158, ID}, F. Becherer ^{54, ID}, P. Bechtle ^{24, ID},

- H.P. Beck 19,^{IP,r}, K. Becker 167,^{IP}, A.J. Beddall 21d,^{IP}, V.A. Bednyakov 38,^{IP}, C.P. Bee 145,^{IP}, L.J. Beemster 15,
 T.A. Beermann 36,^{IP}, M. Begalli 82d,^{IP}, M. Begel 29,^{IP}, A. Behera 145,^{IP}, J.K. Behr 48,^{IP},
 C. Beirao Da Cruz E Silva 36,^{IP}, J.F. Beirer 55,36,^{IP}, F. Beisiegel 24,^{IP}, M. Belfkir 159,^{IP}, G. Bella 151,^{IP},
 L. Bellagamba 23b,^{IP}, A. Bellerive 34,^{IP}, P. Bellos 20,^{IP}, K. Beloborodov 37,^{IP}, N.L. Belyaev 37,^{IP},
 D. Benchekroun 35a,^{IP}, F. Bendebba 35a,^{IP}, Y. Benhammou 151,^{IP}, M. Benoit 29,^{IP}, J.R. Bensinger 26,^{IP},
 S. Bentvelsen 114,^{IP}, L. Beresford 48,^{IP}, M. Beretta 53,^{IP}, E. Bergeaas Kuutmann 161,^{IP}, N. Berger 4,^{IP},
 B. Bergmann 132,^{IP}, J. Beringer 17a,^{IP}, S. Berlendis 7,^{IP}, G. Bernardi 5,^{IP}, C. Bernius 143,^{IP},
 F.U. Bernlochner 24,^{IP}, T. Berry 95,^{IP}, P. Berta 133,^{IP}, A. Berthold 50,^{IP}, I.A. Bertram 91,^{IP}, S. Bethke 110,^{IP},
 A. Betti 75a,75b,^{IP}, A.J. Bevan 94,^{IP}, M. Bhamjee 33c,^{IP}, S. Bhatta 145,^{IP}, D.S. Bhattacharya 166,^{IP},
 P. Bhattacharai 26,^{IP}, V.S. Bhopatkar 121,^{IP}, R. Bi 29,^{ak}, R.M. Bianchi 129,^{IP}, O. Biebel 109,^{IP}, R. Bielski 123,^{IP},
 M. Biglietti 77a,^{IP}, T.R.V. Billoud 132,^{IP}, M. Bindi 55,^{IP}, A. Bingul 21b,^{IP}, C. Bini 75a,75b,^{IP}, A. Biondini 92,^{IP},
 C.J. Birch-sykes 101,^{IP}, G.A. Bird 20,134,^{IP}, M. Birman 169,^{IP}, M. Biros 133,^{IP}, T. Bisanz 36,^{IP},
 E. Bisceglie 43b,43a,^{IP}, D. Biswas 170,^{IP}, A. Bitadze 101,^{IP}, K. Bjørke 125,^{IP}, I. Bloch 48,^{IP}, C. Blocker 26,^{IP},
 A. Blue 59,^{IP}, U. Blumenschein 94,^{IP}, J. Blumenthal 100,^{IP}, G.J. Bobbink 114,^{IP}, V.S. Bobrovnikov 37,^{IP},
 M. Boehler 54,^{IP}, D. Bogavac 36,^{IP}, A.G. Bogdanchikov 37,^{IP}, C. Bohm 47a,^{IP}, V. Boisvert 95,^{IP}, P. Bokan 48,^{IP},
 T. Bold 85a,^{IP}, M. Bomben 5,^{IP}, M. Bona 94,^{IP}, M. Boonekamp 135,^{IP}, C.D. Booth 95,^{IP}, A.G. Borbély 59,^{IP},
 H.M. Borecka-Bielska 108,^{IP}, L.S. Borgna 96,^{IP}, G. Borissov 91,^{IP}, D. Bortoletto 126,^{IP}, D. Boscherini 23b,^{IP},
 M. Bosman 13,^{IP}, J.D. Bossio Sola 36,^{IP}, K. Bouaouda 35a,^{IP}, N. Bouchhar 163,^{IP}, J. Boudreau 129,^{IP},
 E.V. Bouhova-Thacker 91,^{IP}, D. Boumediene 40,^{IP}, R. Bouquet 5,^{IP}, A. Boveia 119,^{IP}, J. Boyd 36,^{IP},
 D. Boye 29,^{IP}, I.R. Boyko 38,^{IP}, J. Bracinik 20,^{IP}, N. Brahimi 62d,^{IP}, G. Brandt 171,^{IP}, O. Brandt 32,^{IP},
 F. Braren 48,^{IP}, B. Brau 103,^{IP}, J.E. Brau 123,^{IP}, K. Brendlinger 48,^{IP}, R. Brener 169,^{IP}, L. Brenner 114,^{IP},
 R. Brenner 161,^{IP}, S. Bressler 169,^{IP}, D. Britton 59,^{IP}, D. Britzger 110,^{IP}, I. Brock 24,^{IP}, G. Brooijmans 41,^{IP},
 W.K. Brooks 137f,^{IP}, E. Brost 29,^{IP}, L.M. Brown 165,^{IP}, T.L. Bruckler 126,^{IP}, P.A. Bruckman de Renstrom 86,^{IP},
 B. Brüers 48,^{IP}, D. Bruncko 28b,^{IP},*, A. Bruni 23b,^{IP}, G. Bruni 23b,^{IP}, M. Bruschi 23b,^{IP}, N. Bruscino 75a,75b,^{IP},
 T. Buanes 16,^{IP}, Q. Buat 138,^{IP}, A.G. Buckley 59,^{IP}, I.A. Budagov 38,^{IP},*, M.K. Bugge 125,^{IP}, O. Bulekov 37,^{IP},
 B.A. Bullard 143,^{IP}, S. Burdin 92,^{IP}, C.D. Burgard 49,^{IP}, A.M. Burger 40,^{IP}, B. Burghgrave 8,^{IP},
 O. Burlayenko 54,^{IP}, J.T.P. Burr 32,^{IP}, C.D. Burton 11,^{IP}, J.C. Burzynski 142,^{IP}, E.L. Busch 41,^{IP},
 V. Büscher 100,^{IP}, P.J. Bussey 59,^{IP}, J.M. Butler 25,^{IP}, C.M. Buttar 59,^{IP}, J.M. Butterworth 96,^{IP},
 W. Buttlinger 134,^{IP}, C.J. Buxo Vazquez 107, A.R. Buzykaev 37,^{IP}, G. Cabras 23b,^{IP}, S. Cabrera Urbán 163,^{IP},
 D. Caforio 58,^{IP}, H. Cai 129,^D, Y. Cai 14a,14e,^{IP}, V.M.M. Cairo 36,^{IP}, O. Cakir 3a,^{IP}, N. Calace 36,^{IP},
 P. Calafiura 17a,^{IP}, G. Calderini 127,^{IP}, P. Calfayan 68,^{IP}, G. Callea 59,^{IP}, L.P. Caloba 82b,^{IP}, D. Calvet 40,^{IP},
 S. Calvet 40,^{IP}, T.P. Calvet 102,^{IP}, M. Calvetti 74a,74b,^{IP}, R. Camacho Toro 127,^{IP}, S. Camarda 36,^{IP},
 D. Camarero Munoz 26,^{IP}, P. Camarri 76a,76b,^{IP}, M.T. Camerlingo 72a,72b,^{IP}, D. Cameron 125,^{IP},
 C. Camincher 165,^{IP}, M. Campanelli 96,^{IP}, A. Camplani 42,^{IP}, V. Canale 72a,72b,^{IP}, A. Canesse 104,^{IP},
 M. Cano Bret 80,^{IP}, J. Cantero 163,^{IP}, Y. Cao 162,^{IP}, F. Capocasa 26,^{IP}, M. Capua 43b,43a,^{IP},
 A. Carbone 71a,71b,^{IP}, R. Cardarelli 76a,^{IP}, J.C.J. Cardenas 8,^{IP}, F. Cardillo 163,^{IP}, T. Carli 36,^{IP}, G. Carlino 72a,^{IP},
 J.I. Carlotto 13,^{IP}, B.T. Carlson 129,^{IP},*, E.M. Carlson 165,156a,^{IP}, L. Carminati 71a,71b,^{IP}, M. Carnesale 75a,75b,^{IP},
 S. Caron 113,^{IP}, E. Carquin 137f,^{IP}, S. Carrá 71a,71b,^{IP}, G. Carratta 23b,23a,^{IP}, F. Carrio Argos 33g,^{IP},
 J.W.S. Carter 155,^{IP}, T.M. Carter 52,^{IP}, M.P. Casado 13,^{IP},*, A.F. Casha 155, M. Caspar 48,^{IP}, E.G. Castiglia 172,^{IP},
 F.L. Castillo 63a,^{IP}, L. Castillo Garcia 13,^{IP}, V. Castillo Gimenez 163,^{IP}, N.F. Castro 130a,130e,^{IP},
 A. Catinaccio 36,^{IP}, J.R. Catmore 125,^{IP}, V. Cavaliere 29,^{IP}, N. Cavalli 23b,23a,^{IP}, V. Cavasinni 74a,74b,^{IP},
 E. Celebi 21a,^{IP}, F. Celli 126,^{IP}, M.S. Centonze 70a,70b,^{IP}, K. Cerny 122,^{IP}, A.S. Cerqueira 82a,^{IP}, A. Cerri 146,^{IP},

- L. Cerrito 76a, 76b, [ID](#), F. Cerutti 17a, [ID](#), A. Cervelli 23b, [ID](#), G. Cesarini 53, [ID](#), S.A. Cetin 21d, [ID](#), Z. Chadi 35a, [ID](#),
 D. Chakraborty 115, [ID](#), M. Chala 130f, [ID](#), J. Chan 170, [ID](#), W.Y. Chan 153, [ID](#), J.D. Chapman 32, [ID](#),
 B. Chargeishvili 149b, [ID](#), D.G. Charlton 20, [ID](#), T.P. Charman 94, [ID](#), M. Chatterjee 19, [ID](#), C. Chauhan 133, [ID](#),
 S. Chekanov 6, [ID](#), S.V. Chekulaev 156a, [ID](#), G.A. Chelkov 38, [ID](#), a, A. Chen 106, [ID](#), B. Chen 151, [ID](#), B. Chen 165, [ID](#),
 H. Chen 14c, [ID](#), H. Chen 29, [ID](#), J. Chen 62c, [ID](#), J. Chen 142, [ID](#), S. Chen 153, [ID](#), S.J. Chen 14c, [ID](#), X. Chen 62c, [ID](#),
 X. Chen 14b, [ID](#), ah, Y. Chen 62a, [ID](#), C.L. Cheng 170, [ID](#), H.C. Cheng 64a, [ID](#), S. Cheong 143, [ID](#), A. Cheplakov 38, [ID](#),
 E. Cheremushkina 48, [ID](#), E. Cherepanova 114, [ID](#), R. Cherkaoui El Moursli 35e, [ID](#), E. Cheu 7, [ID](#), K. Cheung 65, [ID](#),
 L. Chevalier 135, [ID](#), V. Chiarella 53, [ID](#), G. Chiarelli 74a, [ID](#), N. Chiedde 102, [ID](#), G. Chiodini 70a, [ID](#),
 A.S. Chisholm 20, [ID](#), A. Chitan 27b, [ID](#), M. Chitishvili 163, [ID](#), M.V. Chizhov 38, [ID](#), K. Choi 11, [ID](#),
 A.R. Chomont 75a, 75b, [ID](#), Y. Chou 103, [ID](#), E.Y.S. Chow 114, [ID](#), T. Chowdhury 33g, [ID](#), L.D. Christopher 33g, [ID](#),
 K.L. Chu 64a, M.C. Chu 64a, [ID](#), X. Chu 14a, 14e, [ID](#), J. Chudoba 131, [ID](#), J.J. Chwastowski 86, [ID](#), D. Cieri 110, [ID](#),
 K.M. Ciesla 85a, [ID](#), V. Cindro 93, [ID](#), A. Ciocio 17a, [ID](#), F. Cirotto 72a, 72b, [ID](#), Z.H. Citron 169, [ID](#), m, M. Citterio 71a, [ID](#),
 D.A. Ciubotaru 27b, B.M. Ciungu 155, [ID](#), A. Clark 56, [ID](#), P.J. Clark 52, [ID](#), J.M. Clavijo Columbie 48, [ID](#),
 S.E. Clawson 101, [ID](#), C. Clement 47a, 47b, [ID](#), J. Clercx 48, [ID](#), L. Clissa 23b, 23a, [ID](#), Y. Coadou 102, [ID](#),
 M. Cobal 69a, 69c, [ID](#), A. Coccaro 57b, [ID](#), R.F. Coelho Barrue 130a, [ID](#), R. Coelho Lopes De Sa 103, [ID](#),
 S. Coelli 71a, [ID](#), H. Cohen 151, [ID](#), A.E.C. Coimbra 71a, 71b, [ID](#), B. Cole 41, [ID](#), J. Collot 60, [ID](#),
 P. Conde Muiño 130a, 130g, [ID](#), M.P. Connell 33c, [ID](#), S.H. Connell 33c, [ID](#), I.A. Connelly 59, [ID](#), E.I. Conroy 126, [ID](#),
 F. Conventi 72a, [ID](#), aj, H.G. Cooke 20, [ID](#), A.M. Cooper-Sarkar 126, [ID](#), F. Cormier 164, [ID](#), L.D. Corpe 36, [ID](#),
 M. Corradi 75a, 75b, [ID](#), F. Corriveau 104, [ID](#), z, A. Cortes-Gonzalez 18, [ID](#), M.J. Costa 163, [ID](#), F. Costanza 4, [ID](#),
 D. Costanzo 139, [ID](#), B.M. Cote 119, [ID](#), G. Cowan 95, [ID](#), K. Cranmer 117, [ID](#), S. Crépé-Renaudin 60, [ID](#),
 F. Crescioli 127, [ID](#), M. Cristinziani 141, [ID](#), M. Cristoforetti 78a, 78b, [ID](#), d, V. Croft 114, [ID](#), G. Crosetti 43b, 43a, [ID](#),
 A. Cueto 36, [ID](#), T. Cuhadar Donszelmann 160, [ID](#), H. Cui 14a, 14e, [ID](#), Z. Cui 7, [ID](#), W.R. Cunningham 59, [ID](#),
 F. Curcio 43b, 43a, [ID](#), P. Czodrowski 36, [ID](#), M.M. Czurylo 63b, [ID](#), M.J. Da Cunha Sargedas De Sousa 62a, [ID](#),
 J.V. Da Fonseca Pinto 82b, [ID](#), C. Da Via 101, [ID](#), W. Dabrowski 85a, [ID](#), T. Dado 49, [ID](#), S. Dahbi 33g, [ID](#), T. Dai 106, [ID](#),
 C. Dallapiccola 103, [ID](#), M. Dam 42, [ID](#), G. D'amen 29, [ID](#), V. D'Amico 109, [ID](#), J. Damp 100, [ID](#), J.R. Dandoy 128, [ID](#),
 M.F. Daneri 30, [ID](#), M. Danninger 142, [ID](#), V. Dao 36, [ID](#), G. Darbo 57b, [ID](#), S. Darmora 6, [ID](#), S.J. Das 29, [ID](#), ak,
 S. D'Auria 71a, 71b, [ID](#), C. David 156b, [ID](#), T. Davidek 133, [ID](#), B. Davis-Purcell 34, [ID](#), I. Dawson 94, [ID](#), K. De 8, [ID](#),
 R. De Asmundis 72a, [ID](#), N. De Biase 48, [ID](#), S. De Castro 23b, 23a, [ID](#), N. De Groot 113, [ID](#), P. de Jong 114, [ID](#),
 H. De la Torre 107, [ID](#), A. De Maria 14c, [ID](#), A. De Salvo 75a, [ID](#), U. De Sanctis 76a, 76b, [ID](#), A. De Santo 146, [ID](#),
 J.B. De Vivie De Regie 60, [ID](#), D.V. Dedovich 38, [ID](#), J. Degens 114, [ID](#), A.M. Deiana 44, [ID](#), F. Del Corso 23b, 23a, [ID](#),
 J. Del Peso 99, [ID](#), F. Del Rio 63a, [ID](#), F. Deliot 135, [ID](#), C.M. Delitzsch 49, [ID](#), M. Della Pietra 72a, 72b, [ID](#),
 D. Della Volpe 56, [ID](#), A. Dell'Acqua 36, [ID](#), L. Dell'Asta 71a, 71b, [ID](#), M. Delmastro 4, [ID](#), P.A. Delsart 60, [ID](#),
 S. Demers 172, [ID](#), M. Demichev 38, [ID](#), S.P. Denisov 37, [ID](#), L. D'Eramo 115, [ID](#), D. Derendarz 86, [ID](#), F. Derue 127, [ID](#),
 P. Dervan 92, [ID](#), K. Desch 24, [ID](#), K. Dette 155, [ID](#), C. Deutsch 24, [ID](#), F.A. Di Bello 57b, 57a, [ID](#),
 A. Di Ciaccio 76a, 76b, [ID](#), L. Di Ciaccio 4, [ID](#), A. Di Domenico 75a, 75b, [ID](#), C. Di Donato 72a, 72b, [ID](#),
 A. Di Girolamo 36, [ID](#), G. Di Gregorio 5, [ID](#), A. Di Luca 78a, 78b, [ID](#), B. Di Micco 77a, 77b, [ID](#), R. Di Nardo 77a, 77b, [ID](#),
 C. Diaconu 102, [ID](#), F.A. Dias 114, [ID](#), T. Dias Do Vale 142, [ID](#), M.A. Diaz 137a, 137b, [ID](#), F.G. Diaz Capriles 24, [ID](#),
 M. Didenko 163, [ID](#), E.B. Diehl 106, [ID](#), L. Diehl 54, [ID](#), S. Díez Cornell 48, [ID](#), C. Diez Pardos 141, [ID](#),
 C. Dimitriadi 24, 161, [ID](#), A. Dimitrieva 17a, [ID](#), J. Dingfelder 24, [ID](#), I-M. Dinu 27b, [ID](#), S.J. Dittmeier 63b, [ID](#),
 F. Dittus 36, [ID](#), F. Djama 102, [ID](#), T. Djoberava 149b, [ID](#), J.I. Djuvsland 16, [ID](#), C. Doglioni 101, 98, [ID](#), J. Dolejsi 133, [ID](#),
 Z. Dolezal 133, [ID](#), M. Donadelli 82c, [ID](#), B. Dong 107, [ID](#), J. Donini 40, [ID](#), A. D'Onofrio 77a, 77b, [ID](#),
 M. D'Onofrio 92, [ID](#), J. Dopke 134, [ID](#), A. Doria 72a, [ID](#), M.T. Dova 90, [ID](#), A.T. Doyle 59, [ID](#), M.A. Draguet 126, [ID](#),

- E. Drechsler 142, ID, E. Dreyer 169, ID, I. Drivas-koulouris 10, ID, A.S. Drobac 158, ID, M. Drozdova 56, ID,
 D. Du 62a, ID, T.A. du Pree 114, ID, F. Dubinin 37, ID, M. Dubovsky 28a, ID, E. Duchovni 169, ID, G. Duckeck 109, ID,
 O.A. Ducu 27b, ID, D. Duda 110, ID, A. Dudarev 36, ID, E.R. Duden 26, ID, M. D'uffizi 101, ID, L. Duflot 66, ID,
 M. Dührssen 36, ID, C. Dülsen 171, ID, A.E. Dumitriu 27b, ID, M. Dunford 63a, ID, S. Dungs 49, ID,
 K. Dunne 47a, 47b, ID, A. Duperrin 102, ID, H. Duran Yildiz 3a, ID, M. Düren 58, ID, A. Durglishvili 149b, ID,
 B.L. Dwyer 115, ID, G.I. Dyckes 17a, ID, M. Dyndal 85a, ID, S. Dysch 101, ID, B.S. Dziedzic 86, ID,
 Z.O. Earnshaw 146, ID, B. Eckerova 28a, ID, S. Eggebrecht 55, ID, M.G. Eggleston 51,
 E. Egidio Purcino De Souza 127, ID, L.F. Ehrke 56, ID, G. Eigen 16, ID, K. Einsweiler 17a, ID, T. Ekelof 161, ID,
 P.A. Ekman 98, ID, Y. El Ghazali 35b, ID, H. El Jarrari 35e, 148, ID, A. El Moussaouy 35a, ID, V. Ellajosyula 161, ID,
 M. Ellert 161, ID, F. Ellinghaus 171, ID, A.A. Elliot 94, ID, N. Ellis 36, ID, J. Elmsheuser 29, ID, M. Elsing 36, ID,
 D. Emeliyanov 134, ID, Y. Enari 153, ID, I. Ene 17a, ID, S. Epari 13, ID, J. Erdmann 49, ID, P.A. Erland 86, ID,
 M. Errenst 171, ID, M. Escalier 66, ID, C. Escobar 163, ID, E. Etzion 151, ID, G. Evans 130a, ID, H. Evans 68, ID,
 L.S. Evans 95, ID, M.O. Evans 146, ID, A. Ezhilov 37, ID, S. Ezzarqtouni 35a, ID, F. Fabbri 59, ID, L. Fabbri 23b, 23a, ID,
 G. Facini 96, ID, V. Fadeyev 136, ID, R.M. Fakhrutdinov 37, ID, S. Falciano 75a, ID, L.F. Falda Ulhoa Coelho 36, ID,
 P.J. Falke 24, ID, S. Falke 36, ID, J. Faltova 133, ID, C. Fan 162, ID, Y. Fan 14a, ID, Y. Fang 14a, 14e, ID, M. Fanti 71a, 71b, ID,
 M. Faraj 69a, 69b, ID, Z. Farazpay 97, ID, A. Farbin 8, ID, A. Farilla 77a, ID, T. Farooque 107, ID, S.M. Farrington 52, ID,
 F. Fassi 35e, ID, D. Fassouliotis 9, ID, M. Faucci Giannelli 76a, 76b, ID, W.J. Fawcett 32, ID, L. Fayard 66, ID,
 P. Federic 133, ID, P. Federicova 131, ID, O.L. Fedin 37, ID, a, G. Fedotov 37, ID, M. Feickert 170, ID, L. Feligioni 102, ID,
 A. Fell 139, ID, D.E. Fellers 123, ID, C. Feng 62b, ID, M. Feng 14b, ID, Z. Feng 114, ID, M.J. Fenton 160, ID,
 A.B. Fenyuk 37, L. Ferencz 48, ID, R.A.M. Ferguson 91, ID, S.I. Fernandez Luengo 137f, ID, M.J.V. Fernoux 102, ID,
 J. Ferrando 48, ID, A. Ferrari 161, ID, P. Ferrari 114, 113, ID, R. Ferrari 73a, ID, D. Ferrere 56, ID, C. Ferretti 106, ID,
 F. Fiedler 100, ID, A. Filipčič 93, ID, E.K. Filmer 1, ID, F. Filthaut 113, ID, M.C.N. Fiolhais 130a, 130c, ID, c,
 L. Fiorini 163, ID, W.C. Fisher 107, ID, T. Fitschen 101, ID, I. Fleck 141, ID, P. Fleischmann 106, ID, T. Flick 171, ID,
 L. Flores 128, ID, M. Flores 33d, ID, af, L.R. Flores Castillo 64a, ID, F.M. Follega 78a, 78b, ID, N. Fomin 16, ID,
 J.H. Foo 155, ID, B.C. Forland 68, A. Formica 135, ID, A.C. Forti 101, ID, E. Fortin 36, ID, A.W. Fortman 61, ID,
 M.G. Foti 17a, ID, L. Fountas 9, ID, k, D. Fournier 66, ID, H. Fox 91, ID, P. Francavilla 74a, 74b, ID, S. Francescato 61, ID,
 S. Franchellucci 56, ID, M. Franchini 23b, 23a, ID, S. Franchino 63a, ID, D. Francis 36, L. Franco 113, ID,
 L. Franconi 48, ID, M. Franklin 61, ID, G. Frattari 26, ID, A.C. Freegard 94, ID, W.S. Freund 82b, ID, Y.Y. Frid 151, ID,
 N. Fritzsche 50, ID, A. Froch 54, ID, D. Froidevaux 36, ID, J.A. Frost 126, ID, Y. Fu 62a, ID, M. Fujimoto 118, ID,
 E. Fullana Torregrosa 163, ID, *, E. Furtado De Simas Filho 82b, ID, J. Fuster 163, ID, A. Gabrielli 23b, 23a, ID,
 A. Gabrielli 155, ID, P. Gadow 48, ID, G. Gagliardi 57b, 57a, ID, L.G. Gagnon 17a, ID, E.J. Gallas 126, ID,
 B.J. Gallop 134, ID, K.K. Gan 119, ID, S. Ganguly 153, ID, J. Gao 62a, ID, Y. Gao 52, ID, F.M. Garay Walls 137a, 137b, ID,
 B. Garcia 29, ak, C. García 163, ID, A. Garcia Alonso 114, ID, J.E. García Navarro 163, ID, M. Garcia-Sciveres 17a, ID,
 R.W. Gardner 39, ID, D. Garg 80, ID, R.B. Garg 143, ID, q, C.A. Garner 155, S.J. Gasiorowski 138, ID, P. Gaspar 82b, ID,
 G. Gaudio 73a, ID, V. Gautam 13, P. Gauzzi 75a, 75b, ID, I.L. Gavrilenko 37, ID, A. Gavril'yuk 37, ID, C. Gay 164, ID,
 G. Gaycken 48, ID, E.N. Gazis 10, ID, A.A. Geanta 27b, 27e, ID, C.M. Gee 136, ID, C. Gemme 57b, ID,
 M.H. Genest 60, ID, S. Gentile 75a, 75b, ID, S. George 95, ID, W.F. George 20, ID, T. Geralis 46, ID, L.O. Gerlach 55,
 P. Gessinger-Befurt 36, ID, M.E. Geyik 171, ID, M. Ghneimat 141, ID, K. Ghorbanian 94, ID, A. Ghosal 141, ID,
 A. Ghosh 160, ID, A. Ghosh 7, ID, B. Giacobbe 23b, ID, S. Giagu 75a, 75b, ID, P. Giannetti 74a, ID, A. Giannini 62a, ID,
 S.M. Gibson 95, ID, M. Gignac 136, ID, D.T. Gil 85b, ID, A.K. Gilbert 85a, ID, B.J. Gilbert 41, ID, D. Gillberg 34, ID,
 G. Gilles 114, ID, N.E.K. Gillwald 48, ID, L. Ginabat 127, ID, D.M. Gingrich 2, ID, ai, M.P. Giordani 69a, 69c, ID,
 P.F. Giraud 135, ID, G. Giugliarelli 69a, 69c, ID, D. Giugni 71a, ID, F. Giulii 36, ID, k, I. Gkialas 9, ID, k, L.K. Gladilin 37, ID,

- C. Glasman 99, ^{id}, G.R. Gledhill 123, ^{id}, M. Glisic 123, I. Gnesi 43b, ^{id,g}, Y. Go 29, ^{id,ak}, M. Goblirsch-Kolb 36, ^{id},
 B. Gocke 49, ^{id}, D. Godin 108, B. Gokturk 21a, ^{id}, S. Goldfarb 105, ^{id}, T. Golling 56, ^{id}, M.G.D. Gololo 33g,
 D. Golubkov 37, ^{id}, J.P. Gombas 107, ^{id}, A. Gomes 130a, 130b, ^{id}, G. Gomes Da Silva 141, ^{id},
 A.J. Gomez Delegido 163, ^{id}, R. Gonçalo 130a, 130c, ^{id}, G. Gonella 123, ^{id}, L. Gonella 20, ^{id}, A. Gongadze 38, ^{id},
 F. Gonnella 20, ^{id}, J.L. Gonski 41, ^{id}, R.Y. González Andana 52, ^{id}, S. González de la Hoz 163, ^{id},
 S. Gonzalez Fernandez 13, ^{id}, R. Gonzalez Lopez 92, ^{id}, C. Gonzalez Renteria 17a, ^{id}, R. Gonzalez Suarez 161, ^{id},
 S. Gonzalez-Sevilla 56, ^{id}, G.R. Gonzalvo Rodriguez 163, ^{id}, L. Goossens 36, ^{id}, P.A. Gorbounov 37, ^{id},
 B. Gorini 36, ^{id}, E. Gorini 70a, 70b, ^{id}, A. Gorišek 93, ^{id}, T.C. Gosart 128, ^{id}, A.T. Goshaw 51, ^{id}, M.I. Gostkin 38, ^{id},
 S. Goswami 121, ^{id}, C.A. Gottardo 36, ^{id}, M. Gouighri 35b, ^{id}, V. Goumarre 48, ^{id}, A.G. Goussiou 138, ^{id},
 N. Govender 33c, ^{id}, I. Grabowska-Bold 85a, ^{id}, K. Graham 34, ^{id}, E. Gramstad 125, ^{id}, S. Grancagnolo 70a, 70b, ^{id},
 M. Grandi 146, ^{id}, V. Gratchev 37, ^{*,} P.M. Gravila 27f, ^{id}, F.G. Gravili 70a, 70b, ^{id}, H.M. Gray 17a, ^{id},
 M. Greco 70a, 70b, ^{id}, C. Grefe 24, ^{id}, I.M. Gregor 48, ^{id}, P. Grenier 143, ^{id}, C. Grieco 13, ^{id}, A.A. Grillo 136, ^{id},
 K. Grimm 31, ^{id,n}, S. Grinstein 13, ^{id,v}, J.-F. Grivaz 66, ^{id}, E. Gross 169, ^{id}, J. Grosse-Knetter 55, ^{id}, C. Grud 106, ^{id},
 J.C. Grundy 126, ^{id}, L. Guan 106, ^{id}, W. Guan 29, ^{id}, C. Gubbels 164, ^{id}, J.G.R. Guerrero Rojas 163, ^{id},
 G. Guerrieri 69a, 69b, ^{id}, F. Guescini 110, ^{id}, R. Gugel 100, ^{id}, J.A.M. Guhit 106, ^{id}, A. Guida 48, ^{id}, T. Guillemin 4, ^{id},
 E. Guilloton 167, 134, ^{id}, S. Guindon 36, ^{id}, F. Guo 14a, 14e, ^{id}, J. Guo 62c, ^{id}, L. Guo 66, ^{id}, Y. Guo 106, ^{id},
 R. Gupta 48, ^{id}, S. Gurbuz 24, ^{id}, S.S. Gurdasani 54, ^{id}, G. Gustavino 36, ^{id}, M. Guth 56, ^{id}, P. Gutierrez 120, ^{id},
 L.F. Gutierrez Zagazeta 128, ^{id}, C. Gutschow 96, ^{id}, C. Gwenlan 126, ^{id}, C.B. Gwilliam 92, ^{id}, E.S. Haaland 125, ^{id},
 A. Haas 117, ^{id}, M. Habedank 48, ^{id}, C. Haber 17a, ^{id}, H.K. Hadavand 8, ^{id}, A. Hadef 100, ^{id}, S. Hadzic 110, ^{id},
 E.H. Haines 96, ^{id}, M. Haleem 166, ^{id}, J. Haley 121, ^{id}, J.J. Hall 139, ^{id}, G.D. Hallewell 102, ^{id}, L. Halser 19, ^{id},
 K. Hamano 165, ^{id}, H. Hamdaoui 35e, ^{id}, M. Hamer 24, ^{id}, G.N. Hamity 52, ^{id}, E.J. Hampshire 95, ^{id}, J. Han 62b, ^{id},
 K. Han 62a, ^{id}, L. Han 14c, ^{id}, L. Han 62a, ^{id}, S. Han 17a, ^{id}, Y.F. Han 155, ^{id}, K. Hanagaki 83, ^{id}, M. Hance 136, ^{id},
 D.A. Hangal 41, ^{id,ae}, H. Hanif 142, ^{id}, M.D. Hank 128, ^{id}, R. Hankache 101, ^{id}, J.B. Hansen 42, ^{id},
 J.D. Hansen 42, ^{id}, P.H. Hansen 42, ^{id}, K. Hara 157, ^{id}, D. Harada 56, ^{id}, T. Harenberg 171, ^{id}, S. Harkusha 37, ^{id},
 Y.T. Harris 126, ^{id}, N.M. Harrison 119, ^{id}, P.F. Harrison 167, N.M. Hartman 143, ^{id}, N.M. Hartmann 109, ^{id},
 Y. Hasegawa 140, ^{id}, A. Hasib 52, ^{id}, S. Haug 19, ^{id}, R. Hauser 107, ^{id}, M. Havranek 132, ^{id}, C.M. Hawkes 20, ^{id},
 R.J. Hawkings 36, ^{id}, S. Hayashida 111, ^{id}, D. Hayden 107, ^{id}, C. Hayes 106, ^{id}, R.L. Hayes 114, ^{id}, C.P. Hays 126, ^{id},
 J.M. Hays 94, ^{id}, H.S. Hayward 92, ^{id}, F. He 62a, ^{id}, Y. He 154, ^{id}, Y. He 127, ^{id}, N.B. Heatley 94, ^{id},
 V. Hedberg 98, ^{id}, A.L. Heggelund 125, ^{id}, N.D. Hehir 94, ^{id}, C. Heidegger 54, ^{id}, K.K. Heidegger 54, ^{id},
 W.D. Heidorn 81, ^{id}, J. Heilman 34, ^{id}, S. Heim 48, ^{id}, T. Heim 17a, ^{id}, J.G. Heinlein 128, ^{id}, J.J. Heinrich 123, ^{id},
 L. Heinrich 110, ^{id,ag}, J. Hejbal 131, ^{id}, L. Helary 48, ^{id}, A. Held 170, ^{id}, S. Hellesund 16, ^{id}, C.M. Helling 164, ^{id},
 S. Hellman 47a, 47b, ^{id}, C. Helsens 36, ^{id}, R.C.W. Henderson 91, L. Henkelmann 32, ^{id},
 A.M. Henriques Correia 36, H. Herde 98, ^{id}, Y. Hernández Jiménez 145, ^{id}, L.M. Herrmann 24, ^{id},
 T. Herrmann 50, ^{id}, G. Herten 54, ^{id}, R. Hertenberger 109, ^{id}, L. Hervas 36, ^{id}, N.P. Hessey 156a, ^{id}, H. Hibi 84, ^{id},
 S.J. Hillier 20, ^{id}, F. Hinterkeuser 24, ^{id}, M. Hirose 124, ^{id}, S. Hirose 157, ^{id}, D. Hirschbuehl 171, ^{id},
 T.G. Hitchings 101, ^{id}, B. Hiti 93, ^{id}, J. Hobbs 145, ^{id}, R. Hobincu 27e, ^{id}, N. Hod 169, ^{id}, M.C. Hodgkinson 139, ^{id},
 B.H. Hodkinson 32, ^{id}, A. Hoecker 36, ^{id}, J. Hofer 48, ^{id}, T. Holm 24, ^{id}, M. Holzbock 110, ^{id},
 L.B.A.H. Hommels 32, ^{id}, B.P. Honan 101, ^{id}, J. Hong 62c, ^{id}, T.M. Hong 129, ^{id}, J.C. Honig 54, ^{id},
 B.H. Hooberman 162, ^{id}, W.H. Hopkins 6, ^{id}, Y. Horii 111, ^{id}, S. Hou 148, ^{id}, A.S. Howard 93, ^{id}, J. Howarth 59, ^{id},
 J. Hoya 6, ^{id}, M. Hrabovsky 122, ^{id}, A. Hrynevich 48, ^{id}, T. Hrynn'ova 4, ^{id}, P.J. Hsu 65, ^{id}, S.-C. Hsu 138, ^{id},
 Q. Hu 41, ^{id}, Y.F. Hu 14a, 14e, ^{id}, D.P. Huang 96, ^{id}, S. Huang 64b, ^{id}, X. Huang 14c, ^{id}, Y. Huang 62a, ^{id},
 Y. Huang 14a, ^{id}, Z. Huang 101, ^{id}, Z. Hubacek 132, ^{id}, M. Huebner 24, ^{id}, F. Huegging 24, ^{id}, T.B. Huffman 126, ^{id},

- M. Huhtinen ^{36, ID}, S.K. Huiberts ^{16, ID}, R. Hulskens ^{104, ID}, N. Huseynov ^{12, ID, a}, J. Huston ^{107, ID}, J. Huth ^{61, ID}, R. Hyneman ^{143, ID}, G. Iacobucci ^{56, ID}, G. Iakovidis ^{29, ID}, I. Ibragimov ^{141, ID}, L. Iconomidou-Fayard ^{66, ID}, P. Iengo ^{72a, 72b, ID}, R. Iguchi ^{153, ID}, T. Iizawa ^{56, ID}, Y. Ikegami ^{83, ID}, A. Ilg ^{19, ID}, N. Ilic ^{155, ID}, H. Imam ^{35a, ID}, T. Ingebretsen Carlson ^{47a, 47b, ID}, G. Introzzi ^{73a, 73b, ID}, M. Iodice ^{77a, ID}, V. Ippolito ^{75a, 75b, ID}, M. Ishino ^{153, ID}, W. Islam ^{170, ID}, C. Issever ^{18, 48, ID}, S. Istin ^{21a, ID, am}, H. Ito ^{168, ID}, J.M. Iturbe Ponce ^{64a, ID}, R. Iuppa ^{78a, 78b, ID}, A. Ivina ^{169, ID}, J.M. Izen ^{45, ID}, V. Izzo ^{72a, ID}, P. Jacka ^{131, 132, ID}, P. Jackson ^{1, ID}, R.M. Jacobs ^{48, ID}, B.P. Jaeger ^{142, ID}, C.S. Jagfeld ^{109, ID}, P. Jain ^{54, ID}, G. Jäkel ^{171, ID}, K. Jakobs ^{54, ID}, T. Jakoubek ^{169, ID}, J. Jamieson ^{59, ID}, K.W. Janas ^{85a, ID}, A.E. Jaspan ^{92, ID}, M. Javurkova ^{103, ID}, F. Jeanneau ^{135, ID}, L. Jeanty ^{123, ID}, J. Jejelava ^{149a, ID, ac}, P. Jenni ^{54, ID, h}, C.E. Jessiman ^{34, ID}, S. Jézéquel ^{4, ID}, C. Jia ^{62b}, J. Jia ^{145, ID}, X. Jia ^{61, ID}, X. Jia ^{14a, 14e, ID}, Z. Jia ^{14c, ID}, Y. Jiang ^{62a}, S. Jiggins ^{48, ID}, J. Jimenez Pena ^{110, ID}, S. Jin ^{14c, ID}, A. Jinaru ^{27b, ID}, O. Jinnouchi ^{154, ID}, P. Johansson ^{139, ID}, K.A. Johns ^{7, ID}, J.W. Johnson ^{136, ID}, D.M. Jones ^{32, ID}, E. Jones ^{48, ID}, P. Jones ^{32, ID}, R.W.L. Jones ^{91, ID}, T.J. Jones ^{92, ID}, R. Joshi ^{119, ID}, J. Jovicevic ^{15, ID}, X. Ju ^{17a, ID}, J.J. Junggeburth ^{36, ID}, T. Junkermann ^{63a, ID}, A. Juste Rozas ^{13, ID, v}, S. Kabana ^{137e, ID}, A. Kaczmarska ^{86, ID}, M. Kado ^{110, ID}, H. Kagan ^{119, ID}, M. Kagan ^{143, ID}, A. Kahn ⁴¹, A. Kahn ^{128, ID}, C. Kahra ^{100, ID}, T. Kaji ^{168, ID}, E. Kajomovitz ^{150, ID}, N. Kakati ^{169, ID}, C.W. Kalderon ^{29, ID}, A. Kamenshchikov ^{155, ID}, S. Kanayama ^{154, ID}, N.J. Kang ^{136, ID}, D. Kar ^{33g, ID}, K. Karava ^{126, ID}, M.J. Kareem ^{156b, ID}, E. Karentzos ^{54, ID}, I. Karkalias ^{152, ID, f}, S.N. Karpov ^{38, ID}, Z.M. Karpova ^{38, ID}, V. Kartvelishvili ^{91, ID}, A.N. Karyukhin ^{37, ID}, E. Kasimi ^{152, ID, f}, J. Katzy ^{48, ID}, S. Kaur ^{34, ID}, K. Kawade ^{140, ID}, T. Kawamoto ^{135, ID}, G. Kawamura ⁵⁵, E.F. Kay ^{165, ID}, F.I. Kaya ^{158, ID}, S. Kazakos ^{13, ID}, V.F. Kazanin ^{37, ID}, Y. Ke ^{145, ID}, J.M. Keaveney ^{33a, ID}, R. Keeler ^{165, ID}, G.V. Kehris ^{61, ID}, J.S. Keller ^{34, ID}, A.S. Kelly ⁹⁶, D. Kelsey ^{146, ID}, J.J. Kempster ^{146, ID}, K.E. Kennedy ^{41, ID}, P.D. Kennedy ^{100, ID}, O. Kepka ^{131, ID}, B.P. Kerridge ^{167, ID}, S. Kersten ^{171, ID}, B.P. Kerševan ^{93, ID}, S. Keshri ^{66, ID}, L. Keszeghova ^{28a, ID}, S. Ketabchi Haghighat ^{155, ID}, M. Khandoga ^{127, ID}, A. Khanov ^{121, ID}, A.G. Kharlamov ^{37, ID}, T. Kharlamova ^{37, ID}, E.E. Khoda ^{138, ID}, T.J. Khoo ^{18, ID}, G. Khoriauli ^{166, ID}, J. Khubua ^{149b, ID}, Y.A.R. Khwaira ^{66, ID}, M. Kiehn ^{36, ID}, A. Kilgallon ^{123, ID}, D.W. Kim ^{47a, 47b, ID}, Y.K. Kim ^{39, ID}, N. Kimura ^{96, ID}, A. Kirchhoff ^{55, ID}, C. Kirfel ^{24, ID}, J. Kirk ^{134, ID}, A.E. Kiryunin ^{110, ID}, T. Kishimoto ^{153, ID}, D.P. Kisliuk ¹⁵⁵, C. Kitsaki ^{10, ID}, O. Kivernyk ^{24, ID}, M. Klassen ^{63a, ID}, C. Klein ^{34, ID}, L. Klein ^{166, ID}, M.H. Klein ^{106, ID}, M. Klein ^{92, ID}, S.B. Klein ^{56, ID}, U. Klein ^{92, ID}, P. Klimek ^{36, ID}, A. Klimentov ^{29, ID}, T. Klioutchnikova ^{36, ID}, P. Kluit ^{114, ID}, S. Kluth ^{110, ID}, E. Kneringer ^{79, ID}, T.M. Knight ^{155, ID}, A. Knue ^{54, ID}, R. Kobayashi ^{87, ID}, M. Kocian ^{143, ID}, P. Kodyš ^{133, ID}, D.M. Koeck ^{123, ID}, P.T. Koenig ^{24, ID}, T. Koffas ^{34, ID}, M. Kolb ^{135, ID}, I. Koletsou ^{4, ID}, T. Komarek ^{122, ID}, K. Köneke ^{54, ID}, A.X.Y. Kong ^{1, ID}, T. Kono ^{118, ID}, N. Konstantinidis ^{96, ID}, B. Konya ^{98, ID}, R. Kopeliansky ^{68, ID}, S. Koperny ^{85a, ID}, K. Korcyl ^{86, ID}, K. Kordas ^{152, ID, f}, G. Koren ^{151, ID}, A. Korn ^{96, ID}, S. Korn ^{55, ID}, I. Korolkov ^{13, ID}, N. Korotkova ^{37, ID}, B. Kortman ^{114, ID}, O. Kortner ^{110, ID}, S. Kortner ^{110, ID}, W.H. Kostecka ^{115, ID}, V.V. Kostyukhin ^{141, ID}, A. Kotsokechagia ^{135, ID}, A. Kotwal ^{51, ID}, A. Koulouris ^{36, ID}, A. Kourkoumeli-Charalampidi ^{73a, 73b, ID}, C. Kourkoumelis ^{9, ID}, E. Kourlitis ^{6, ID}, O. Kovanda ^{146, ID}, R. Kowalewski ^{165, ID}, W. Kozanecki ^{135, ID}, A.S. Kozhin ^{37, ID}, V.A. Kramarenko ^{37, ID}, G. Kramberger ^{93, ID}, P. Kramer ^{100, ID}, M.W. Krasny ^{127, ID}, A. Krasznahorkay ^{36, ID}, J.A. Kremer ^{100, ID}, T. Kresse ^{50, ID}, J. Kretzschmar ^{92, ID}, K. Kreul ^{18, ID}, P. Krieger ^{155, ID}, S. Krishnamurthy ^{103, ID}, M. Krivos ^{133, ID}, K. Krizka ^{20, ID}, K. Kroeninger ^{49, ID}, H. Kroha ^{110, ID}, J. Kroll ^{131, ID}, J. Kroll ^{128, ID}, K.S. Krowpman ^{107, ID}, U. Kruchonak ^{38, ID}, H. Krüger ^{24, ID}, N. Krumnack ⁸¹, M.C. Kruse ^{51, ID}, J.A. Krzysiak ^{86, ID}, O. Kuchinskaia ^{37, ID}, S. Kuday ^{3a, ID}, S. Kuehn ^{36, ID}, R. Kuesters ^{54, ID}, T. Kuhl ^{48, ID}, V. Kukhtin ^{38, ID}, Y. Kulchitsky ^{37, ID, a}, S. Kuleshov ^{137d, 137b, ID}, M. Kumar ^{33g, ID}, N. Kumari ^{102, ID}, A. Kupco ^{131, ID}, T. Kupfer ⁴⁹, A. Kupich ^{37, ID}, O. Kuprash ^{54, ID},

- H. Kurashige^{84, ID}, L.L. Kurchaninov^{156a, ID}, O. Kurdysh^{66, ID}, Y.A. Kurochkin^{37, ID}, A. Kurova^{37, ID}, M. Kuze^{154, ID}, A.K. Kvam^{103, ID}, J. Kvita^{122, ID}, T. Kwan^{104, ID}, N.G. Kyriacou^{106, ID}, L.A.O. Laatu^{102, ID}, C. Lacasta^{163, ID}, F. Lacava^{75a, 75b, ID}, H. Lacker^{18, ID}, D. Lacour^{127, ID}, N.N. Lad^{96, ID}, E. Ladygin^{38, ID}, B. Laforge^{127, ID}, T. Lagouri^{137e, ID}, S. Lai^{55, ID}, I.K. Lakomiec^{85a, ID}, N. Lalloue^{60, ID}, J.E. Lambert^{120, ID}, S. Lammers^{68, ID}, W. Lampl^{7, ID}, C. Lampoudis^{152, ID, f}, A.N. Lancaster^{115, ID}, E. Lançon^{29, ID}, U. Landgraf^{54, ID}, M.P.J. Landon^{94, ID}, V.S. Lang^{54, ID}, R.J. Langenberg^{103, ID}, A.J. Lankford^{160, ID}, F. Lanni^{36, ID}, K. Lantzsch^{24, ID}, A. Lanza^{73a, ID}, A. Lapertosa^{57b, 57a, ID}, J.F. Laporte^{135, ID}, T. Lari^{71a, ID}, F. Lasagni Manghi^{23b, ID}, M. Lassnig^{36, ID}, V. Latonova^{131, ID}, A. Laudrain^{100, ID}, A. Laurier^{150, ID}, S.D. Lawlor^{95, ID}, Z. Lawrence^{101, ID}, M. Lazzaroni^{71a, 71b, ID}, B. Le¹⁰¹, E.M. Le Boulicaut^{51, ID}, B. Leban^{93, ID}, A. Lebedev^{81, ID}, M. LeBlanc^{36, ID}, F. Ledroit-Guillon^{60, ID}, A.C.A. Lee⁹⁶, G.R. Lee^{16, ID}, S.C. Lee^{148, ID}, S. Lee^{47a, 47b, ID}, T.F. Lee^{92, ID}, L.L. Leeuw^{33c, ID}, H.P. Lefebvre^{95, ID}, M. Lefebvre^{165, ID}, C. Leggett^{17a, ID}, K. Lehmann^{142, ID}, G. Lehmann Miotti^{36, ID}, M. Leigh^{56, ID}, W.A. Leight^{103, ID}, A. Leisos^{152, ID, u}, M.A.L. Leite^{82c, ID}, C.E. Leitgeb^{48, ID}, R. Leitner^{133, ID}, K.J.C. Leney^{44, ID}, T. Lenz^{24, ID}, S. Leone^{74a, ID}, C. Leonidopoulos^{52, ID}, A. Leopold^{144, ID}, C. Leroy^{108, ID}, R. Les^{107, ID}, C.G. Lester^{32, ID}, M. Levchenko^{37, ID}, J. Levêque^{4, ID}, D. Levin^{106, ID}, L.J. Levinson^{169, ID}, M.P. Lewicki^{86, ID}, D.J. Lewis^{4, ID}, A. Li^{5, ID}, B. Li^{62b, ID}, C. Li^{62a}, C-Q. Li^{62c, ID}, H. Li^{62a, ID}, H. Li^{62b, ID}, H. Li^{14c, ID}, H. Li^{62b, ID}, J. Li^{62c, ID}, K. Li^{138, ID}, L. Li^{62c, ID}, M. Li^{14a, 14e, ID}, Q.Y. Li^{62a, ID}, S. Li^{14a, 14e, ID}, S. Li^{62d, 62c, ID, e}, T. Li^{62b, ID}, X. Li^{104, ID}, Z. Li^{62b, ID}, Z. Li^{126, ID}, Z. Li^{104, ID}, Z. Li^{92, ID}, Z. Li^{14a, 14e, ID}, Z. Liang^{14a, ID}, M. Liberatore^{48, ID}, B. Liberti^{76a, ID}, K. Lie^{64c, ID}, J. Lieber Marin^{82b, ID}, H. Lien^{68, ID}, K. Lin^{107, ID}, R.A. Linck^{68, ID}, R.E. Lindley^{7, ID}, J.H. Lindon^{2, ID}, A. Linss^{48, ID}, E. Lipeles^{128, ID}, A. Lipniacka^{16, ID}, A. Lister^{164, ID}, J.D. Little^{4, ID}, B. Liu^{14a, ID}, B.X. Liu^{142, ID}, D. Liu^{62d, 62c, ID}, J.B. Liu^{62a, ID}, J.K.K. Liu^{32, ID}, K. Liu^{62d, 62c, ID}, M. Liu^{62a, ID}, M.Y. Liu^{62a, ID}, P. Liu^{14a, ID}, Q. Liu^{62d, 138, 62c, ID}, X. Liu^{62a, ID}, Y. Liu^{14d, 14e, ID}, Y.L. Liu^{106, ID}, Y.W. Liu^{62a, ID}, J. Llorente Merino^{142, ID}, S.L. Lloyd^{94, ID}, E.M. Lobodzinska^{48, ID}, P. Loch^{7, ID}, S. Loffredo^{76a, 76b, ID}, T. Lohse^{18, ID}, K. Lohwasser^{139, ID}, E. Loiacono^{48, ID}, M. Lokajicek^{131, ID, *, ID}, J.D. Lomas^{20, ID}, J.D. Long^{162, ID}, I. Longarini^{160, ID}, L. Longo^{70a, 70b, ID}, R. Longo^{162, ID}, I. Lopez Paz^{67, ID}, A. Lopez Solis^{48, ID}, J. Lorenz^{109, ID}, N. Lorenzo Martinez^{4, ID}, A.M. Lory^{109, ID}, X. Lou^{47a, 47b, ID}, X. Lou^{14a, 14e, ID}, A. Lounis^{66, ID}, J. Love^{6, ID}, P.A. Love^{91, ID}, G. Lu^{14a, 14e, ID}, M. Lu^{80, ID}, S. Lu^{128, ID}, Y.J. Lu^{65, ID}, H.J. Lubatti^{138, ID}, C. Luci^{75a, 75b, ID}, F.L. Lucio Alves^{14c, ID}, A. Lucotte^{60, ID}, F. Luehring^{68, ID}, I. Luise^{145, ID}, O. Lukianchuk^{66, ID}, O. Lundberg^{144, ID}, B. Lund-Jensen^{144, ID}, N.A. Luongo^{123, ID}, M.S. Lutz^{151, ID}, D. Lynn^{29, ID}, H. Lyons^{92, ID}, R. Lysak^{131, ID}, E. Lytken^{98, ID}, V. Lyubushkin^{38, ID}, T. Lyubushkina^{38, ID}, M.M. Lyukova^{145, ID}, H. Ma^{29, ID}, L.L. Ma^{62b, ID}, Y. Ma^{96, ID}, D.M. Mac Donell^{165, ID}, G. Maccarrone^{53, ID}, J.C. MacDonald^{139, ID}, R. Madar^{40, ID}, W.F. Mader^{50, ID}, J. Maeda^{84, ID}, T. Maeno^{29, ID}, M. Maerker^{50, ID}, H. Maguire^{139, ID}, A. Maio^{130a, 130b, 130d, ID}, K. Maj^{85a, ID}, O. Majersky^{48, ID}, S. Majewski^{123, ID}, N. Makovec^{66, ID}, V. Maksimovic^{15, ID}, B. Malaescu^{127, ID}, Pa. Malecki^{86, ID}, V.P. Maleev^{37, ID}, F. Malek^{60, ID}, D. Malito^{43b, 43a, ID}, U. Mallik^{80, ID}, C. Malone^{32, ID}, S. Maltezos^{10, ID}, S. Malyukov^{38, ID}, J. Mamuzic^{13, ID}, G. Mancini^{53, ID}, G. Manco^{73a, 73b, ID}, J.P. Mandalia^{94, ID}, I. Mandić^{93, ID}, L. Manhaes de Andrade Filho^{82a, ID}, I.M. Maniatis^{169, ID}, J. Manjarres Ramos^{102, ID, ad}, D.C. Mankad^{169, ID}, A. Mann^{109, ID}, B. Mansoulie^{135, ID}, S. Manzoni^{36, ID}, A. Marantis^{152, ID, u}, G. Marchiori^{5, ID}, M. Marcisovsky^{131, ID}, C. Marcon^{71a, 71b, ID}, M. Marinescu^{20, ID}, M. Marjanovic^{120, ID}, E.J. Marshall^{91, ID}, Z. Marshall^{17a, ID}, S. Marti-Garcia^{163, ID}, T.A. Martin^{167, ID}, V.J. Martin^{52, ID}, B. Martin dit Latour^{16, ID}, L. Martinelli^{75a, 75b, ID}, M. Martinez^{13, ID, v}, P. Martinez Agullo^{163, ID}, V.I. Martinez Outschoorn^{103, ID}, P. Martinez Suarez^{13, ID}, S. Martin-Haugh^{134, ID}, V.S. Martoiu^{27b, ID}, A.C. Martyniuk^{96, ID}, A. Marzin^{36, ID},

- S.R. Maschek 110, , D. Mascione 78a, 78b, , L. Masetti 100, , T. Mashimo 153, , J. Masik 101, ,
 A.L. Maslennikov 37, , L. Massa 23b, , P. Massarotti 72a, 72b, , P. Mastrandrea 74a, 74b, ,
 A. Mastroberardino 43b, 43a, , T. Masubuchi 153, , T. Mathisen 161, , N. Matsuzawa 153, J. Maurer 27b, ,
 B. Maček 93, , D.A. Maximov 37, , R. Mazini 148, , I. Maznas 152, , f, M. Mazza 107, , S.M. Mazza 136, ,
 C. Mc Ginn 29, , J.P. Mc Gowan 104, , S.P. Mc Kee 106, , E.F. McDonald 105, , A.E. McDougall 114, ,
 J.A. Mcfayden 146, , R.P. McGovern 128, , G. Mcchedlidze 149b, , R.P. Mckenzie 33g, , T.C. McLachlan 48, ,
 D.J. McLaughlin 96, , K.D. McLean 165, , S.J. McMahon 134, , P.C. McNamara 105, , C.M. Mcpartland 92, ,
 R.A. McPherson 165, , z, T. Megy 40, , S. Mehlhase 109, , A. Mehta 92, , D. Melini 150, ,
 B.R. Mellado Garcia 33g, , A.H. Melo 55, , F. Meloni 48, , A.M. Mendes Jacques Da Costa 101, ,
 H.Y. Meng 155, , L. Meng 91, , S. Menke 110, , M. Mentink 36, , E. Meoni 43b, 43a, , C. Merlassino 126, ,
 L. Merola 72a, 72b, , C. Meroni 71a, 71b, , G. Merz 106, O. Meshkov 37, , J. Metcalfe 6, , A.S. Mete 6, ,
 C. Meyer 68, , J-P. Meyer 135, , R.P. Middleton 134, , L. Mijović 52, , G. Mikenberg 169, ,
 M. Mikestikova 131, , M. Mikuž 93, , H. Mildner 139, , A. Milic 36, , C.D. Milke 44, , D.W. Miller 39, ,
 L.S. Miller 34, , A. Milov 169, , D.A. Milstead 47a, 47b, T. Min 14c, A.A. Minaenko 37, , I.A. Minashvili 149b, ,
 L. Mince 59, , A.I. Mincer 117, , B. Mindur 85a, , M. Mineev 38, , Y. Mino 87, , L.M. Mir 13, ,
 M. Miralles Lopez 163, , M. Mironova 17a, , M.C. Missio 113, , T. Mitani 168, , A. Mitra 167, ,
 V.A. Mitsou 163, , O. Miu 155, , P.S. Miyagawa 94, , Y. Miyazaki 89, A. Mizukami 83, , T. Mkrtchyan 63a, ,
 M. Mlinarevic 96, , T. Mlinarevic 96, , M. Mlynarikova 36, , S. Mobius 55, , K. Mochizuki 108, ,
 P. Moder 48, , P. Mogg 109, , A.F. Mohammed 14a, 14e, , S. Mohapatra 41, , G. Mokgatitswane 33g, ,
 B. Mondal 141, , S. Mondal 132, , G. Monig 146, , K. Mönig 48, , E. Monnier 102, ,
 L. Monsonis Romero 163, J. Montejo Berlingen 83, , M. Montella 119, , F. Monticelli 90, ,
 N. Morange 66, , A.L. Moreira De Carvalho 130a, , M. Moreno Llácer 163, , C. Moreno Martinez 56, ,
 P. Morettini 57b, , S. Morgenstern 36, , M. Morii 61, , M. Morinaga 153, , A.K. Morley 36, ,
 F. Morodei 75a, 75b, , L. Morvaj 36, , P. Moschovakos 36, , B. Moser 36, , M. Mosidze 149b, ,
 T. Moskalets 54, , P. Moskvitina 113, , J. Moss 31, , o, E.J.W. Moyse 103, , O. Mtintsilana 33g, ,
 S. Muanza 102, , J. Mueller 129, , D. Muenstermann 91, , R. Müller 19, , G.A. Mullier 161, ,
 J.J. Mullin 128, D.P. Mungo 155, , J.L. Munoz Martinez 13, , D. Munoz Perez 163, ,
 F.J. Munoz Sanchez 101, , M. Murin 101, , W.J. Murray 167, 134, , A. Murrone 71a, 71b, , J.M. Muse 120, ,
 M. Muškinja 17a, , C. Mwewa 29, , A.G. Myagkov 37, , a, A.J. Myers 8, , A.A. Myers 129, , G. Myers 68, ,
 M. Myska 132, , B.P. Nachman 17a, , O. Nackenhorst 49, , A. Nag 50, , K. Nagai 126, , K. Nagano 83, ,
 J.L. Nagle 29, , ak, E. Nagy 102, , A.M. Nairz 36, , Y. Nakahama 83, , K. Nakamura 83, , H. Nanjo 124, ,
 R. Narayan 44, , E.A. Narayanan 112, , I. Naryshkin 37, , M. Naseri 34, , C. Nass 24, , G. Navarro 22a, ,
 J. Navarro-Gonzalez 163, , R. Nayak 151, , A. Nayaz 18, , P.Y. Nechaeva 37, , F. Nechansky 48, ,
 L. Nedic 126, , T.J. Neep 20, , A. Negri 73a, 73b, , M. Negrini 23b, , C. Nellist 114, , C. Nelson 104, ,
 K. Nelson 106, , S. Nemecek 131, , M. Nessi 36, , i, M.S. Neubauer 162, , F. Neuhaus 100, ,
 J. Neundorf 48, , R. Newhouse 164, , P.R. Newman 20, , C.W. Ng 129, , Y.W.Y. Ng 48, , B. Ngair 35e, ,
 H.D.N. Nguyen 108, , R.B. Nickerson 126, , R. Nicolaidou 135, , J. Nielsen 136, , M. Niemeyer 55, ,
 N. Nikiforou 36, , V. Nikolaenko 37, , a, I. Nikolic-Audit 127, , K. Nikolopoulos 20, , P. Nilsson 29, ,
 I. Ninca 48, , H.R. Nindhito 56, , G. Ninio 151, , A. Nisati 75a, , N. Nishu 2, , R. Nisius 110, ,
 J-E. Nitschke 50, , E.K. Nkademeng 33g, , S.J. Noacco Rosende 90, , T. Nobe 153, , D.L. Noel 32, ,
 T. Nommensen 147, , M.A. Nomura 29, M.B. Norfolk 139, , R.R.B. Norisam 96, , B.J. Norman 34, ,
 J. Novak 93, , T. Novak 48, , L. Novotny 132, , R. Novotny 112, , L. Nozka 122, , K. Ntekas 160, ,

- N.M.J. Nunes De Moura Junior 82b, , E. Nurse 96, J. Ocariz 127, , A. Ochi 84, , I. Ochoa 130a, ,
 S. Oerdekk 161, , J.T. Offermann 39, , A. Ogrodnik 85a, , A. Oh 101, , C.C. Ohm 144, , H. Oide 83, ,
 R. Oishi 153, , M.L. Ojeda 48, , Y. Okazaki 87, , M.W. O'Keefe 92, Y. Okumura 153, ,
 L.F. Oleiro Seabra 130a, , S.A. Olivares Pino 137d, , D. Oliveira Damazio 29, , D. Oliveira Goncalves 82a, ,
 J.L. Oliver 160, , M.J.R. Olsson 160, , A. Olszewski 86, , Ö.O. Öncel 54, , D.C. O'Neil 142, , A.P. O'Neill 19, ,
 A. Onofre 130a, 130e, , P.U.E. Onyisi 11, , M.J. Oreglia 39, , G.E. Orellana 90, , D. Orestano 77a, 77b, ,
 N. Orlando 13, , R.S. Orr 155, , V. O'Shea 59, , R. Ospanov 62a, , G. Otero y Garzon 30, , H. Otomo 89, ,
 P.S. Ott 63a, , G.J. Ottino 17a, , M. Ouchrif 35d, , J. Ouellette 29, , F. Ould-Saada 125, , M. Owen 59, ,
 R.E. Owen 134, , K.Y. Oyulmaz 21a, , V.E. Ozcan 21a, , N. Ozturk 8, , S. Ozturk 21d, , H.A. Pacey 32, ,
 A. Pacheco Pages 13, , C. Padilla Aranda 13, , G. Padovano 75a, 75b, , S. Pagan Griso 17a, ,
 G. Palacino 68, , A. Palazzo 70a, 70b, , S. Palestini 36, , J. Pan 172, , T. Pan 64a, , D.K. Panchal 11, ,
 C.E. Pandini 114, , J.G. Panduro Vazquez 95, , H. Pang 14b, , P. Pani 48, , G. Panizzo 69a, 69c, ,
 L. Paolozzi 56, , C. Papadatos 108, , S. Parajuli 44, , A. Paramonov 6, , C. Paraskevopoulos 10, ,
 D. Paredes Hernandez 64b, , T.H. Park 155, , M.A. Parker 32, , F. Parodi 57b, 57a, , E.W. Parrish 115, ,
 V.A. Parrish 52, , J.A. Parsons 41, , U. Parzefall 54, , B. Pascual Dias 108, , L. Pascual Dominguez 151, ,
 F. Pasquali 114, , E. Pasqualucci 75a, , S. Passaggio 57b, , F. Pastore 95, , P. Pasuwan 47a, 47b, ,
 P. Patel 86, , U.M. Patel 51, , J.R. Pater 101, , T. Pauly 36, , J. Pearkes 143, , M. Pedersen 125, ,
 R. Pedro 130a, , S.V. Peleganchuk 37, , O. Penc 36, , E.A. Pender 52, , H. Peng 62a, , K.E. Penski 109, ,
 M. Penzin 37, , B.S. Peralva 82d, , A.P. Pereira Peixoto 60, , L. Pereira Sanchez 47a, 47b, ,
 D.V. Perepelitsa 29, , ak, E. Perez Codina 156a, , M. Perganti 10, , L. Perini 71a, 71b, , *, H. Pernegger 36, ,
 A. Perrevoort 113, , O. Perrin 40, , K. Peters 48, , R.F.Y. Peters 101, , B.A. Petersen 36, , T.C. Petersen 42, ,
 E. Petit 102, , V. Petousis 132, , C. Petridou 152, , f, A. Petrukhin 141, , M. Pettee 17a, ,
 N.E. Pettersson 36, , A. Petukhov 37, , K. Petukhova 133, , A. Peyaud 135, , R. Pezoa 137f, ,
 L. Pezzotti 36, , G. Pezzullo 172, , T.M. Pham 170, , T. Pham 105, , P.W. Phillips 134, , M.W. Phipps 162, ,
 G. Piacquadio 145, , E. Pianori 17a, , F. Piazza 71a, 71b, , R. Piegaia 30, , D. Pietreanu 27b, ,
 A.D. Pilkington 101, , M. Pinamonti 69a, 69c, , J.L. Pinfold 2, , B.C. Pinheiro Pereira 130a, ,
 C. Pitman Donaldson 96, D.A. Pizzi 34, , L. Pizzimento 76a, 76b, , A. Pizzini 114, , M.-A. Pleier 29, ,
 V. Plesanovs 54, V. Pleskot 133, , E. Plotnikova 38, G. Poddar 4, , R. Poettgen 98, , L. Poggioli 127, ,
 D. Pohl 24, , I. Pokharel 55, , S. Polacek 133, , G. Polesello 73a, , A. Poley 142, 156a, , R. Polifka 132, ,
 A. Polini 23b, , C.S. Pollard 167, , Z.B. Pollock 119, , V. Polychronakos 29, , E. Pompa Pacchi 75a, 75b, ,
 D. Ponomarenko 113, , L. Pontecorvo 36, , S. Popa 27a, , G.A. Popeneciu 27d, ,
 D.M. Portillo Quintero 156a, , S. Pospisil 132, , P. Postolache 27c, , K. Potamianos 126, , P.A. Potepa 85a, ,
 I.N. Potrap 38, , C.J. Potter 32, , H. Potti 1, , T. Poulsen 48, , J. Poveda 163, , M.E. Pozo Astigarraga 36, ,
 A. Prades Ibanez 163, , M.M. Prapa 46, , J. Pretel 54, , D. Price 101, , M. Primavera 70a, ,
 M.A. Principe Martin 99, , R. Privara 122, , M.L. Proffitt 138, , N. Proklova 128, , K. Prokofiev 64c, ,
 G. Proto 76a, 76b, , S. Protopopescu 29, , J. Proudfoot 6, , M. Przybycien 85a, , W.W. Przygoda 85b, ,
 J.E. Puddefoot 139, , D. Pudzha 37, , D. Pyatiizbyantseva 37, , J. Qian 106, , D. Qichen 101, , Y. Qin 101, ,
 T. Qiu 52, , A. Quadt 55, , M. Queitsch-Maitland 101, , G. Quetant 56, , G. Rabanal Bolanos 61, ,
 D. Rafanoharana 54, , F. Ragusa 71a, 71b, , J.L. Rainbolt 39, , J.A. Raine 56, , S. Rajagopalan 29, ,
 E. Ramakoti 37, , K. Ran 48, 14e, , N.P. Rapheeza 33g, , V. Raskina 127, , D.F. Rassloff 63a, , S. Rave 100, ,
 B. Ravina 55, , I. Ravinovich 169, , M. Raymond 36, , A.L. Read 125, , N.P. Readioff 139, ,
 D.M. Rebuzzi 73a, 73b, , G. Redlinger 29, , K. Reeves 26, , J.A. Reidelsturz 171, , D. Reikher 151,

- A. Rej ^{141, ID}, C. Rembser ^{36, ID}, A. Renardi ^{48, ID}, M. Renda ^{27b, ID}, M.B. Rendel ¹¹⁰, F. Renner ^{48, ID},
 A.G. Rennie ^{59, ID}, S. Resconi ^{71a, ID}, M. Ressegotti ^{57b, 57a, ID}, E.D. Resseguei ^{17a, ID}, S. Rettie ^{36, ID},
 J.G. Reyes Rivera ^{107, ID}, B. Reynolds ¹¹⁹, E. Reynolds ^{17a, ID}, M. Rezaei Estabragh ^{171, ID}, O.L. Rezanova ^{37, ID},
 P. Reznicek ^{133, ID}, N. Ribaric ^{91, ID}, E. Ricci ^{78a, 78b, ID}, R. Richter ^{110, ID}, S. Richter ^{47a, 47b, ID},
 E. Richter-Was ^{85b, ID}, M. Ridel ^{127, ID}, S. Ridouani ^{35d, ID}, P. Rieck ^{117, ID}, P. Riedler ^{36, ID},
 M. Rijssenbeek ^{145, ID}, A. Rimoldi ^{73a, 73b, ID}, M. Rimoldi ^{48, ID}, L. Rinaldi ^{23b, 23a, ID}, T.T. Rinn ^{29, ID},
 M.P. Rinnagel ^{109, ID}, G. Ripellino ^{161, ID}, I. Riu ^{13, ID}, P. Rivadeneira ^{48, ID}, J.C. Rivera Vergara ^{165, ID},
 F. Rizatdinova ^{121, ID}, E. Rizvi ^{94, ID}, C. Rizzi ^{56, ID}, B.A. Roberts ^{167, ID}, B.R. Roberts ^{17a, ID},
 S.H. Robertson ^{104, ID, z}, M. Robin ^{48, ID}, D. Robinson ^{32, ID}, C.M. Robles Gajardo ^{137f},
 M. Robles Manzano ^{100, ID}, A. Robson ^{59, ID}, A. Rocchi ^{76a, 76b, ID}, C. Roda ^{74a, 74b, ID}, S. Rodriguez Bosca ^{63a, ID},
 Y. Rodriguez Garcia ^{22a, ID}, A. Rodriguez Rodriguez ^{54, ID}, A.M. Rodríguez Vera ^{156b, ID}, S. Roe ³⁶,
 J.T. Roemer ^{160, ID}, A.R. Roepe-Gier ^{136, ID}, J. Roggel ^{171, ID}, O. Røhne ^{125, ID}, R.A. Rojas ^{103, ID},
 C.P.A. Roland ^{68, ID}, J. Roloff ^{29, ID}, A. Romaniouk ^{37, ID}, E. Romano ^{73a, 73b, ID}, M. Romano ^{23b, ID},
 A.C. Romero Hernandez ^{162, ID}, N. Rompotis ^{92, ID}, L. Roos ^{127, ID}, S. Rosati ^{75a, ID}, B.J. Rosser ^{39, ID},
 E. Rossi ^{4, ID}, E. Rossi ^{72a, 72b, ID}, L.P. Rossi ^{57b, ID}, L. Rossini ^{48, ID}, R. Rosten ^{119, ID}, M. Rotaru ^{27b, ID},
 B. Rottler ^{54, ID}, C. Rougier ^{102, ID, ad}, D. Rousseau ^{66, ID}, D. Rousso ^{32, ID}, A. Roy ^{162, ID}, S. Roy-Garand ^{155, ID},
 A. Rozanov ^{102, ID}, Y. Rozen ^{150, ID}, X. Ruan ^{33g, ID}, A. Rubio Jimenez ^{163, ID}, A.J. Ruby ^{92, ID},
 V.H. Ruelas Rivera ^{18, ID}, T.A. Ruggeri ^{1, ID}, A. Ruggiero ^{126, ID}, A. Ruiz-Martinez ^{163, ID}, A. Rummler ^{36, ID},
 Z. Rurikova ^{54, ID}, N.A. Rusakovich ^{38, ID}, H.L. Russell ^{165, ID}, J.P. Rutherford ^{7, ID}, K. Rybacki ⁹¹,
 M. Rybar ^{133, ID}, E.B. Rye ^{125, ID}, A. Ryzhov ^{37, ID}, J.A. Sabater Iglesias ^{56, ID}, P. Sabatini ^{163, ID},
 L. Sabetta ^{75a, 75b, ID}, H.F-W. Sadrozinski ^{136, ID}, F. Safai Tehrani ^{75a, ID}, B. Safarzadeh Samani ^{146, ID},
 M. Safdari ^{143, ID}, S. Saha ^{104, ID}, M. Sahin soy ^{110, ID}, M. Saimpert ^{135, ID}, M. Saito ^{153, ID}, T. Saito ^{153, ID},
 D. Salamani ^{36, ID}, A. Salnikov ^{143, ID}, J. Salt ^{163, ID}, A. Salvador Salas ^{13, ID}, D. Salvatore ^{43b, 43a, ID},
 F. Salvatore ^{146, ID}, A. Salzburger ^{36, ID}, D. Sammel ^{54, ID}, D. Sampsonidis ^{152, ID, f}, D. Sampsonidou ^{123, 62c, ID},
 J. Sánchez ^{163, ID}, A. Sanchez Pineda ^{4, ID}, V. Sanchez Sebastian ^{163, ID}, H. Sandaker ^{125, ID}, C.O. Sander ^{48, ID},
 J.A. Sandesara ^{103, ID}, M. Sandhoff ^{171, ID}, C. Sandoval ^{22b, ID}, D.P.C. Sankey ^{134, ID}, T. Sano ^{87, ID},
 A. Sansoni ^{53, ID}, L. Santi ^{75a, 75b, ID}, C. Santoni ^{40, ID}, H. Santos ^{130a, 130b, ID}, S.N. Santpur ^{17a, ID},
 A. Santra ^{169, ID}, K.A. Saoucha ^{139, ID}, J.G. Saraiva ^{130a, 130d, ID}, J. Sardain ^{7, ID}, O. Sasaki ^{83, ID}, K. Sato ^{157, ID},
 C. Sauer ^{63b, ID}, F. Sauerburger ^{54, ID}, E. Sauvan ^{4, ID}, P. Savard ^{155, ID, ai}, R. Sawada ^{153, ID}, C. Sawyer ^{134, ID},
 L. Sawyer ^{97, ID}, I. Sayago Galvan ^{163, ID}, C. Sbarra ^{23b, ID}, A. Sbrizzi ^{23b, 23a, ID}, T. Scanlon ^{96, ID},
 J. Schaarschmidt ^{138, ID}, P. Schacht ^{110, ID}, D. Schaefer ^{39, ID}, U. Schäfer ^{100, ID}, A.C. Schaffer ^{66, 44, ID},
 D. Schaile ^{109, ID}, R.D. Schamberger ^{145, ID}, E. Schanet ^{109, ID}, C. Scharf ^{18, ID}, M.M. Schefer ^{19, ID},
 V.A. Schegelsky ^{37, ID}, D. Scheirich ^{133, ID}, F. Schenck ^{18, ID}, M. Schernau ^{160, ID}, C. Scheulen ^{55, ID},
 C. Schiavi ^{57b, 57a, ID}, E.J. Schioppa ^{70a, 70b, ID}, M. Schioppa ^{43b, 43a, ID}, B. Schlag ^{143, ID, q}, K.E. Schleicher ^{54, ID},
 S. Schlenker ^{36, ID}, J. Schmeing ^{171, ID}, M.A. Schmidt ^{171, ID}, K. Schmieden ^{100, ID}, C. Schmitt ^{100, ID},
 S. Schmitt ^{48, ID}, L. Schoeffel ^{135, ID}, A. Schoening ^{63b, ID}, P.G. Scholer ^{54, ID}, E. Schopf ^{126, ID}, M. Schott ^{100, ID},
 J. Schovancova ^{36, ID}, S. Schramm ^{56, ID}, F. Schroeder ^{171, ID}, H-C. Schultz-Coulon ^{63a, ID}, M. Schumacher ^{54, ID},
 B.A. Schumm ^{136, ID}, Ph. Schune ^{135, ID}, H.R. Schwartz ^{136, ID}, A. Schwartzman ^{143, ID}, T.A. Schwarz ^{106, ID},
 Ph. Schwemling ^{135, ID}, R. Schwienhorst ^{107, ID}, A. Sciandra ^{136, ID}, G. Sciolla ^{26, ID}, F. Scuri ^{74a, ID}, F. Scutti ¹⁰⁵,
 C.D. Sebastiani ^{92, ID}, K. Sedlaczek ^{49, ID}, P. Seema ^{18, ID}, S.C. Seidel ^{112, ID}, A. Seiden ^{136, ID}, B.D. Seidlitz ^{41, ID},
 C. Seitz ^{48, ID}, J.M. Seixas ^{82b, ID}, G. Sekhniaidze ^{72a, ID}, S.J. Sekula ^{44, ID}, L. Selem ^{4, ID},
 N. Semprini-Cesari ^{23b, 23a, ID}, S. Sen ^{51, ID}, D. Sengupta ^{56, ID}, V. Senthilkumar ^{163, ID}, L. Serin ^{66, ID},

- L. Serkin 69a, 69b, , M. Sessa 77a, 77b, , H. Severini 120, , F. Sforza 57b, 57a, , A. Sfyrla 56, ,
 E. Shabalina 55, , R. Shaheen 144, , J.D. Shahinian 128, , D. Shaked Renous 169, , L.Y. Shan 14a, ,
 M. Shapiro 17a, , A. Sharma 36, , A.S. Sharma 164, , P. Sharma 80, , S. Sharma 48, , P.B. Shatalov 37, ,
 K. Shaw 146, , S.M. Shaw 101, , Q. Shen 62c, 5, , P. Sherwood 96, , L. Shi 96, , C.O. Shimmin 172, ,
 Y. Shimogama 168, , J.D. Shinner 95, , I.P.J. Shipsey 126, , S. Shirabe 60, , M. Shiyakova 38, , x,
 J. Shlomi 169, , M.J. Shochet 39, , J. Shojaei 105, , D.R. Shope 125, , S. Shrestha 119, , al, E.M. Shrif 33g, ,
 M.J. Shroff 165, , P. Sicho 131, , A.M. Sickles 162, , E. Sideras Haddad 33g, , A. Sidoti 23b, , F. Siegert 50, ,
 Dj. Sijacki 15, , R. Sikora 85a, , F. Sili 90, , J.M. Silva 20, , M.V. Silva Oliveira 36, , S.B. Silverstein 47a, ,
 S. Simion 66, R. Simoniello 36, , E.L. Simpson 59, , H. Simpson 146, , L.R. Simpson 106, , N.D. Simpson 98, ,
 S. Simsek 21d, , S. Sindhu 55, , P. Sinervo 155, , S. Singh 142, , S. Singh 155, , S. Sinha 48, ,
 S. Sinha 33g, , M. Sioli 23b, 23a, , I. Siral 36, , S.Yu. Sivoklokov 37, , *, J. Sjölin 47a, 47b, , A. Skaf 55, ,
 E. Skorda 98, , P. Skubic 120, , M. Slawinska 86, , V. Smakhtin 169, B.H. Smart 134, , J. Smiesko 36, ,
 S.Yu. Smirnov 37, , Y. Smirnov 37, , L.N. Smirnova 37, , a, O. Smirnova 98, , A.C. Smith 41, ,
 E.A. Smith 39, , H.A. Smith 126, , J.L. Smith 92, , R. Smith 143, M. Smizanska 91, , K. Smolek 132, ,
 A.A. Snesarev 37, , H.L. Snoek 114, , S. Snyder 29, , R. Sobie 165, , z, A. Soffer 151, ,
 C.A. Solans Sanchez 36, , E.Yu. Soldatov 37, , U. Soldevila 163, , A.A. Solodkov 37, , S. Solomon 54, ,
 A. Soloshenko 38, , K. Solovieva 54, , O.V. Solovyanov 40, , V. Solovyev 37, , P. Sommer 36, ,
 A. Sonay 13, , W.Y. Song 156b, , J.M. Sonneveld 114, , A. Sopczak 132, , A.L. Sopio 96, , F. Sopkova 28b, ,
 V. Sothilingam 63a, , S. Sottocornola 68, , R. Soualah 116b, , Z. Soumaimi 35e, , D. South 48, ,
 S. Spagnolo 70a, 70b, , M. Spalla 110, , D. Sperlich 54, , G. Spigo 36, , M. Spina 146, , S. Spinali 91, ,
 D.P. Spiteri 59, , M. Spousta 133, , E.J. Staats 34, , A. Stabile 71a, 71b, , R. Stamen 63a, ,
 M. Stamenkovic 114, , A. Stampekkis 20, , M. Standke 24, , E. Stanecka 86, , M.V. Stange 50, ,
 B. Stanislaus 17a, , M.M. Stanitzki 48, , M. Stankaityte 126, , B. Stapf 48, , E.A. Starchenko 37, ,
 G.H. Stark 136, , J. Stark 102, , ad, D.M. Starko 156b, P. Staroba 131, , P. Starovoitov 63a, , S. Stärz 104, ,
 R. Staszewski 86, , G. Stavropoulos 46, , J. Steentoft 161, , P. Steinberg 29, , B. Stelzer 142, 156a, ,
 H.J. Stelzer 129, , O. Stelzer-Chilton 156a, , H. Stenzel 58, , T.J. Stevenson 146, , G.A. Stewart 36, ,
 J.R. Stewart 121, , M.C. Stockton 36, , G. Stoica 27b, , M. Stolarski 130a, , S. Stonjek 110, ,
 A. Straessner 50, , J. Strandberg 144, , S. Strandberg 47a, 47b, , M. Strauss 120, , T. Strebler 102, ,
 P. Strizenec 28b, , R. Ströhmer 166, , D.M. Strom 123, , L.R. Strom 48, , R. Stroynowski 44, ,
 A. Strubig 47a, 47b, , S.A. Stucci 29, , B. Stugu 16, , J. Stupak 120, , N.A. Styles 48, , D. Su 143, ,
 S. Su 62a, , W. Su 62d, 138, 62c, , X. Su 62a, 66, , K. Sugizaki 153, , V.V. Sulin 37, , M.J. Sullivan 92, ,
 D.M.S. Sultan 78a, 78b, , L. Sultanaliyeva 37, , S. Sultansoy 3b, , T. Sumida 87, , S. Sun 106, , S. Sun 170, ,
 O. Sunneborn Gudnadottir 161, , M.R. Sutton 146, , M. Svatos 131, , M. Swiatlowski 156a, ,
 T. Swirski 166, , I. Sykora 28a, , M. Sykora 133, , T. Sykora 133, , D. Ta 100, , K. Tackmann 48, , w,
 A. Taffard 160, , R. Tafirout 156a, , J.S. Tafoya Vargas 66, , R.H.M. Taibah 127, , R. Takashima 88, ,
 E.P. Takeva 52, , Y. Takubo 83, , M. Talby 102, , A.A. Talyshев 37, , K.C. Tam 64b, , N.M. Tamir 151, ,
 A. Tanaka 153, , J. Tanaka 153, , R. Tanaka 66, , M. Tanasini 57b, 57a, , Z. Tao 164, , S. Tapia Araya 137f, ,
 S. Tapprogge 100, , A. Tarek Abouelfadl Mohamed 107, , S. Tarem 150, , K. Tariq 62b, , G. Tarna 102, 27b, ,
 G.F. Tartarelli 71a, , P. Tas 133, , M. Tasevsky 131, , E. Tassi 43b, 43a, , A.C. Tate 162, , G. Tateno 153, ,
 Y. Tayalati 35e, , y, G.N. Taylor 105, , W. Taylor 156b, , H. Teagle 92, , A.S. Tee 170, ,
 R. Teixeira De Lima 143, , P. Teixeira-Dias 95, , J.J. Teoh 155, , K. Terashi 153, , J. Terron 99, ,
 S. Terzo 13, , M. Testa 53, , R.J. Teuscher 155, , z, A. Thaler 79, , O. Theiner 56, , N. Themistokleous 52, ,

- T. Theveneaux-Pelzer ^{102, ID}, O. Thielmann ^{171, ID}, D.W. Thomas ⁹⁵, J.P. Thomas ^{20, ID}, E.A. Thompson ^{17a, ID}, P.D. Thompson ^{20, ID}, E. Thomson ^{128, ID}, Y. Tian ^{55, ID}, V. Tikhomirov ^{37, ID, a}, Yu.A. Tikhonov ^{37, ID}, S. Timoshenko ³⁷, E.X.L. Ting ^{1, ID}, P. Tipton ^{172, ID}, S.H. Tlou ^{33g, ID}, A. Tnourji ^{40, ID}, K. Todome ^{23b,23a, ID}, S. Todorova-Nova ^{133, ID}, S. Todt ⁵⁰, M. Togawa ^{83, ID}, J. Tojo ^{89, ID}, S. Tokár ^{28a, ID}, K. Tokushuku ^{83, ID}, O. Toldaiev ^{68, ID}, R. Tombs ^{32, ID}, M. Tomoto ^{83,111, ID}, L. Tompkins ^{143, ID, q}, K.W. Topolnicki ^{85b, ID}, E. Torrence ^{123, ID}, H. Torres ^{102, ID, ad}, E. Torró Pastor ^{163, ID}, M. Toscani ^{30, ID}, C. Tosciri ^{39, ID}, M. Tost ^{11, ID}, D.R. Tovey ^{139, ID}, A. Traeet ¹⁶, I.S. Trandafir ^{27b, ID}, T. Trefzger ^{166, ID}, A. Tricoli ^{29, ID}, I.M. Trigger ^{156a, ID}, S. Trincaz-Duvold ^{127, ID}, D.A. Trischuk ^{26, ID}, B. Trocmé ^{60, ID}, C. Troncon ^{71a, ID}, L. Truong ^{33c, ID}, M. Trzebinski ^{86, ID}, A. Trzupek ^{86, ID}, F. Tsai ^{145, ID}, M. Tsai ^{106, ID}, A. Tsiamis ^{152, ID, f}, P.V. Tsiareshka ³⁷, S. Tsigaridas ^{156a, ID}, A. Tsirigotis ^{152, ID, u}, V. Tsiskaridze ^{145, ID}, E.G. Tskhadadze ^{149a, ID}, M. Tsopoulou ^{152, ID, f}, Y. Tsujikawa ^{87, ID}, I.I. Tsukerman ^{37, ID}, V. Tsulaia ^{17a, ID}, S. Tsuno ^{83, ID}, O. Tsur ¹⁵⁰, D. Tsybychev ^{145, ID}, Y. Tu ^{64b, ID}, A. Tudorache ^{27b, ID}, V. Tudorache ^{27b, ID}, A.N. Tuna ^{36, ID}, S. Turchikhin ^{38, ID}, I. Turk Cakir ^{3a, ID}, R. Turra ^{71a, ID}, T. Turtuvshin ^{38, ID, aa}, P.M. Tuts ^{41, ID}, S. Tzamarias ^{152, ID, f}, P. Tzanis ^{10, ID}, E. Tzovara ^{100, ID}, K. Uchida ¹⁵³, F. Ukegawa ^{157, ID}, P.A. Ulloa Poblete ^{137c, ID}, E.N. Umaka ^{29, ID}, G. Unal ^{36, ID}, M. Unal ^{11, ID}, A. Undrus ^{29, ID}, G. Unel ^{160, ID}, J. Urban ^{28b, ID}, P. Urquijo ^{105, ID}, G. Usai ^{8, ID}, R. Ushioda ^{154, ID}, M. Usman ^{108, ID}, Z. Uysal ^{21b, ID}, L. Vacavant ^{102, ID}, V. Vacek ^{132, ID}, B. Vachon ^{104, ID}, K.O.H. Vadla ^{125, ID}, T. Vafeiadis ^{36, ID}, A. Vaitkus ^{96, ID}, C. Valderanis ^{109, ID}, E. Valdes Santurio ^{47a,47b, ID}, M. Valente ^{156a, ID}, S. Valentinetto ^{23b,23a, ID}, A. Valero ^{163, ID}, E. Valiente Moreno ^{163, ID}, A. Vallier ^{102, ID, ad}, J.A. Valls Ferrer ^{163, ID}, D.R. Van Arneman ^{114, ID}, T.R. Van Daalen ^{138, ID}, P. Van Gemmeren ^{6, ID}, M. Van Rijnbach ^{125,36, ID}, S. Van Stroud ^{96, ID}, I. Van Vulpen ^{114, ID}, M. Vanadia ^{76a,76b, ID}, W. Vandelli ^{36, ID}, M. Vandenbroucke ^{135, ID}, E.R. Vandewall ^{121, ID}, D. Vannicola ^{151, ID}, L. Vannoli ^{57b,57a, ID}, R. Vari ^{75a, ID}, E.W. Varnes ^{7, ID}, C. Varni ^{17a, ID}, T. Varol ^{148, ID}, D. Varouchas ^{66, ID}, L. Varriale ^{163, ID}, K.E. Varvell ^{147, ID}, M.E. Vasile ^{27b, ID}, L. Vaslin ⁴⁰, G.A. Vasquez ^{165, ID}, F. Vazeille ^{40, ID}, T. Vazquez Schroeder ^{36, ID}, J. Veatch ^{31, ID}, V. Vecchio ^{101, ID}, M.J. Veen ^{103, ID}, I. Veliscek ^{126, ID}, L.M. Veloce ^{155, ID}, F. Veloso ^{130a,130c, ID}, S. Veneziano ^{75a, ID}, A. Ventura ^{70a,70b, ID}, A. Verbytskyi ^{110, ID}, M. Verducci ^{74a,74b, ID}, C. Vergis ^{24, ID}, M. Verissimo De Araujo ^{82b, ID}, W. Verkerke ^{114, ID}, J.C. Vermeulen ^{114, ID}, C. Vernieri ^{143, ID}, P.J. Verschueren ^{95, ID}, M. Vessella ^{103, ID}, M.C. Vetterli ^{142, ID, ai}, A. Vgenopoulos ^{152, ID, f}, N. Viaux Maira ^{137f, ID}, T. Vickey ^{139, ID}, O.E. Vickey Boeriu ^{139, ID}, G.H.A. Viehhauser ^{126, ID}, L. Vigani ^{63b, ID}, M. Villa ^{23b,23a, ID}, M. Villaplana Perez ^{163, ID}, E.M. Villhauer ⁵², E. Vilucchi ^{53, ID}, M.G. Vincter ^{34, ID}, G.S. Virdee ^{20, ID}, A. Vishwakarma ^{52, ID}, C. Vittori ^{36, ID}, I. Vivarelli ^{146, ID}, V. Vladimirov ¹⁶⁷, E. Voevodina ^{110, ID}, F. Vogel ^{109, ID}, P. Vokac ^{132, ID}, J. Von Ahnen ^{48, ID}, E. Von Toerne ^{24, ID}, B. Vormwald ^{36, ID}, V. Vorobel ^{133, ID}, K. Vorobev ^{37, ID}, M. Vos ^{163, ID}, K. Voss ^{141, ID}, J.H. Vossebeld ^{92, ID}, M. Vozak ^{114, ID}, L. Vozdecky ^{94, ID}, N. Vranjes ^{15, ID}, M. Vranjes Milosavljevic ^{15, ID}, M. Vreeswijk ^{114, ID}, R. Vuillermet ^{36, ID}, O. Vujinovic ^{100, ID}, I. Vukotic ^{39, ID}, S. Wada ^{157, ID}, C. Wagner ¹⁰³, J.M. Wagner ^{17a, ID}, W. Wagner ^{171, ID}, S. Wahdan ^{171, ID}, H. Wahlberg ^{90, ID}, R. Wakasa ^{157, ID}, M. Wakida ^{111, ID}, J. Walder ^{134, ID}, R. Walker ^{109, ID}, W. Walkowiak ^{141, ID}, A. Wall ^{128, ID}, A.Z. Wang ^{170, ID}, C. Wang ^{100, ID}, C. Wang ^{62c, ID}, H. Wang ^{17a, ID}, J. Wang ^{64a, ID}, R.-J. Wang ^{100, ID}, R. Wang ^{61, ID}, R. Wang ^{6, ID}, S.M. Wang ^{148, ID}, S. Wang ^{62b, ID}, T. Wang ^{62a, ID}, W.T. Wang ^{80, ID}, X. Wang ^{14c, ID}, X. Wang ^{162, ID}, X. Wang ^{62c, ID}, Y. Wang ^{62d, ID}, Y. Wang ^{14c, ID}, Z. Wang ^{106, ID}, Z. Wang ^{62d,51,62c, ID}, Z. Wang ^{106, ID}, A. Warburton ^{104, ID}, R.J. Ward ^{20, ID}, N. Warrack ^{59, ID}, A.T. Watson ^{20, ID}, H. Watson ^{59, ID}, M.F. Watson ^{20, ID}, G. Watts ^{138, ID}, B.M. Waugh ^{96, ID}, C. Weber ^{29, ID}, H.A. Weber ^{18, ID}, M.S. Weber ^{19, ID}, S.M. Weber ^{63a, ID}, C. Wei ^{62a,}

- Y. Wei ^{126, ID}, A.R. Weidberg ^{126, ID}, E.J. Weik ^{117, ID}, J. Weingarten ^{49, ID}, M. Weirich ^{100, ID}, C. Weiser ^{54, ID}, C.J. Wells ^{48, ID}, T. Wenaus ^{29, ID}, B. Wendland ^{49, ID}, T. Wengler ^{36, ID}, N.S. Wenke ^{110, ID}, N. Wermes ^{24, ID}, M. Wessels ^{63a, ID}, K. Whalen ^{123, ID}, A.M. Wharton ^{91, ID}, A.S. White ^{61, ID}, A. White ^{8, ID}, M.J. White ^{1, ID}, D. Whiteson ^{160, ID}, L. Wickremasinghe ^{124, ID}, W. Wiedenmann ^{170, ID}, C. Wiel ^{50, ID}, M. Wielers ^{134, ID}, C. Wiglesworth ^{42, ID}, L.A.M. Wiik-Fuchs ^{54, ID}, D.J. Wilbern ^{120, ID}, H.G. Wilkens ^{36, ID}, D.M. Williams ^{41, ID}, H.H. Williams ^{128, ID}, S. Williams ^{32, ID}, S. Willocq ^{103, ID}, B.J. Wilson ^{101, ID}, P.J. Windischhofer ^{39, ID}, F. Winklmeier ^{123, ID}, B.T. Winter ^{54, ID}, J.K. Winter ^{101, ID}, M. Wittgen ^{143, ID}, M. Wobisch ^{97, ID}, R. Wölker ^{126, ID}, J. Wollrath ^{160, ID}, M.W. Wolter ^{86, ID}, H. Wolters ^{130a, 130c, ID}, V.W.S. Wong ^{164, ID}, A.F. Wongel ^{48, ID}, S.D. Worm ^{48, ID}, B.K. Wosiek ^{86, ID}, K.W. Woźniak ^{86, ID}, K. Wright ^{59, ID}, J. Wu ^{14a, 14e, ID}, M. Wu ^{64a, ID}, M. Wu ^{113, ID}, S.L. Wu ^{170, ID}, X. Wu ^{56, ID}, Y. Wu ^{62a, ID}, Z. Wu ^{135, 62a, ID}, J. Wuerzinger ^{110, ID}, T.R. Wyatt ^{101, ID}, B.M. Wynne ^{52, ID}, S. Xella ^{42, ID}, L. Xia ^{14c, ID}, M. Xia ^{14b, ID}, J. Xiang ^{64c, ID}, X. Xiao ^{106, ID}, M. Xie ^{62a, ID}, X. Xie ^{62a, ID}, S. Xin ^{14a, 14e, ID}, J. Xiong ^{17a, ID}, I. Xiotidis ^{146, ID}, D. Xu ^{14a, ID}, H. Xu ^{62a, ID}, H. Xu ^{62a, ID}, L. Xu ^{62a, ID}, R. Xu ^{128, ID}, T. Xu ^{106, ID}, Y. Xu ^{14b, ID}, Z. Xu ^{62b, ID}, Z. Xu ^{14a, ID}, B. Yabsley ^{147, ID}, S. Yacoob ^{33a, ID}, N. Yamaguchi ^{89, ID}, Y. Yamaguchi ^{154, ID}, H. Yamauchi ^{157, ID}, T. Yamazaki ^{17a, ID}, Y. Yamazaki ^{84, ID}, J. Yan ^{62c, ID}, S. Yan ^{126, ID}, Z. Yan ^{25, ID}, H.J. Yang ^{62c, 62d, ID}, H.T. Yang ^{62a, ID}, S. Yang ^{62a, ID}, T. Yang ^{64c, ID}, X. Yang ^{62a, ID}, X. Yang ^{14a, ID}, Y. Yang ^{44, ID}, Y. Yang ^{62a, ID}, Z. Yang ^{62a, 106, ID}, W-M. Yao ^{17a, ID}, Y.C. Yap ^{48, ID}, H. Ye ^{14c, ID}, H. Ye ^{55, ID}, J. Ye ^{44, ID}, S. Ye ^{29, ID}, X. Ye ^{62a, ID}, Y. Yeh ^{96, ID}, I. Yeletskikh ^{38, ID}, B.K. Yeo ^{17a, ID}, M.R. Yexley ^{91, ID}, P. Yin ^{41, ID}, K. Yorita ^{168, ID}, S. Younas ^{27b, ID}, C.J.S. Young ^{54, ID}, C. Young ^{143, ID}, Y. Yu ^{62a, ID}, M. Yuan ^{106, ID}, R. Yuan ^{62b, ID}, L. Yue ^{96, ID}, M. Zaazoua ^{35e, ID}, B. Zabinski ^{86, ID}, E. Zaid ^{52, ID}, T. Zakareishvili ^{149b, ID}, N. Zakharchuk ^{34, ID}, S. Zambito ^{56, ID}, J.A. Zamora Saa ^{137d, 137b, ID}, J. Zang ^{153, ID}, D. Zanzi ^{54, ID}, O. Zaplatilek ^{132, ID}, C. Zeitnitz ^{171, ID}, H. Zeng ^{14a, ID}, J.C. Zeng ^{162, ID}, D.T. Zenger Jr ^{26, ID}, O. Zenin ^{37, ID}, T. Ženiš ^{28a, ID}, S. Zenz ^{94, ID}, S. Zerradi ^{35a, ID}, D. Zerwas ^{66, ID}, M. Zhai ^{14a, 14e, ID}, B. Zhang ^{14c, ID}, D.F. Zhang ^{139, ID}, J. Zhang ^{62b, ID}, J. Zhang ^{6, ID}, K. Zhang ^{14a, 14e, ID}, L. Zhang ^{14c, ID}, P. Zhang ^{14a, 14e, ID}, R. Zhang ^{170, ID}, S. Zhang ^{106, ID}, T. Zhang ^{153, ID}, X. Zhang ^{62c, ID}, X. Zhang ^{62b, ID}, Y. Zhang ^{62c, 5, ID}, Z. Zhang ^{17a, ID}, Z. Zhang ^{66, ID}, H. Zhao ^{138, ID}, P. Zhao ^{51, ID}, T. Zhao ^{62b, ID}, Y. Zhao ^{136, ID}, Z. Zhao ^{62a, ID}, A. Zhemchugov ^{38, ID}, K. Zheng ^{162, ID}, X. Zheng ^{62a, ID}, Z. Zheng ^{143, ID}, D. Zhong ^{162, ID}, B. Zhou ^{106, ID}, C. Zhou ^{170, ID}, H. Zhou ^{7, ID}, N. Zhou ^{62c, ID}, Y. Zhou ^{7, ID}, C.G. Zhu ^{62b, ID}, J. Zhu ^{106, ID}, Y. Zhu ^{62c, ID}, Y. Zhu ^{62a, ID}, X. Zhuang ^{14a, ID}, K. Zhukov ^{37, ID}, V. Zhulanov ^{37, ID}, N.I. Zimine ^{38, ID}, J. Zinsser ^{63b, ID}, M. Ziolkowski ^{141, ID}, L. Živković ^{15, ID}, A. Zoccoli ^{23b, 23a, ID}, K. Zoch ^{56, ID}, T.G. Zorbas ^{139, ID}, O. Zormpa ^{46, ID}, W. Zou ^{41, ID}, L. Zwalinski ^{36, ID}

¹ Department of Physics, University of Adelaide, Adelaide; Australia² Department of Physics, University of Alberta, Edmonton AB; Canada³ ^(a) Department of Physics, Ankara University, Ankara; ^(b) Division of Physics, TOBB University of Economics and Technology, Ankara; Türkiye⁴ LAPP, Université Savoie Mont Blanc, CNRS/IN2P3, Annecy; France⁵ APC, Université Paris Cité, CNRS/IN2P3, Paris; France⁶ High Energy Physics Division, Argonne National Laboratory, Argonne IL; United States of America⁷ Department of Physics, University of Arizona, Tucson AZ; United States of America⁸ Department of Physics, University of Texas at Arlington, Arlington TX; United States of America⁹ Physics Department, National and Kapodistrian University of Athens, Athens; Greece¹⁰ Physics Department, National Technical University of Athens, Zografou; Greece¹¹ Department of Physics, University of Texas at Austin, Austin TX; United States of America¹² Institute of Physics, Azerbaijan Academy of Sciences, Baku; Azerbaijan¹³ Institut de Física d'Altes Energies (IFAE), Barcelona Institute of Science and Technology, Barcelona; Spain¹⁴ ^(a) Institute of High Energy Physics, Chinese Academy of Sciences, Beijing; ^(b) Physics Department, Tsinghua University, Beijing; ^(c) Department of Physics, Nanjing University, Nanjing;^(d) School of Science, Shenzhen Campus of Sun Yat-sen University; ^(e) University of Chinese Academy of Science (UCAS), Beijing; China¹⁵ Institute of Physics, University of Belgrade, Belgrade; Serbia¹⁶ Department for Physics and Technology, University of Bergen, Bergen; Norway¹⁷ ^(a) Physics Division, Lawrence Berkeley National Laboratory, Berkeley CA; ^(b) University of California, Berkeley CA; United States of America¹⁸ Institut für Physik, Humboldt Universität zu Berlin, Berlin; Germany¹⁹ Albert Einstein Center for Fundamental Physics and Laboratory for High Energy Physics, University of Bern, Bern; Switzerland²⁰ School of Physics and Astronomy, University of Birmingham, Birmingham; United Kingdom

- 21 ^(a) Department of Physics, Bogazici University, Istanbul; ^(b) Department of Physics Engineering, Gaziantep University, Gaziantep; ^(c) Department of Physics, Istanbul University, Istanbul;
^(d) Istaninte University, Sariyer, Istanbul; Türkiye
- 22 ^(a) Facultad de Ciencias y Centro de Investigaciones, Universidad Antonio Nariño, Bogotá; ^(b) Departamento de Física, Universidad Nacional de Colombia, Bogotá; Colombia
- 23 ^(a) Dipartimento di Fisica e Astronomia A. Righi, Università di Bologna, Bologna; ^(b) INFN Sezione di Bologna; Italy
- 24 Physikalisches Institut, Universität Bonn, Bonn; Germany
- 25 Department of Physics, Boston University, Boston MA; United States of America
- 26 Department of Physics, Brandeis University, Waltham MA; United States of America
- 27 ^(a) Transilvania University of Brasov, Brasov; ^(b) Horia Hulubei National Institute of Physics and Nuclear Engineering, Bucharest; ^(c) Department of Physics, Alexandru Ioan Cuza University of Iasi, Iasi; ^(d) National Institute for Research and Development of Isotopic and Molecular Technologies, Physics Department, Cluj-Napoca; ^(e) University Politehnica Bucharest, Bucharest; ^(f) West University in Timisoara, Timisoara; ^(g) Faculty of Physics, University of Bucharest, Bucharest; Romania
- 28 ^(a) Faculty of Mathematics, Physics and Informatics, Comenius University, Bratislava; ^(b) Department of Subnuclear Physics, Institute of Experimental Physics of the Slovak Academy of Sciences, Kosice; Slovak Republic
- 29 Physics Department, Brookhaven National Laboratory, Upton NY; United States of America
- 30 Universidad de Buenos Aires, Facultad de Ciencias Exactas y Naturales, Departamento de Física, y CONICET, Instituto de Física de Buenos Aires (IFIBA), Buenos Aires; Argentina
- 31 California State University, CA; United States of America
- 32 Cavendish Laboratory, University of Cambridge, Cambridge; United Kingdom
- 33 ^(a) Department of Physics, University of Cape Town, Cape Town; ^(b) iThemba Labs, Western Cape; ^(c) Department of Mechanical Engineering Science, University of Johannesburg, Johannesburg; ^(d) National Institute of Physics, University of the Philippines Diliman (Philippines); ^(e) University of South Africa, Department of Physics, Pretoria; ^(f) University of Zululand, KwaDlangezwa; ^(g) School of Physics, University of the Witwatersrand, Johannesburg; South Africa
- 34 Department of Physics, Carleton University, Ottawa ON; Canada
- 35 ^(a) Faculté des Sciences Ain Chock, Réseau Universitaire de Physique des Hautes Energies - Université Hassan II, Casablanca; ^(b) Faculté des Sciences, Université Ibn-Tofail, Kénitra; ^(c) Faculté des Sciences Semlalia, Université Cadi Ayyad, LPHEA-Marrakech; ^(d) LPMR, Faculté des Sciences, Université Mohamed Premier, Oujda; ^(e) Faculté des sciences, Université Mohammed V, Rabat; ^(f) Institute of Applied Physics, Mohammed VI Polytechnic University, Ben Guerir; Morocco
- 36 CERN, Geneva; Switzerland
- 37 Affiliated with an institute covered by a cooperation agreement with CERN
- 38 Affiliated with an international laboratory covered by a cooperation agreement with CERN
- 39 Enrico Fermi Institute, University of Chicago, Chicago IL; United States of America
- 40 LPC, Université Clermont Auvergne, CNRS/IN2P3, Clermont-Ferrand; France
- 41 Nevis Laboratory, Columbia University, Irvington NY; United States of America
- 42 Niels Bohr Institute, University of Copenhagen, Copenhagen; Denmark
- 43 ^(a) Dipartimento di Fisica, Università della Calabria, Rende; ^(b) INFN Gruppo Collegato di Cosenza, Laboratori Nazionali di Frascati; Italy
- 44 Physics Department, Southern Methodist University, Dallas TX; United States of America
- 45 Physics Department, University of Texas at Dallas, Richardson TX; United States of America
- 46 National Centre for Scientific Research "Demokritos", Agia Paraskevi; Greece
- 47 ^(a) Department of Physics, Stockholm University; ^(b) Oskar Klein Centre, Stockholm; Sweden
- 48 Deutsches Elektronen-Synchrotron DESY, Hamburg and Zeuthen; Germany
- 49 Fakultät Physik, Technische Universität Dortmund, Dortmund; Germany
- 50 Institut für Kern- und Teilchenphysik, Technische Universität Dresden, Dresden; Germany
- 51 Department of Physics, Duke University, Durham NC; United States of America
- 52 SUPA - School of Physics and Astronomy, University of Edinburgh, Edinburgh; United Kingdom
- 53 INFN e Laboratori Nazionali di Frascati, Frascati; Italy
- 54 Physikalisches Institut, Albert-Ludwigs-Universität Freiburg, Freiburg; Germany
- 55 II. Physikalisches Institut, Georg-August-Universität Göttingen, Göttingen; Germany
- 56 Département de Physique Nucléaire et Corpusculaire, Université de Genève, Genève; Switzerland
- 57 ^(a) Dipartimento di Fisica, Università di Genova, Genova; ^(b) INFN Sezione di Genova; Italy
- 58 II. Physikalisches Institut, Justus-Liebig-Universität Giessen, Giessen; Germany
- 59 SUPA - School of Physics and Astronomy, University of Glasgow, Glasgow; United Kingdom
- 60 LPSC, Université Grenoble Alpes, CNRS/IN2P3, Grenoble INP, Grenoble; France
- 61 Laboratory for Particle Physics and Cosmology, Harvard University, Cambridge MA; United States of America
- 62 ^(a) Department of Modern Physics and State Key Laboratory of Particle Detection and Electronics, University of Science and Technology of China, Hefei; ^(b) Institute of Frontier and Interdisciplinary Science and Key Laboratory of Particle Physics and Particle Irradiation (MOE), Shandong University, Qingdao; ^(c) School of Physics and Astronomy, Shanghai Jiao Tong University, Key Laboratory for Particle Astrophysics and Cosmology (MOE), SKLPPC, Shanghai; ^(d) Tsung-Dao Lee Institute, Shanghai; China
- 63 ^(a) Kirchhoff-Institut für Physik, Ruprecht-Karls-Universität Heidelberg, Heidelberg; ^(b) Physikalisches Institut, Ruprecht-Karls-Universität Heidelberg, Heidelberg; Germany
- 64 ^(a) Department of Physics, Chinese University of Hong Kong, Shatin, N.T., Hong Kong; ^(b) Department of Physics, University of Hong Kong, Hong Kong; ^(c) Department of Physics and Institute for Advanced Study, Hong Kong University of Science and Technology, Clear Water Bay, Kowloon, Hong Kong; China
- 65 Department of Physics, National Tsing Hua University, Hsinchu; Taiwan
- 66 IJCLab, Université Paris-Saclay, CNRS/IN2P3, 91405, Orsay; France
- 67 Centro Nacional de Microelectrónica (IMB-CNM-CSIC), Barcelona; Spain
- 68 Department of Physics, Indiana University, Bloomington IN; United States of America
- 69 ^(a) INFN Gruppo Collegato di Udine, Sezione di Trieste, Udine; ^(b) ICTP, Trieste; ^(c) Dipartimento Politecnico di Ingegneria e Architettura, Università di Udine, Udine; Italy
- 70 ^(a) INFN Sezione di Lecce; ^(b) Dipartimento di Matematica e Fisica, Università del Salento, Lecce; Italy
- 71 ^(a) INFN Sezione di Milano; ^(b) Dipartimento di Fisica, Università di Milano, Milano; Italy
- 72 ^(a) INFN Sezione di Napoli; ^(b) Dipartimento di Fisica, Università di Napoli, Napoli; Italy
- 73 ^(a) INFN Sezione di Pavia; ^(b) Dipartimento di Fisica, Università di Pavia, Pavia; Italy
- 74 ^(a) INFN Sezione di Pisa; ^(b) Dipartimento di Fisica E. Fermi, Università di Pisa, Pisa; Italy
- 75 ^(a) INFN Sezione di Roma; ^(b) Dipartimento di Fisica, Sapienza Università di Roma, Roma; Italy
- 76 ^(a) INFN Sezione di Roma Tor Vergata; ^(b) Dipartimento di Fisica, Università di Roma Tor Vergata, Roma; Italy
- 77 ^(a) INFN Sezione di Roma Tre; ^(b) Dipartimento di Matematica e Fisica, Università Roma Tre, Roma; Italy
- 78 ^(a) INFN-TIFPA; ^(b) Università degli Studi di Trento, Trento; Italy
- 79 Universität Innsbruck, Department of Astro and Particle Physics, Innsbruck; Austria
- 80 University of Iowa, Iowa City IA; United States of America
- 81 Department of Physics and Astronomy, Iowa State University, Ames IA; United States of America
- 82 ^(a) Departamento de Engenharia Elétrica, Universidade Federal de Juiz de Fora (UFJF), Juiz de Fora; ^(b) Universidade Federal do Rio De Janeiro COPPE/EE/IF, Rio de Janeiro; ^(c) Instituto de Física, Universidade de São Paulo, São Paulo; ^(d) Rio de Janeiro State University, Rio de Janeiro; Brazil
- 83 KEK, High Energy Accelerator Research Organization, Tsukuba; Japan
- 84 Graduate School of Science, Kobe University, Kobe; Japan
- 85 ^(a) AGH University of Krakow, Faculty of Physics and Applied Computer Science, Krakow; ^(b) Marian Smoluchowski Institute of Physics, Jagiellonian University, Krakow; Poland
- 86 Institute of Nuclear Physics Polish Academy of Sciences, Krakow; Poland
- 87 Faculty of Science, Kyoto University, Kyoto; Japan
- 88 Kyoto University of Education, Kyoto; Japan

- ⁸⁹ Research Center for Advanced Particle Physics and Department of Physics, Kyushu University, Fukuoka; Japan
⁹⁰ Instituto de Física La Plata, Universidad Nacional de La Plata and CONICET, La Plata; Argentina
⁹¹ Physics Department, Lancaster University, Lancaster; United Kingdom
⁹² Oliver Lodge Laboratory, University of Liverpool, Liverpool; United Kingdom
⁹³ Department of Experimental Particle Physics, Jožef Stefan Institute and Department of Physics, University of Ljubljana, Ljubljana; Slovenia
⁹⁴ School of Physics and Astronomy, Queen Mary University of London, London; United Kingdom
⁹⁵ Department of Physics, Royal Holloway University of London, Egham; United Kingdom
⁹⁶ Department of Physics and Astronomy, University College London, London; United Kingdom
⁹⁷ Louisiana Tech University, Ruston LA; United States of America
⁹⁸ Fysiska institutionen, Lunds universitet, Lund; Sweden
⁹⁹ Departamento de Física Teórica C-15 and CIAFF, Universidad Autónoma de Madrid, Madrid; Spain
¹⁰⁰ Institut für Physik, Universität Mainz, Mainz; Germany
¹⁰¹ School of Physics and Astronomy, University of Manchester, Manchester; United Kingdom
¹⁰² CPPM, Aix-Marseille Université, CNRS/IN2P3, Marseille; France
¹⁰³ Department of Physics, University of Massachusetts, Amherst MA; United States of America
¹⁰⁴ Department of Physics, McGill University, Montreal QC; Canada
¹⁰⁵ School of Physics, University of Melbourne, Victoria; Australia
¹⁰⁶ Department of Physics, University of Michigan, Ann Arbor MI; United States of America
¹⁰⁷ Department of Physics and Astronomy, Michigan State University, East Lansing MI; United States of America
¹⁰⁸ Group of Particle Physics, University of Montreal, Montreal QC; Canada
¹⁰⁹ Fakultät für Physik, Ludwig-Maximilians-Universität München, München; Germany
¹¹⁰ Max-Planck-Institut für Physik (Werner-Heisenberg-Institut), München; Germany
¹¹¹ Graduate School of Science and Kobayashi-Maskawa Institute, Nagoya University, Nagoya; Japan
¹¹² Department of Physics and Astronomy, University of New Mexico, Albuquerque NM; United States of America
¹¹³ Institute for Mathematics, Astrophysics and Particle Physics, Radboud University/Nikhef, Nijmegen; Netherlands
¹¹⁴ Nikhef National Institute for Subatomic Physics and University of Amsterdam, Amsterdam; Netherlands
¹¹⁵ Department of Physics, Northern Illinois University, DeKalb IL; United States of America
¹¹⁶ ^(a) New York University Abu Dhabi, Abu Dhabi; ^(b) University of Sharjah, Sharjah; United Arab Emirates
¹¹⁷ Department of Physics, New York University, New York NY; United States of America
¹¹⁸ Ochanomizu University, Otsuka, Bunkyo-ku, Tokyo; Japan
¹¹⁹ Ohio State University, Columbus OH; United States of America
¹²⁰ Homer L. Dodge Department of Physics and Astronomy, University of Oklahoma, Norman OK; United States of America
¹²¹ Department of Physics, Oklahoma State University, Stillwater OK; United States of America
¹²² Palacký University, Joint Laboratory of Optics, Olomouc; Czech Republic
¹²³ Institute for Fundamental Science, University of Oregon, Eugene, OR; United States of America
¹²⁴ Graduate School of Science, Osaka University, Osaka; Japan
¹²⁵ Department of Physics, University of Oslo, Oslo; Norway
¹²⁶ Department of Physics, Oxford University, Oxford; United Kingdom
¹²⁷ LPNHE, Sorbonne Université, Université Paris Cité, CNRS/IN2P3, Paris; France
¹²⁸ Department of Physics, University of Pennsylvania, Philadelphia PA; United States of America
¹²⁹ Department of Physics and Astronomy, University of Pittsburgh, Pittsburgh PA; United States of America
¹³⁰ ^(a) Laboratório de Instrumentação e Física Experimental de Partículas - LIP, Lisboa; ^(b) Departamento de Física, Faculdade de Ciências, Universidade de Lisboa, Lisboa; ^(c) Departamento de Física, Universidade de Coimbra, Coimbra; ^(d) Centro de Física Nuclear da Universidade de Lisboa, Lisboa; ^(e) Departamento de Física, Universidade do Minho, Braga; ^(f) Departamento de Física Teórica y del Cosmos, Universidad de Granada, Granada (Spain); ^(g) Departamento de Física, Instituto Superior Técnico, Universidade de Lisboa, Lisboa; Portugal
¹³¹ Institute of Physics of the Czech Academy of Sciences, Prague; Czech Republic
¹³² Czech Technical University in Prague, Prague; Czech Republic
¹³³ Charles University, Faculty of Mathematics and Physics, Prague; Czech Republic
¹³⁴ Particle Physics Department, Rutherford Appleton Laboratory, Didcot; United Kingdom
¹³⁵ IRFU, CEA, Université Paris-Saclay, Gif-sur-Yvette; France
¹³⁶ Santa Cruz Institute for Particle Physics, University of California Santa Cruz, Santa Cruz CA; United States of America
¹³⁷ ^(a) Departamento de Física, Pontificia Universidad Católica de Chile, Santiago; ^(b) Millennium Institute for Subatomic physics at high energy frontier (SAPHIR), Santiago; ^(c) Instituto de Investigación Multidisciplinario en Ciencia y Tecnología, y Departamento de Física, Universidad de La Serena; ^(d) Universidad Andres Bello, Department of Physics, Santiago; ^(e) Instituto de Alta Investigación, Universidad de Tarapacá, Arica; ^(f) Departamento de Física, Universidad Técnica Federico Santa María, Valparaíso; Chile
¹³⁸ Department of Physics, University of Washington, Seattle WA; United States of America
¹³⁹ Department of Physics and Astronomy, University of Sheffield, Sheffield; United Kingdom
¹⁴⁰ Department of Physics, Shinshu University, Nagano; Japan
¹⁴¹ Department Physik, Universität Siegen, Siegen; Germany
¹⁴² Department of Physics, Simon Fraser University, Burnaby BC; Canada
¹⁴³ SLAC National Accelerator Laboratory, Stanford CA; United States of America
¹⁴⁴ Department of Physics, Royal Institute of Technology, Stockholm; Sweden
¹⁴⁵ Departments of Physics and Astronomy, Stony Brook University, Stony Brook NY; United States of America
¹⁴⁶ Department of Physics and Astronomy, University of Sussex, Brighton; United Kingdom
¹⁴⁷ School of Physics, University of Sydney, Sydney; Australia
¹⁴⁸ Institute of Physics, Academia Sinica, Taipei; Taiwan
¹⁴⁹ ^(a) E. Andronikashvili Institute of Physics, Iv. Javakhishvili Tbilisi State University, Tbilisi; ^(b) High Energy Physics Institute, Tbilisi State University, Tbilisi; ^(c) University of Georgia, Tbilisi; Georgia
¹⁵⁰ Department of Physics, Technion, Israel Institute of Technology, Haifa; Israel
¹⁵¹ Raymond and Beverly Sackler School of Physics and Astronomy, Tel Aviv University, Tel Aviv; Israel
¹⁵² Department of Physics, Aristotle University of Thessaloniki, Thessaloniki; Greece
¹⁵³ International Center for Elementary Particle Physics and Department of Physics, University of Tokyo, Tokyo; Japan
¹⁵⁴ Department of Physics, Tokyo Institute of Technology, Tokyo; Japan
¹⁵⁵ Department of Physics, University of Toronto, Toronto ON; Canada
¹⁵⁶ ^(a) TRIUMF, Vancouver BC; ^(b) Department of Physics and Astronomy, York University, Toronto ON; Canada
¹⁵⁷ Division of Physics and Tomonaga Center for the History of the Universe, Faculty of Pure and Applied Sciences, University of Tsukuba, Tsukuba; Japan
¹⁵⁸ Department of Physics and Astronomy, Tufts University, Medford MA; United States of America
¹⁵⁹ United Arab Emirates University, Al Ain; United Arab Emirates
¹⁶⁰ Department of Physics and Astronomy, University of California Irvine, Irvine CA; United States of America
¹⁶¹ Department of Physics and Astronomy, University of Uppsala, Uppsala; Sweden
¹⁶² Department of Physics, University of Illinois, Urbana IL; United States of America
¹⁶³ Instituto de Física Corpuscular (IFIC), Centro Mixto Universidad de Valencia - CSIC, Valencia; Spain

- ¹⁶⁴ Department of Physics, University of British Columbia, Vancouver BC; Canada
¹⁶⁵ Department of Physics and Astronomy, University of Victoria, Victoria BC; Canada
¹⁶⁶ Fakultät für Physik und Astronomie, Julius-Maximilians-Universität Würzburg, Würzburg; Germany
¹⁶⁷ Department of Physics, University of Warwick, Coventry; United Kingdom
¹⁶⁸ Waseda University, Tokyo; Japan
¹⁶⁹ Department of Particle Physics and Astrophysics, Weizmann Institute of Science, Rehovot; Israel
¹⁷⁰ Department of Physics, University of Wisconsin, Madison WI; United States of America
¹⁷¹ Fakultät für Mathematik und Naturwissenschaften, Fachgruppe Physik, Bergische Universität Wuppertal, Wuppertal; Germany
¹⁷² Department of Physics, Yale University, New Haven CT; United States of America

- ^a Also Affiliated with an institute covered by a cooperation agreement with CERN.
^b Also at An-Najah National University, Nablus; Palestine.
^c Also at Borough of Manhattan Community College, City University of New York, New York NY; United States of America.
^d Also at Bruno Kessler Foundation, Trento; Italy.
^e Also at Center for High Energy Physics, Peking University; China.
^f Also at Center for Interdisciplinary Research and Innovation (CIRI-AUTH), Thessaloniki; Greece.
^g Also at Centro Studi e Ricerche Enrico Fermi; Italy.
^h Also at CERN, Geneva; Switzerland.
ⁱ Also at Département de Physique Nucléaire et Corpusculaire, Université de Genève, Genève; Switzerland.
^j Also at Departament de Fisica de la Universitat Autònoma de Barcelona, Barcelona; Spain.
^k Also at Department of Financial and Management Engineering, University of the Aegean, Chios; Greece.
^l Also at Department of Physics and Astronomy, Michigan State University, East Lansing MI; United States of America.
^m Also at Department of Physics, Ben Gurion University of the Negev, Beer Sheva; Israel.
ⁿ Also at Department of Physics, California State University, East Bay; United States of America.
^o Also at Department of Physics, California State University, Sacramento; United States of America.
^p Also at Department of Physics, King's College London, London; United Kingdom.
^q Also at Department of Physics, Stanford University, Stanford CA; United States of America.
^r Also at Department of Physics, University of Fribourg, Fribourg; Switzerland.
^s Also at Department of Physics, University of Thessaly; Greece.
^t Also at Department of Physics, Westmont College, Santa Barbara; United States of America.
^u Also at Hellenic Open University, Patras; Greece.
^v Also at Institut Catalana de Recerca i Estudis Avancats, ICREA, Barcelona; Spain.
^w Also at Institut für Experimentalphysik, Universität Hamburg, Hamburg; Germany.
^x Also at Institute for Nuclear Research and Nuclear Energy (INRNE) of the Bulgarian Academy of Sciences, Sofia; Bulgaria.
^y Also at Institute of Applied Physics, Mohammed VI Polytechnic University, Ben Guerir; Morocco.
^z Also at Institute of Particle Physics (IPP); Canada.
^{aa} Also at Institute of Physics and Technology, Ulaanbaatar; Mongolia.
^{ab} Also at Institute of Physics, Azerbaijan Academy of Sciences, Baku; Azerbaijan.
^{ac} Also at Institute of Theoretical Physics, Ilia State University, Tbilisi; Georgia.
^{ad} Also at L2IT, Université de Toulouse, CNRS/IN2P3, UPS, Toulouse; France.
^{ae} Also at Lawrence Livermore National Laboratory, Livermore; United States of America.
^{af} Also at National Institute of Physics, University of the Philippines Diliman (Philippines); Philippines.
^{ag} Also at Technical University of Munich, Munich; Germany.
^{ah} Also at The Collaborative Innovation Center of Quantum Matter (CICQM), Beijing; China.
^{ai} Also at TRIUMF, Vancouver BC; Canada.
^{aj} Also at Università di Napoli Parthenope, Napoli; Italy.
^{ak} Also at University of Colorado Boulder, Department of Physics, Colorado; United States of America.
^{al} Also at Washington College, Maryland; United States of America.
^{am} Also at Yeditepe University, Physics Department, Istanbul; Türkiye.
^{*} Deceased.